# INFORMATION TO USERS

This manuscript has been reproduced from the microfilm master. UMI films the text directly from the original or copy submitted. Thus, some thesis and dissertation copies are in typewriter face, while others may be from any type of computer printer.

**The quality of this reproduction is dependent upon the quality of the copy submitted.** Broken or indistinct print, colored or poor quality illustrations and photographs, print bleedthrough, substandard margins, and improper alignment can adversely affect reproduction.

In the unlikely event that the author did not send UMI a complete manuscript and there are missing pages, these will be noted. Also, if unauthorized copyright material had to be removed, a note will indicate the deletion.

Oversize materials (e.g., maps, drawings, charts) are reproduced by sectioning the original, beginning at the upper left-hand corner and continuing from left to right in equal sections with small overlaps.

Photographs included in the original manuscript have been reproduced xerographically in this copy. Higher quality 6" x 9" black and white photographic prints are available for any photographs or illustrations appearing in this copy for an additional charge. Contact UMI directly to order.

ProQuest Information and Learning
300 North Zeeb Road, Ann Arbor, MI 48106-1346 USA
800-521-0600

UMI®

Downloaded from SHAREOK. Persistent Handle URL: https://hdl.handle.net/11244/423

NOTE TO USERS

This reproduction is the best copy available.

UMI

UNIVERSITY OF OKLAHOMA

GRADUATE COLLEGE

# IMPACT OF PHYSIOLOGICAL STATE AND MACRO-NUTRIENT RATIO ON MICROBIAL SURFACE THERMODYNAMICS AND TRANSPORT

A Dissertation

SUBMITTED TO THE GRADUATE FACULTY

In partial fulfillment of the requirements for the

degree of

Doctor of Philosophy

By

Gang Chen

Norman, Oklahoma
2002

UMI Number: 3040839

UMI®

UMI Microform 3040839

Copyright 2002 by ProQuest Information and Learning Company.
All rights reserved. This microform edition is protected against
unauthorized copying under Title 17, United States Code.

ProQuest Information and Learning Company
300 North Zeeb Road
P.O. Box 1346
Ann Arbor, MI 48106-1346

© Copyright by Gang Chen, 2002
All Right Reserved

# IMPACT OF PHYSIOLOGICAL STATE AND MACRO-NUTRIENT RATIO ON MICROBIAL SURFACE THERMODYNAMICS AND TRANSPORT

A Dissertation

APPROVED FOR THE

SCHOOL OF CIVIL ENGINEERING AND ENVIRONMENTAL SCIENCE

By

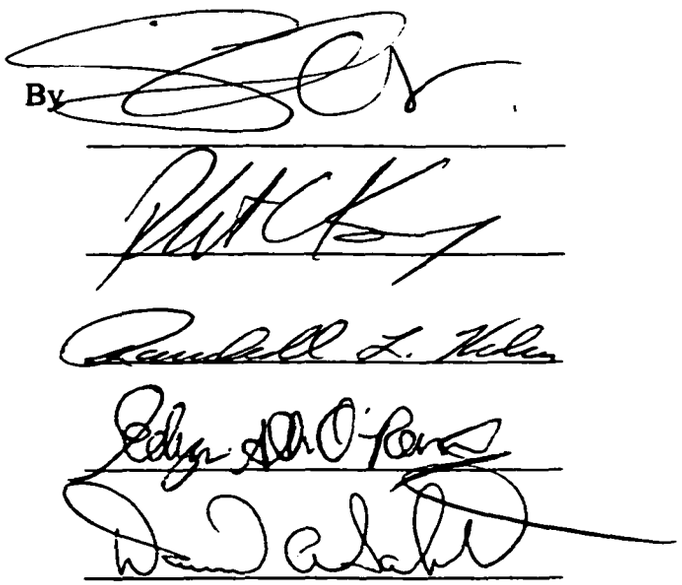

## DEDICATION

This dissertation is dedicated to my wife Lili and my daughter Qiqi, also to my father-in-law Honglong Zhu and mother-in-law Ruixiang Zhang for their encouragement and support.

## ACKNOWLEDGEMENTS

Words are always meaningless in expressing my gratitude to my advisor, Dr. Strevett. Throughout my study at the University of Oklahoma, his invaluable advice and encouragement are always with me. He is more than a mentor to me in every aspect. I would also like to express my many thanks to my committee members: Dr. Knox for his encouragement and always being there for me, Dr. Sabatini for his unique insight into my research and suggestions, Dr. Kolar for his valuable advice in modeling and support through my course of study, and Dr. O'Rear for his valuable input to my research from the Bioengineering's point of view.

I wish to thank Carrie Evenson, Md. Shaheed, Jose Baeza, Jacklin Simmons, Chetan Goudar and Jane Sund for their advice and assistance. I would also like to thank the CEES staff for their support.

## TABLE OF CONTENTS

Page

DEDICATION ..... iv
ACKNOWLEDGEMENT ..... v
TABLE OF CONTENTS ..... vi
LIST OF TABLES ..... ix
LIST OF ILLUSTRATIONS ..... xi
PREFACE ..... xiii

CHAPTER 1 Overview ..... 1

CHAPTER 2 Impact of Surface Thermodynamics on Bacterial Transport
Abstract ..... 3
Introduction ..... 3
Model Development ..... 5
Materials ..... 11
Experiment Protocols ..... 12
Results and Discussion ..... 17
Interactions in Aqueous Media ..... 17
Impact of Physiological State on Surface Thermodynamics ..... 21
Impact of Surface Thermodynamics on Deposition Coefficient ..... 23
Conclusions ..... 29
Acknowledgements ..... 29
References ..... 31

CHAPTER 3 Impact of Carbon and Nitrogen Conditions on E. coli Growth and Surface Thermodynamics
Abstract ..... 34
Introduction ..... 35
Materials ..... 37
Experiment Protocols ..... 39
Results ..... 42
Discussion ..... 47
Impact of Carbon and Nitrogen on Microbial Cell Growth ..... 47
Lipopolysaccharide Production ..... 51
Surface Thermodynamics ..... 53
Conclusions ..... 55
Acknowledgements ..... 56
References 56

CHAPTER 4 Surface Free Energy Relationships Used to Evaluate Microbial Transport
Abstract ..... 58
Introduction ..... 59

Model Development ..... 61
Materials ..... 66
Experiment Protocols ..... 68
Results and Discussion ..... 72
Deposition Coefficient ..... 79
Retardation factor ..... 81
Acknowledgements ..... 84
References ..... 84

CHAPTER 5 Microbial Deposition in Porous Media: A Surface Thermodynamic Investigation
Abstract ..... 89
Introduction ..... 90
Materials and Methods ..... 91
Result ..... 100
Discussion ..... 104
Clean Bed Collision Efficiency ..... 104
Blocking Factor ..... 106
Conclusions ..... 109
Acknowledgements ..... 110
References ..... 110

CHAPTER 6 Determination of Microbial Sorption Isotherms from Column Experiments
Abstract ..... 113
Introduction ..... 113
Materials and Methods ..... 116
Result ..... 123
Discussion ..... 128
Conclusions ..... 131
Acknowledgements ..... 132
References ..... 132

CHAPTER 7 Effect of Flow Rate on Microbial Transport
Abstract ..... 136
Introduction ..... 136
Experiment Protocols ..... 138
Results and Discussion ..... 140
Acknowledgements ..... 143
References ..... 143

CHAPTER 8 Impact of Bacterial Extracellular Polymers on Lindane Transport
Abstract ..... 145
Introduction ..... 146
Materials ..... 149
Experiment Protocols ..... 150

Results and Discussion ..... 156
Lindane Transport in the Absence of the ECPs ..... 156
Lindane Transport in the Presence of the ECPs ..... 161
Impact of Lindane Transport by the ECPs Extracted from Different Microorganisms ..... 161
Impact of Lindane Transport by the Same ECPs in Different Medium Matrices ..... 164
Surface Thermodynamic and Infrared Spectroscopy (IR) Study of the ECPs ..... 166
Impact of ECP Concentrations on Lindane Transport ..... 169
Summary ..... 169
Acknowledgements ..... 171
References ..... 171

CHAPTER 9 Conclusions ..... 174

APPENDIX I ..... 177

APPENDIX II ..... 186

APPENDIX III ..... 187

APPENDIX IV ..... 188

APPENDIX V ..... 189

APPENDIX VI ..... 190

APPENDIX VII ..... 191

APPENDIX VIII ..... 192

APPENDIX IX ..... 193

## LIST OF TABLES


Page

Table 2.1: Summary of the Parameters Used in Column Experiment ..... 16

Table 2.2: Surface Thermodynamics of the Microorganisms and the Media ..... 18

Table 2.3: Free Energies of the Interactions between Microorganisms and the Media ..... 20

Table 2.4: Relevant Transmissions of Different Functional Groups from Infrared Spectroscopy ..... 24

Table 3.1: Carbon and Nitrogen Sources in Different Medium Formations ..... 38

Table 3.2: Summary of the Growth and Surface Thermodynamic Properties of *E. coli* Cultured under Different Medium Formations ..... 43

Table 3.3: Summary of the Free Energy Values of the Half Reactions and Theoretically Calculated Growth Parameters ..... 50

Table 4.1: Summary of the Parameters Used in Column Experiment ..... 73

Table 4.2: Surface Thermodynamic Properties of the Microorganisms and the Media ..... 76

Table 4.3: The Deposition Coefficient $k_c$ and Collision Efficiency $\alpha$ as a Function of Lewis Acid/Base Free Energy at the Closest Approach $\Delta G_{132}^{AB}$ and Retardation Factor R as a Function of van der Waals Free Energy at the Last Interaction Inflection Point $\Delta G_{132}^{LW}$ ..... 80

Table 5.1: Summary of the Parameters Used in Column Experiment ..... 97

Table 5.2: Bacterial and Medium Surface Thermodynamic Properties ..... 101

Table 5.3: Interaction Free Energies and Corresponding Clean Bed Collision Efficiency $\alpha_0$ and Blocking Factor B ..... 102

Table 5.4: van der Waals, Lewis Acid/Base and Electrostatic Interaction Free Energies ..... 108

Table 6.1: Summary of the Parameters Used in Column Experiment ..... 123

Table 6.2: Bacterial and Medium Surface Thermodynamic Properties ..... 127

Table 6.3: Interaction Free Energies at the Secondary Minimum ..... 127

Table 7.1: Summary of the Parameters Used in Column Experiment ..... 140

Table 8.1: Retardation Factor and Fraction Recovery of Lindane in the Absence and Presence of the ECPs Extracted at a Concentration of 30 mg/l ..... 159

Table 8.2: Surface Thermodynamic Properties of the ECPs ..... 167

## LIST OF ILLUSTRATIONS


Page

Figure 2.1: Breakthrough Curves of the Bacterial Strains at Stationary State in Silica gel and CRA Columns ..... 16

Figure 2.2: $-\Delta G_{132}^{TOT}$ ( $\times 10^{-18}$ J) and Deposition Coefficient ($hr^{-1}$) as a Function of Bacterial Strains for Silica gel and CRA ..... 25

Figure 2.3: Deposition Coefficient as a Function of $-\Delta G_{132}^{TOT}$ ( $\times 10^{-18}$ J) for Silica gel and CRA ..... 27

Figure 3.1: *E. coli* Growth under Different Carbon and Nitrogen Conditions with Ammonia Serving as the Nitrogen Source ..... 44

Figure 3.2: *E. coli* Growth under Different Carbon and Nitrogen Conditions with Nitrate Serving as the Nitrogen Source ..... 45

Figure 4.1: BTCs of the Bacteria on Silica gel and COA ..... 72

Figure 4.2: Free Energies between E. coli and Silica gel with Respect to Distance ..... 77

Figure 4.3: The Retardation Factor R as a Function of the Free Energy of van der Waals Interactions at the Last Inflection Point ..... 82

Figure 5.1: Collision Efficiency, $\alpha$ versus Cell Surface Coverage, $\phi$ ..... 103

Figure 5.2: $Ln\alpha_0$ versus $\Delta G_{132}^{TOT}/1000$ Kt ..... 106

Figure 5.3: LnB versus $\Delta G_{131}^{TOT}/1000$ kT ..... 107

Figure 6.1: BTCs of the microbes in COA ..... 124

Figure 6.2: Microbial Sorption Isotherms ..... 126

Figure 6.3: Theoretical Simulations of the Microbial BTCs in COA ..... 130

Figure 7.1: Deposition Coefficient, $k_c$ versus Flow Rate ..... 141

Figure 8.1: BTCs of Lindane in the Absence and Presence of Extracellular Polymers (30 mg/l) in a CRA and COA Column ..... 157

Figure 8.2: Linear Sorption Isotherms of Lindane in CRA and COA ..... 160

Figure 8.3: Linear Sorption Isotherms of Lindane in the ECPs ..... 162

Figure 8.4: Linear Sorption Isotherms of the ECPs in the Media.....163

Figure 8.5: Effect of $K_{om}^{d}$ on the Retardation Factor of Lindane at Different $K_{dom}^{s}$ values.....165

Figure 8.6: Infrared Spectroscopy of the ECPs .....168

Figure 8.7: Effect of ECP Concentration on the Facilitated Lindane Transport .....170

## PREFACE

A quantitative understanding of microbial migration in geological formations is critical to predict the dissemination of microbes in the environment and to evaluate the efficacy of microbially mediated *in situ* pollutant degradation. The key event that retards the movement of microorganisms in the saturated zone is their interactions with matrix surfaces, which may result in adhesion. These interactions are determined by surface thermodynamic properties of the microorganisms and the matrix. The extended DLVO theory, which includes a short-range hydrophobic force, provides a theoretical framework for describing and predicting these interactions. Because of the variable nature of bacterial cell surfaces with the microorganisms' physiological state and macro-nutrient ratio, the surface thermodynamics are highly dependent on the cell's growth state and such dependence requires quantification. Finally, hydrodynamic forces may be significant in determining the surface-surface interactions and should be included in a complete description of microorganism migration. These interfacial interactions can be related to microbial transport in porous media.

Two types of models are often used to describe the transport of micro-size particles (colloids or biocolloids) in porous media: the Deep-Bed Filtration Model and the Convection-Dispersion Model. The Deep-Bed Filtration Model describes a process in which colloidal particles present in the flowing suspension are deposited within the porous media. The deposition of the colloids is considered to be irreversible and no consideration is given to hydrodynamic forces that may remove the particles from the surface and suspend them again in the flowing fluid. The Convection-Dispersion Model

describes the movement and spreading of the colloids during transport based on the assumption that given long enough time, all the particles transported can be recovered. Each model has its own parameter for describing the transport. The Deep-Bed Filtration Model utilizes the deposition coefficient, a parameter that describes irreversible adsorption (i.e., deposition) of the colloids on the media; while the Convection-Dispersion Model uses the retardation factor, a parameter that describes reversible adsorption (i.e., retardation) of the colloids when passing through the media.

As both deposition and retardation occur during bacterial transport, the deposition coefficient and retardation factor have been widely used individually in describing the transport of bacteria through porous media. Rijnaarts *et al.* has demonstrated that a combination of both parameters is required to accurately describe microbial transport in porous media. This study is to relate deposition and retardation to surface interactions between microbes and porous media, which are determined by the surface thermodynamics of the microbes and the media as well as the radius of the microbes.

# CHAPTER 1

## OVERVIEW

This dissertation consists of nine chapters corresponding to overview, six different referred journal articles, one research communication and conclusion. Chapter 2 discusses the impact of microbial physiological states on microbial surface thermodynamics and surface thermodynamic models are developed to calculate interfacial interactions based on independently determined surface thermodynamic data. It has been published in *Environmental Microbiology*, 3: 237- 245. Revalidation of the conclusion using other microbial strains is recommended by Dr. Kolar during defense. Chapter 3 focuses on the impact of macro-nutrient ratio on microbial growth and surface thermodynamics. A correlation between microbial growth and their surface thermodynamics is established. This chapter has been submitted to *Environmental Microbiology*. Chapter 4 discusses the use of retardation factor and deposition coefficient in describing microbial transport in the subsurface. Reversible and irreversible sorption of microbes in porous media are distinguished and relationships between retardation factor and deposition coefficient and interfacial interaction free energies are established. This chapter has appeared in *Journal of Environmental Engineering* 128: 408-415. More discussion on model simulation, especially the use of other modeling methods is recommeded during defense. Chapter 5 focuses on microbial deposition or irreversible sorption in porous media. The impact of deposited microbial cells on the deposition of suspended cells in the solution is also investigated. This work has been submitted to *Environmental Engineering Science* and is under review. Chapter 6 deals with reversible sorption of microbes in porous media, where microbial sorption

isotherms are determined from column experiments. This work has been submitted to *Water Resources Research* and is under review. Chapter 7 discusses the effect of flow rate on microbial transport and will be submitted to *Water Resources Research* as a research communication. Chapter 8 talks about the application of extracellular polymers (ECPs) from indigenous microorganisms. The impact of ECPs on the enhancement of the transport of a model pesticide of lindane is investigated. This part of work has appeared in *Environmental Engineering Science*, 18: 191 – 203. This research was done earlier than Chapter 6, so linear lindane sorption isotherms were assumed. Whereas, nonlinear isotherms may describe lidane sorption more accurately according to the experimental results from Chapter 6. Chapter 9 summarizes the conclusions of this research. Applications of the concepts and theories developed in this research are also discussed.

# CHAPTER 2

# IMPACT OF SURFACE THERMODYNAMICS ON BACTERIAL TRANSPORT


## Abstract

In this paper, microbial surface thermodynamics was correlated with bacterial transport in saturated porous media. The surface thermodynamics was characterized by contact-angle measurement and the wicking method, which was related to surface free energies of Lifshitz-van der Waals interaction, Lewis acid-base interaction, and electrostatic interaction between the bacteria and the medium matrix. Transport of three different strains of bacteria present at three physiological states was measured in columns of silica gel and sand from the Canadian River Alluvium (Norman, OK). Microorganisms in the stationary state had the highest deposit on solid matrix, compared to logarithmic and decay states. The deposition correlated with the total surface free energy ($\Delta G_{132}^{TOT}$), and the differences in $\Delta G_{132}^{TOT}$ were mainly controlled by the Lewis acid/base interaction. Infrared spectroscopy showed that the increased deposition correlated to an increase in the hydrogen-bonding functional groups on the cell surfaces.



Key words: surface thermodynamics, *Escherichia coli, Pseudomonas fluorescens, Bacillus subtilis*, deposition coefficient, and bacterial transport.


## Introduction

Stenstrom (1989) reported that the adhesions of *Salmonella typhimurium*, *Streptococcus faecalis*, *Streptococcus faecium*, *Escherichia coli*, *Citrobacter freundii*, *Shigella sonnei*,

and *Shigella boydii* to the mineral particles quartz, albite, feldspar, and magnetite were correlated with the hydrophobicity of the cell surfaces as measured by hydrophobic interaction chromatography. Other studies have also reported that hydrophobicity is the dominant interaction mechanism for explaining cell adhesion to abiotic surfaces (van der Mei *et al.*, 1991 and van Loosdrecht *et al.*, 1987). According to van Oss (1994), hydrophobicity can be determined by surface free energy. Therefore, it is hypothesized that surface free energy should play an important role in bacterial adhesion and transport.

Grasso *et al.* (1996) found that *Pseudomonas aeruginosa* cells exhibited different surface free energies at different physiological growth phases, which predicated that bacterial physiological growth state would influence the bacterial surface free energy. This influence is due to the change in outer membrane functional proteins resulting from physiological and metabolic changes during the growth cycle (Singleton *et al.*, 1997). Mercer *et al.* (1993) demonstrated that *E. coli* increased the number of galactose-binding proteins which mediated the chemotactic signal at low growth rate (chemotactic sensitivity coefficient was $1.4 \times 10^3$ $cm^2/s$ for growth rate of 0.1 $hr^{-1}$ compared with $0.5 \times 10^3$ $cm^2/s$ for growth rates greater than 0.3 $hr^{-1}$). This supports the hypothesis that changes in outer membrane proteins occur with changes in physiological growth rate. The changes of the functional proteins can alter the overall outer membrane hydrophobicity, which, in fact, will be demonstrated by the change of bacterial surface free energy. Since surface free energy plays an important role in bacterial transport, the bacterial transport may be impacted by the bacterial physiological growth phase.

The objectives of this study were to (1) examine the surface thermodynamics of the bacteria at different physiological states as well as the surface thermodynamics of the medium matrix; (2) develop models that can be used to estimate the interactions between the bacteria and the matrix based on independently determined surface thermodynamics; and (3) relate the interaction forces to the observed bacterial transport. This correlation will help better understand the impact of surface thermodynamics on the transport of bacteria in the subsurface and will offer a guide for *in-situ* bioremediation.

**Model Development**

*Surface thermodynamics* Interactions between biotic and abiotic surfaces that should be considered in aqueous media are: apolar, or Lifshitz-van der Waals (LW) interaction; polar, electron-donor/electron-acceptor, or Lewis acid-base (AB) interaction; and electrostatic (EL) interaction (van Oss, 1994). During contact-angle measurements, the Gibbs energies $\Delta G_{y0132}{}^{LW}$ and $\Delta G_{y0132}{}^{AB}$ for two parallel plates (designated as 1 and 2) at a distance of closest approach, $y_0$ (assumed to be 1.57 Å by van Oss, 1994), immersed in water (3) can be determined by (Meinders *et al.*, 1995):

$$\Delta G^{LW}_{y_0\ 132} = -2(\sqrt{\gamma_3^{LW}} - \sqrt{\gamma_2^{LW}})(\sqrt{\gamma_3^{LW}} - \sqrt{\gamma_1^{LW}}) \quad (1)$$

$$\Delta G^{AB}_{y_0\ 132} = 2\sqrt{\gamma_3^+}(\sqrt{\gamma_1^-} + \sqrt{\gamma_2^-} - \sqrt{\gamma_3^-}) + 2\sqrt{\gamma_3^-}(\sqrt{\gamma_1^+} + \sqrt{\gamma_2^+} - \sqrt{\gamma_3^+}) - 2\sqrt{\gamma_1^+\gamma_2^-} - 2\sqrt{\gamma_1^-\gamma_2^+} \quad (2)$$

where $\gamma^{LW}$ is the Liftshitz-van der Waals component of surface tension ($mJ/m^2$); $\gamma^+$ the electron-acceptor parameter and $\gamma^-$ the electron-donor parameter of Lewis acid/base component of the surface tension ($mJ/m^2$), which can be determined by Young-Dupré's equation (van Oss, 1994):

$$(1+\cos\theta)\gamma_L = 2(\sqrt{\gamma_S^{LW}\gamma_L^{LW}} + \sqrt{\gamma_S^+\gamma_L^-} + \sqrt{\gamma_S^-\gamma_L^+}) \quad (3)$$

in which $\gamma_L$ is the surface tension of the liquid that is used for the measurements ($mJ/m^2$) and can be calculated from:

$$\gamma_L = \gamma_L^{LW} + 2\sqrt{\gamma_L^-\gamma_L^+} \quad (4)$$

By using three or more different liquids with known $\gamma_L^{LW}$, $\gamma_L^+$, and $\gamma_L^-$ values, the unknown solid surface thermodynamic parameters, $\gamma_S^{LW}$, $\gamma_S^+$, and $\gamma_S^-$ can be estimated. Based on equations (3) and (4), $\gamma_S^{LW}$ can be easily obtained by using one apolar liquid. This occurs because there is no Lewis acid/base component contribution (i.e., $\gamma_L^+ = \gamma_L^- = 0$) for apolar liquids; the liquid surface tension is completely equal to the Liftshitz-van der Waals component ($\gamma_L = \gamma_L^{LW}$). By using the apolar liquid with surface tension already known, the only dependent variable in equation (3) is $\gamma_S^{LW}$, and the independent variable is $\theta$. Once $\gamma_S^{LW}$ is determined, $\gamma_S^+$ and $\gamma_S^-$ can be estimated by using two more polar liquids with known $\gamma_L^{LW}$, $\gamma_L^+$, and $\gamma_L^-$ values.

The Gibbs free energies of interactions between plates, 1, $\Delta G_{y_0131}^{LW}$ and $\Delta G_{y_0131}^{AB}$, at a distance of closest approach, $y_0$, immersed in water, 3, can be calculated by substituting subscript 2 for 1 in equations (1) and (2).

Assuming the microorganisms can be modeled as a sphere having a radius that is at least one order of magnitude less than that of the soil matrix, a sphere-flat plate configuration can be adopted to simplify the interactions between the microorganisms and the matrix. The distance-dependent Lifshitz-Van der Waals interaction between the microorganisms,

1 (sphere-sphere), and between a spherical microorganism, 1, and a flat plate soil matrix, 2 (sphere-plate), are (van Oss, 1994):

$$\Delta G_{131}^{LW}(\text{sphere}-\text{sphere}) = \frac{AR}{12y} \tag{5}$$

$$\Delta G_{132}^{LW}(\text{sphere}-\text{plate}) = \frac{AR}{6y} \tag{6}$$

in which y is the distance between the microorganisms (sphere) or between the microorganisms (sphere) and the matrix (flat plate) measured from the outer edge of the sphere (m); R the radius of the microorganism and A the Hamaker constant, which can be obtained from the Gibbs free energy at distance of closest approach, i.e.,

$$A = 12\,\pi\, y_0^2\, \Delta G_{y0}^{LW} \tag{7}$$

Thus, the Lifshitz-Van der Waals interaction per microorganism can be expressed by:

$$\Delta G(y)_{131}^{LW} = \pi \Delta G_{y_0 131}^{LW} \frac{y_0^2 R}{y} \tag{8}$$

$$\Delta G(y)_{132}^{LW} = 2\pi \Delta G_{y_0 132}^{LW} \frac{y_0^2 R}{y} \tag{9}$$

The acid-base interaction $\Delta G_{132}^{AB}$ per microorganism decays exponentially from the Gibbs free energy value at the distance of closest approach (Meinders *et al.*, 1995):

$$\Delta G(y)_{131}^{AB} = \pi R y_0 \Delta G_{y_0 131}^{AB} e^{(y_0 - y)/\lambda} \tag{10}$$

$$\Delta G(y)_{132}^{AB} = 2\pi R y_0 \Delta G_{y_0 132}^{AB} e^{(y_0 - y)/\lambda} \tag{11}$$

in which $\lambda$ is the decay length of water, justified to be 0.6 nm for pure water (van Oss, 1994).

The electrostatic interaction $\Delta G_{132}^{EL}$ per microorganism can be evaluated by (constant potential approach) (valid for $\kappa y > 10$, van Oss, 1994):

$$\Delta G(y)_{131}^{EL} = \pi\varepsilon\varepsilon_0 R\psi_{01}^2[\mathrm{Ln}(\frac{1+e^{-\kappa y}}{1-e^{-\kappa y}}) + \mathrm{Ln}(1-e^{-2\kappa y})] \quad (12)$$

$$\Delta G(y)_{132}^{EL} = \pi\varepsilon\varepsilon_0 R[2\psi_{01}\psi_{02}\mathrm{Ln}(\frac{1+e^{-\kappa y}}{1-e^{-\kappa y}}) + (\psi_{01}^2 + \psi_{02}^2)\mathrm{Ln}(1-e^{-2\kappa y})] \quad (13)$$

where $\varepsilon$ and $\varepsilon_0$ are the relative dielectric permittivity of water (78.55 for water at 25°C) and permittivity under vaccum ($8.854 \times 10^{-12}$ C/V·m) respectively; $1/\kappa$ the Debye-Hückel length and an estimation of the effective thickness of the electrical double layer (Marshall *et al.*, 1984) which equals to 1000 nm for DI water; $\psi_{01}$, $\psi_{02}$ potentials at the surfaces of the microorganisms and the matrix, which can be calculated based on the following equation:

$$\psi_0 = \zeta(1 + z/R)\exp(\kappa z) \quad (14)$$

where $\zeta$ is the zeta potential measured at the slipping plate that can be easily measured; z the distance from the particles surface to the slipping plate that is generally on the order of 5 Å (van Oss, 1994).

Based on equations (8) to (13), when the microorganisms approach each other or the media at a distance larger than the effective thickness of the electrical double layers, the bacteria are repelled from the medium particles due to the electrostatic forces. The electrostatic repulsion may be overcome by the hydrodynamic forces and Brownian movements. As the bacteria approach the medium particles, the double layers become superimposed, and the Lifshitz-van der Waals and Lewis acid/base interactions increase

dramatically with a decrease in distance between the surfaces. The electrostatic forces can be ignored because the superimposition of the double layers neutralizes the electrostatic charges. In this study, the interactions were evaluated at the distance of closest approach (y=1.57 Å) where physical "contact" that leads to the actual attachment can occur. At this distance, the double layers are totally superimposed and thus the electrostatic (EL) interaction can be neglected.

In this study, as the radii of the medium particles were three orders greater in magnitude than the microorganisms, the interactions between the medium particles were assumed a semi-infinite flat parallel slabs configuration. The Gibbs free energies $\Delta G_{232}^{LW}$ and $\Delta G_{232}^{AB}$ were thus calculated directly from equations (1) and (2). Therefore, the Gibbs free energies $\Delta G_{232}^{LW}$, $\Delta G_{232}^{AB}$ and $\Delta G_{232}^{TOT}$ were expressed in the unit of $mJ/m^2$ instead of J.

*Bacterial transport* Bacterial transport was evaluated by column tests. Deposition coefficient is adopted for the description of bacterial transport based on Bolster *et al.*'s (1998) theory:

$$\frac{K_c L}{V} = -\ln(fr) + \frac{\ln^2(fr)}{Pe} \tag{15}$$

where $K_c$ is the deposition coefficient ($hr^{-1}$); L the length of the column (m); V the pore velocity (m/s); fr fraction recovery; and Pe Peclet number. Deposition coefficient can be calculated provided that fraction recovery and Pe are known. Fraction recovery of the bacteria can be measured by adenosine triphosphate (ATP) analysis. Pe is determined by

study of the breakthrough curves (BTCs) from a conservative tracer of sodium chloride based on the following equation (Annable *et al.*, 1997 and Jin *et al.*, 1995):

$$\sigma^2 = \tau^2 \cdot [\frac{2}{Pe} - \frac{2}{Pe^2} \cdot (1 - e^{-Pe})] \tag{16}$$

where $\sigma$ is the standard deviation and $\tau$ is the measured average residence time for the tracer in the reactor, and they can be calculated by:

$$\tau = \frac{\int_0^\infty t \cdot C(t)dt}{\int_0^\infty C(t)dt} \tag{17}$$

$$\sigma^2 = \frac{\int_0^\infty C(t)(t-\tau)^2 dt}{\int_0^\infty C(t)dt} = \frac{\int_0^\infty \tau^2 \cdot C(t)dt}{\int_0^\infty C(t)dt} - \tau^2 \tag{18}$$

C is the measured concentration of the tracer at the outlet of the column (mg/l) and t the elapsed time from the initial injection of the tracer (sec).

Typically, deposition coefficients are estimated by fitting transport models to the measured BTCs of bacteria eluted from either packed columns or cores of intact aquifer materials. This calculation requires the estimation of porosity, size and density of bacteria, temperature, and column length and neglects of dispersion. Bolster *et al.* (1998) found that the fraction of bacteria recovered was a function of both the deposition coefficients and the Peclet number through calculations using an analytical solution to the nondimensional form of the transport equation. Based on this theory, deposition

coefficients can be easily determined by the measurement of the fraction of bacterial recovery and the Peclet number. Bolster *et al.* (1998) tested this utility for a suite of experiments, and the results indicated that a simple measurement – fraction recovery of bacteria – can be used to obtain an accurate value for deposition coefficient. However, with bacterial fraction recovery and Peclet number, detailed information such as the distribution of bacteria within the column cannot be obtained and it is only valid for 1-D transport modeling studies. The detailed 3-D distribution information is usually a necessity for studies such as *in situ* bioremediation. Even with this limitation, the deposition coefficient is sufficient to evaluate bacterial transport for many general-purpose studies, such as the one described herein.

**Materials**

The bacteria selected for this study included *Echerichia coli, Pseudomonas fluorescens, Bacillus subtilis*, which were the typical representatives of rod-shaped bacteria *Enterobacteriaceae, Pseudomonadaceas*, and *Bacillaceae.* The *E. coli* strain used in this research was *E. coli* HB101, a plasmidless non-fimbriated bacterium, obtained from ATCC (Catalog No.-33694). It was cultured on Luria Broth medium (Sigma L-3522) at 37°C; *P. fluorescens* (P-17) and *B. subtilis* were also obtained from ATCC (Catalog No.-49642 and 6051a) and were grown on Nutrient Broth (Difco 0003) at 26°C and 30°C, respectively. Physiological states of the bacteria were quantified through biochemical assay using ATP analysis. After inoculated on the Gyrotory Water Bath Shaker (New Brunswick Scientific Co. Inc. Model G76), 50 μm of culture was sampled at a time interval of 30 minutes. The number of viable bacterial cells was obtained based on the

light emitted by the reaction of ATP extracted from cells with the enzyme, luciferase, measured by a luminometer (Turner Design, TD-20/20). Thus the bacterial growth curves were obtained and used as the references for the determination of physiological states. For column tests, bacterial strains collected at different physiological states (predetermined by ATP assay) were centrifuged at 2500 RPM (Damon/IEC Divison) for 15 min to separate the strains from the media. After washing twice with Nano-pure deionized water (NPDI), the strains were resuspended in NPDI by agitating on a Wrist Action Shaker (Burrell Scientific, Model 75) for 15 min. The hydrodynamic radius of the bacteria were obtained based on the methods described by Meinders *et al.* (1995).

Porous media used for this research included silica gel from Fisher Scientific (100-200 mesh) and sand (alluvial sand) from the Canadian River Alluvium (CRA) (Norman, OK). Before being packed in the column, silica gel was sterilized at 121°C for 20 min. CRA was sampled from the closed Norman landfill. The organic fraction and hydraulic conductivity of CRA were reported to be $0.0480 \pm 0.0056$ and $(1.6 \pm 0.3) \times 10^{-3}$ cm/s (Karapanagioti et al., 1999). Due to concerns of the structural and chemical alterations, CRA was not sterilized. Instead, it was air dried and stored desiccated until use to minimize the bacterial activity.

**Experiment Protocol**

The surface free energies of the media, silica gel and CRA, were studied using the wicking method (Wålinder and Gardner, 1999 and Ku *et al.*, 1985), which was done by

measuring the velocity of capillary rise through a porous layer and thus obtaining cos(θ) via Washburn's equation (van Oss, 1994):

$$h^2 = (D \cdot t \cdot \gamma_L \cdot \cos\theta) \cdot (2 \cdot \mu)^{-1} \quad (19)$$

where h is the height (m) of capillary rise of liquid (L) at time (t); $\gamma_L$ the total surface tension of the wicking liquid ($mJ/m^2$); $\mu$ the viscosity of liquid ($N \cdot s/m^2$) and D the average interstitial pore size (m). By using a liquid with low surface tension, such as methanol ($\gamma = 22.5$ $mJ/m^2$) or hexane ($\gamma = 18.4$ $mJ/m^2$), the average interstitial pore size D can be obtained from equation (19) because methanol or hexane is expected to spread over the solid surface during the wicking measurement with $\cos\theta=1$. Once D was determined, an apolar liquid, diiodomethane and three polar liquids, glycerol, water, and formamine were applied to estimate their relevant cosθ values. Each measurement was repeated 30 times. Careful consideration should be given in the selection of liquids used during the wicking measurement. Weakly polar surfaces do not bind strongly with polar liquids, and strongly polar surfaces attract many types of impurities and are more soluble in polar liquids. Therefore, three polar liquids were used and two suitable ones were used for the determination of $\gamma^+$ and $\gamma^-$.

The surface free energies of the microorganisms were measured by contact-angle measurement (Contact-angle Meter, Tantec) following the method described by Grasso *et al.*(1996). Similar to the preparation of the bacterial solution for column experiments, bacterial strains collected at different physiological growth states (predetermined by ATP analysis) were washed twice with NPDI, and then resuspended in NPDI. The bacterial solution was vacuum filtered on silver metal membrane filters (0.45 μm, Osmonic, Inc.)

and air-dried for about 30 minutes before the contact-angle measurements were taken. The amount of cells on the silver filter was approximately 13 mg to ensure multi-layer covering of the membrane and the moisture content should be kept in the range of 25% to 30% (Grasso *et al.*, 1996). Similarly to the wicking measurement, one apolar liquid, diiodomethane and three polar liquids, glycerol, water, and formamine (two used for the final calculation) were adopted. Each measurement was repeated 30 times and the average values of the results together with the average results from the wicking measurements were to fit into equations (1) to (11) for the calculation of the Lifshitz-Van der Waals and Lewis acid-base interactions.

$\zeta$-potentials of the microorganisms and the matrix particles were measured using Lazer Zee Meter (Model 501, Pen Kem, Inc.), which was also repeated 30 times. Similar to the contact-angle measurement, bacterial strains were washed twice with NPDI and suspended in NPDI. The medium matrix particles were first ground and then suspended in NPDI. The average results were to fit in equations (12) to (14) for the estimation of the electrostatic interaction.

Column tests for these three strains over a range of physiological states in silica gel and CRA were conducted using a column from Kimble-Kontes with 2.5-cm ID x 15-cm length at a flow rate of 0.03 ml/sec that simulated the natural hydraulic gradient. The column ID and length were chosen to avoid side-wall effects and minimize transport short-circuiting while maintaining the same physiological state at a flow rate of 0.03 ml/sec. The media used for the column experiments, silica gel and CRA, were gently dry

packed into the column by continuously agitating to prevent stratification, after which the column was saturated by 5 pore volumes of DI using a peristaltic pump (Masterflex, Cole-Parmer). A conservative tracer (chloride) BTC was obtained separately to determine *Pe*. The conductivity (μmhos) of the tracer instead of concentration was measured and used in equations (16) to (18) to estimate *Pe*. For each run, 10 ml of bacterial solution (concentration predetermined by ATP analysis) was injected by a syringe from an injection inlet port. The column was continuously flushed with DI for up to 50 pore volumes until no cells could be detected from the elution collected by a fraction collector. The fraction recovery was obtained by numerically integrating the area under the BTCs of the bacteria and then normalizing by the initial bacterial concentration. Each run was done in triplicate. Relevant parameters used in the column experiment are summarized in Table 2.1 and the BTCs of *B. subtilis*, *E. coli*, and *P. fluorescens* at their stationary state in silica gel and CRA are shown in Figure 2.1.

Bacterial surface components were analyzed using infrared spectroscopy (IR) (Perkin-Elmer, 283B). Potassium bromide was used as the crystalline medium. Air-dried bacterial strains of these three microorganisms collected at different physiological state were mixed with potassium bromide to make crystal media before they were put into IR for the analysis. Each sample was evaluated in triplicates and the inconsistency of the peaks of relative transmission was within 5% (95% CI, t-test). The frequencies of the peaks were referred to the library of reference curves (Barnes, 1944).

**Table 2.1 Summary of the Parameters Used in Column Experiment**

| Microorganisms | Radius |
|---|---|
| *E. coli* | 0.5 μm |
| *P. fluorescens* | 0.3 μm |
| *B. subtilis* | 1.0 μm |
| **Porous Media** | **Size** |
| Silica gel | 100-200 mesh (0.1 mm) |
| CRA | ~ 0.8 mm |

| Column Experiment | |
|---|---|
| Column | 2.5-cm ID x 15-cm Length |
| Flow Rate | 0.03 ml/sec |
| *Pe* | 13.89 (silica gel) and 48.1 (CRA) |

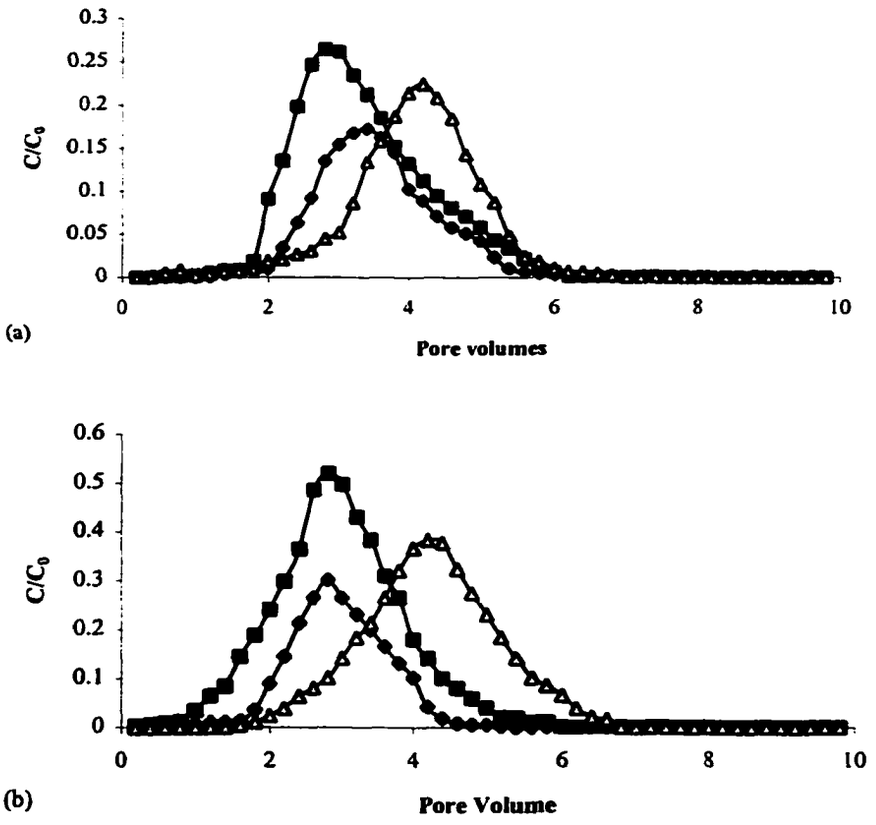


**Figure 2.1** Break through curves of the bacterial strains at stationary state in (a) silica gel and (b) CRA columns ■ *B. subtilis*, ◆ *P. fluorescens* and ▲ *E. coli*

**Results and Discussion**

*Interactions in the aqueous media* Surface thermodynamic properties of the microorganisms in different physiological states and surface thermodynamic properties of the media are summarized in Table 2.2. From Table 2.2, it can be seen that all the microorganisms as well as silica gel and CRA were negatively charged (negative $\zeta$-potential values), which resulted in the repulsive electrostatic interaction. Also, there was very little change in $\zeta$-potential values for the microorganisms at different physiological states, however, there were some differences among the bacteria examined. For different media, $\zeta$-potentials were significantly different (95% CI, t-test). Also it was found that all the microorganisms and the media exhibited a monopolar surface ($\gamma_l^-$ was at least one order of magnitude greater than $\gamma_l^+$, van Oss, 1994).

The free energy of Lifshitz-van der Waals interaction, $\Delta G_{131}^{LW}$, between microorganisms, 1, immersed in water, 3, was negative for all the microorganisms and physiological states. This result follows the prediction by van Oss (1994) that $\Delta G_{131}^{LW}$ is always negative, which is reasonable since the Lifshitz-van der Waals interaction between the same materials immersed in aqueous media should always be attractive. $\Delta G_{131}^{AB}$, the free energy of Lewis acid/base interaction between microorganisms, 1, immersed in water, 3 was positive, viz., repulsive for all the microorganisms at all the three physiological states because of the microorganisms' monopolar surface.

**Table 2.2 Surface Thermodynamics of the Microorganisms and the Media**

| Strain* | ζ-potential (mV) | $\gamma_1^+$ (mJ/m$^2$) | $\gamma_1^-$ (mJ/m$^2$) | $\gamma_1^{LW}$ (mJ/m$^2$) | $\Delta G_{131}^{LW}$ ($10^{-18}$ J) | $\Delta G_{131}^{AB}$ ($10^{-18}$ J) | $\Delta G_{131}^{TOT}$ ($10^{-18}$ J) |
|---|---|---|---|---|---|---|---|
| *E. coli* L | -16.4±0.4 | 0.72 | 57.19 | 39.62 | -1.30 | 13.18 | 11.88 |
| *E. coli* S | -16.3±0.3 | 0.59 | 58.98 | 39.11 | -1.24 | 11.20 | 9.96 |
| *E. coli* D | -16.5±0.2 | 0.56 | 57.87 | 39.62 | -1.30 | 13.07 | 11.77 |
| *P. fluorescens* L | -19.5±0.3 | 1.32 | 56.00 | 36.49 | -0.56 | 8.62 | 8.06 |
| *P. fluorescens* S | -18.9±0.2 | 1.29 | 56.83 | 36.49 | -0.56 | 7.91 | 7.35 |
| *P. fluorescens* D | -19.0±0.5 | 1.29 | 55.82 | 37.02 | -0.59 | 8.75 | 8.16 |
| *B. subtilis* L | -22.9±0.4 | 0.07 | 57.59 | 45.03 | -4.11 | 25.01 | 20.9 |
| *B. subtilis* S | -22.8±0.4 | 0.08 | 59.88 | 44.64 | -3.99 | 22.41 | 18.42 |
| *B. subtilis* D | -22.8±0.4 | 0.09 | 57.55 | 44.64 | -3.99 | 24.96 | 20.97 |
| Media | ξ-potential (mV) | $\gamma_2^+$ (mJ/m$^2$) | $\gamma_2^-$ (mJ/m$^2$) | $\gamma_2^{LW}$ (mJ/m$^2$) | $\Delta G_{232}^{LW}$ (mJ/m$^2$) | $\Delta G_{232}^{AB}$ (mJ/m$^2$) | $\Delta G_{232}^{TOT}$ (mJ/m$^2$) |
| Silica Gel | -42.3±0.8 | 0.003 | 11.71 | 25.72 | -0.32 | -32.52 | 32.84 |
| Sand | -28.1±0.6 | 0.473 | 12.52 | 24.58 | -0.17 | -20.03 | -20.20 |

* L — logarithmic state, S — stationary state, D — decay state.

Free energies of interactions between the microorganisms and the media are summarized in Table 2.3. From Table 2.3, it was found that $\Delta G_{132}^{LW}$, the free energy of Lifshitz-van der Waals interaction between microorganisms, 1, and the medium matrix, 2, immersed in water, 3 was negative, which indicated a net attraction occurred. This is due to the fact that the microorganisms, 1, had the highest Lifshitz-van der Waals free energy of cohesion *in vacuo*, while water, 3, had the least (by study of the Lifshitz-van der Waals component of surface tension) (van Oss, 1994). Also, both silica gel and CRA exhibited a monopolar surface. Due to the monopolar surfaces of both the microorganisms and the porous media, $\Delta G_{132}^{AB}$, the free energy of Lewis acid/base interaction between microorganisms, 1, and the medium matrix, 2, immersed in water, 3 was negative, i.e., an attractive interaction.

Total free energies of interactions between the microorganisms, 1, immersed in water, 3, $\Delta G_{131}^{TOT}$ (sum of $\Delta G_{131}^{LW}$ and $\Delta G_{131}^{AB}$), were positive for all the microorganisms used in this study, which indicated that the interactions between the microorganisms in the aqueous medium were repulsive. This results in a mono-dispersed microorganism suspension in water rather than aggregation. From the surface thermodynamic perspective, a colloid is hydrophilic when $\Delta G_{131}^{TOT} > 0$. Therefore all the microorganisms studied at all three physiological states exhibit a predominant hydrophilic surface. $\Delta G_{131}^{AB}$ was the major driving force for this hydrophilicity as it was one order magnitude greater than that of $\Delta G_{131}^{LW}$.

**Table 2.3 Free Energies of the Interactions between the Microorganisms and the Media**

| Strain* | $^{a}\Delta G_{132}^{LW}$ ($10^{-18}$ J) | $^{a}\Delta G_{132}^{AB}$ ($10^{-18}$ J) | $^{a}\Delta G_{132}^{TOT}$ ($10^{-18}$ J) | $^{b}\Delta G_{132}^{LW}$ ($10^{-18}$ J) | $^{b}\Delta G_{132}^{AB}$ ($10^{-18}$ J) | $^{b}\Delta G_{132}^{TOT}$ ($10^{-18}$ J) |
|---|---|---|---|---|---|---|
| *E. coli* L | -0.65 | -5.63 | -6.28 | -0.46 | -4.55 | -5.01 |
| *E. coli* S | -0.63 | -6.08 | -6.71 | -0.45 | -4.93 | -5.38 |
| *E. coli* D | -0.65 | -5.67 | -6.32 | -0.46 | -4.57 | -5.03 |
| *P. fluorescens* L | -0.33 | -3.44 | -3.77 | -0.23 | -2.79 | -3.02 |
| *P. fluorescens* S | -0.33 | -3.58 | -3.91 | -0.23 | -2.92 | -3.15 |
| *P. fluorescens* D | -0.34 | -3.39 | -3.73 | -0.24 | -2.75 | -2.99 |
| *B. subtilis* L | -1.62 | -9.67 | -11.29 | -1.16 | -7.60 | -8.76 |
| *B. subtilis* S | -1.60 | -10.28 | -11.88 | -1.15 | -8.93 | -10.08 |
| *B. subtilis* D | -1.60 | -9.74 | -11.34 | -1.15 | -7.66 | -8.81 |

* L — logarithmic state, S — stationary state, D — decay state.

a Free energies of the interactions between the microorganisms and silica gel.

b Free energies of the interactions between the microorganisms and CRA.

Total free energies of interaction between the microorganisms, 1, and silica gel or CRA, 2, immersed in water, 3, $\Delta G_{132}^{TOT}$ (sum of $\Delta G_{132}^{LW}$ and $\Delta G_{132}^{AB}$), at the closest approach were always negative and therefore, attractive forces played a significant role when the microorganisms were close to the media. This explains why attachment occurs when microorganisms pass through porous media. Similar to $\Delta G_{131}^{TOT}$, $\Delta G_{132}^{AB}$ was the driving force for $\Delta G_{132}^{TOT}$.

*Impact of physiological state on surface thermodynamics* van Oss (1994) has previously suggested that the $\gamma^{LW}$ values for a considerable number of biological and many other organic materials are typically equal to 40 mJ/m$^2$ with minor variability. This was supported herein with $\gamma^{LW}$ values for all the three microorganisms at different growth states being in the range from 36 mJ/m$^2$ to 45 mJ/m$^2$. As $\gamma^{LW}$ was obtained by using the apolar liquid, diiodomethane on the microorganisms, and the microorganisms were essentially monopolar, the monopolarity did not affect the cohesion of diiodomethane (van Oss, 1994). Therefore, the contact-angle that was determined by the cohesive interactions in the apolar liquid resulted in a relatively constant $\gamma^{LW}$ value. Because $\gamma^{LW}$ remained relatively constant, $\Delta G_{131}^{LW}$ and $\Delta G_{132}^{LW}$ (given the condition that the porous medium was the same) did not change significantly (t-test, 95% CI) from logarithmic state to stationary state and decay state.

As the microorganisms were monopolar, $\gamma^-$ played a more important role than $\gamma^+$ in determining the Lewis acid-base interaction between the microorganisms, viz., $\Delta G_{131}^{AB}$ and between the microorganisms and the media, viz., $\Delta G_{132}^{AB}$. Since $\Delta G_{131}^{AB}$ and

$\Delta G_{132}^{AB}$ were the major contributors for $\Delta G_{131}^{TOT}$ and $\Delta G_{132}^{TOT}$, $\gamma^-$ appeared primarily responsible for the stability of the bacterial suspension (Grasso *et al.*, 1996) and their interactions with the media. In stationary state, $\gamma^-$ value increased by 1.5% ~ 4% from logarithmic state and this made $\Delta G_{131}^{AB}$ decrease by 8% ~ 15% and $\Delta G_{132}^{AB}$ decrease (negatively increased) by 4% ~ 8% for silica gel and 5% ~ 18% for CRA. Accordingly, $\Delta G_{131}^{TOT}$ decreased by 8% ~ 16% and $\Delta G_{132}^{TOT}$ decreased by 4% ~ 7% for silica gel and 4% ~ 15% for CRA. This suggested that the hydrophilicity of the microorganisms decreased and the attractive forces between the microorganisms and the porous media increased when changing from logarithmic state to stationary state. This observation is consistent with the fact that less hydrophilicity (more hydrophobicity) increases the potential of the adsorption of the microorganisms on the porous media. Conversely, there was no significant change (t-test, 95% CI) from logarithmic state to decay state (The change of $\gamma^- < 1.2\%$, the change of $\Delta G_{132}^{TOT} < 1.0\%$ for silica gel and CRA).

To develop an explanation for this phenomenon, further investigation was performed through the study of chemical structure of the bacterial surfaces in different physiological states. By using infrared spectroscopy (IR), the bacteria surfaces were found to be characterized by a variety of different functional groups of aldehydes (RCOH) (peaks shown at wavenumber of 1700 $cm^{-1}$), ketones (RCOR) (1680 $cm^{-1}$), carboxylic acids (RCOOH, $RCOO^-$) (1690 $cm^{-1}$, 1600 $cm^{-1}$), carbonyl groups ($CH_3CO$-) (1320 $cm^{-1}$), peptide bond (-CO-NH-) (1500 $cm^{-1}$), ethers (-$CH_2$-O-, $CH_3$-O-, -C-O-C-) (1000 $cm^{-1}$, 980 $cm^{-1}$, 1060 $cm^{-1}$), ethenyl groups (-CH=CH-, >C=$CH_2$, -CH=$CH_2$) (700 $cm^{-1}$, 830 $cm^{-1}$, 860 $cm^{-1}$), etc., as well as hydrogen (H-) (2900 $cm^{-1}$) and (hydroxyl) (OH-) (3600

$cm^{-1}$), which were due to the contribution of water (Barnes *et al.*,1944). As seen in Table 2.4, microorganisms had more functional groups that favored the electron-donor parameter, $\gamma^-$, (hydrogen-binding groups) such as RCOH, which showed peaks at wavenumber between 1400 and 1700 $cm^{-1}$ in stationary state than in logarithmic and decay states. The relevant transmission of RCOH for *B. subtilis* outer membrane decreased from 21.7% in logarithmic state to 8.8% in stationary state and bounced back to 19.8% again in decay state. A similar observation was made for *E. coli* (35.5%, 20.3%, and 30.4%) and *P. fluorescens* (39.6%, 30.5%, and 38.1%). This increase in functional groups like RCOH from logarithmic to stationary state explained the increase in $\gamma^-$ value by $1.5 \sim 4\%$.

*Impact of Surface Thermodynamics on Deposition Coefficients* From column experiments, deposition coefficient as a function of strains and physiological states was obtained based on equation (15). Analysis of the results revealed that the deposition coefficient was related to $\Delta G_{132}^{TOT}$, the total free energy of interactions between the microorganisms, 1, and the porous media, 2, immersed in water, 3. Higher deposition coefficient values coincided with a lower (higher in negative) value of $\Delta G_{132}^{TOT}$. As compared to *E. coli* and *P. fluorescens*, *B. subtilis* showed greater deposition coefficient values due to its lower (higher in negative) $\Delta G_{132}^{TOT}$ values. Figure 2.2 (a) and (b) illustrated the deposition coefficient and $\Delta G_{132}^{TOT}$ values for all the three bacteria at all

**Table 2.4 Relevant Transmissions of Different Functional Groups from Infrared Spectroscopy**

| Strain* | RCOH | RCOR | RCOOH | $RCOO^-$ | $CH_3CO$- | -CO-NH- | $-CH_2-O-$ | $CH_3-O-$ | -C-O-C- | -CH=CH- | $>C=CH_2$ | $-CH=CH_2$ |
|---|---|---|---|---|---|---|---|---|---|---|---|---|
| *E. coli* L | 35.5 | 42.1 | N/A | 49.2 | 58.2 | 45.1 | 62.8 | N/A | 60.1 | 60.1 | 76.5 | 77.6 |
| *E. coli* S | 20.3 | 21.2 | N/A | 32.3 | 55.1 | 44.2 | 60.9 | N/A | 62.2 | 62.5 | 78.3 | 76.4 |
| *E. coli* D | 30.4 | 35.4 | N/A | 39.1 | 56.7 | 50.1 | 68.2 | N/A | 72.4 | 62.4 | 78.1 | 76.1 |
| *P. fluorescens* L | 39.6 | N/A | N/A | 55.5 | 74.4 | 75.2 | 54.4 | N/A | 57.8 | 72.3 | 72.8 | 66.4 |
| *P. fluorescens* S | 30.5 | N/A | N/A | 50.4 | 62.2 | 58.4 | 50.0 | N/A | 61.9 | 82.8 | 82.2 | 78.2 |
| *P. fluorescens* D | 38.1 | N/A | N/A | 52.3 | 62.5 | 58.2 | 52.1 | N/A | 60.5 | 82.2 | 78.4 | 76.5 |
| *B. subtilis* L | 21.7 | 27.5 | N/A | 32.0 | 30.2 | 39.3 | 40.5 | N/A | 40.7 | 40.1 | 45.5 | 40.4 |
| *B. subtilis* S | 8.8 | 18.4 | N/A | 10.8 | 30.0 | 19.8 | 35.7 | N/A | 36.5 | 46.7 | 48.2 | 42.2 |
| *B. subtilis* D | 19.8 | 29.2 | N/A | 30.2 | 32.5 | 30.1 | 37.4 | N/A | 36.2 | 46.1 | 44.8 | 38.7 |

* L — logarithmic state, S — stationary state, D — decay state.

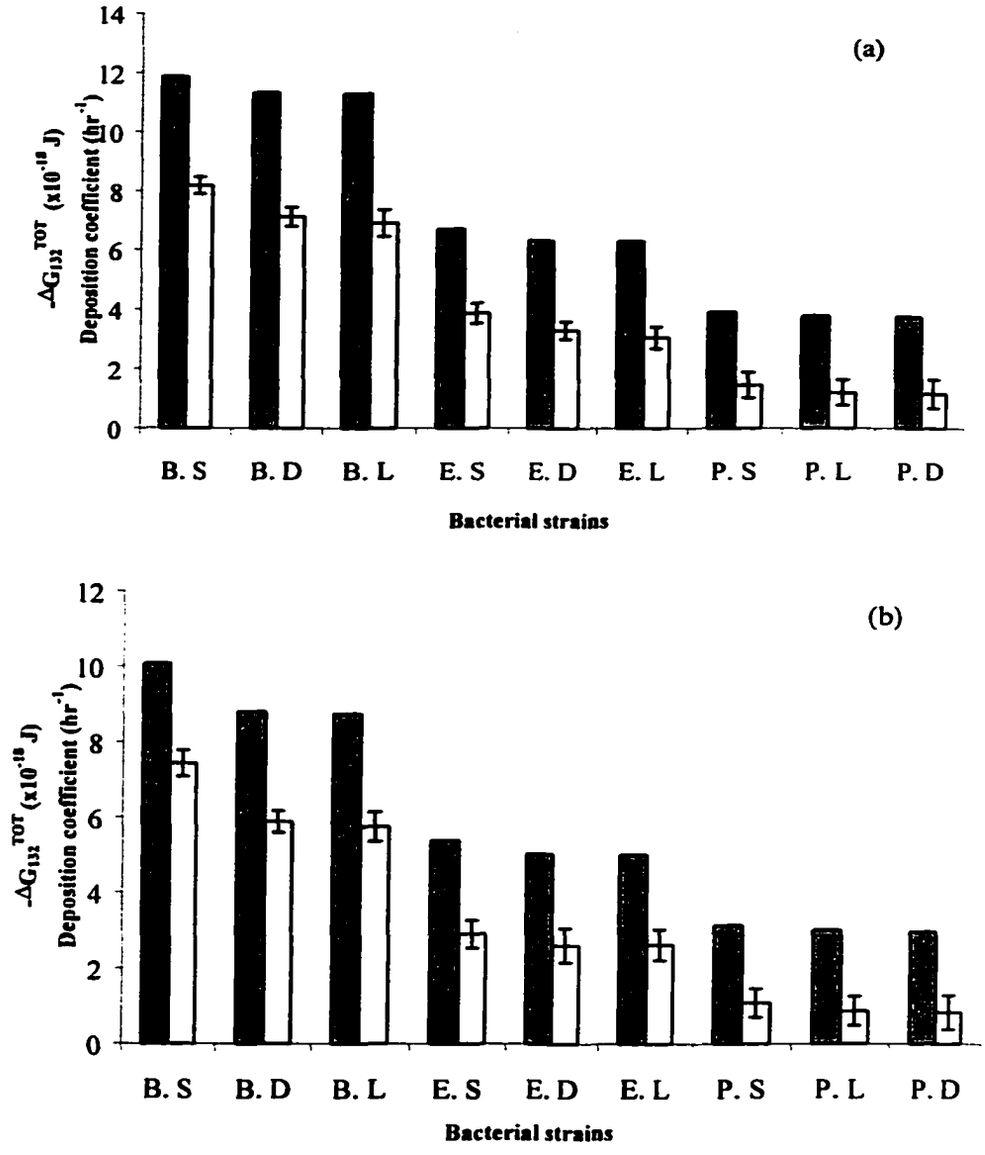


**Figure 2.2** $-\Delta G_{132}^{TOT}$($\times 10^{-18}$ J) and deposition coefficient ($hr^{-1}$) as a function of bacterial strains for (a) silica gel and (b) CRA B. — *B. subtilis*, E. — *E. coli*, P. — *P. fluorescens*; L — logarithmic state, S — stationary state, D — decay state; ■ — $-\Delta G_{132}^{TOT}$, □ — deposition coefficient.

the three physiological states on silica gel and CRA, respectively. For the microorganisms studied and in the stationary state, *B. subtilis* had the lowest $\Delta G_{132}^{TOT}$ values ($-11.88\times10^{-18}$ J for silica gel and $-10.08\times10^{-18}$ J for CRA), *P. fluorescens* had the highest ($-3.91\times10^{-18}$ J and $-3.15\times10^{-18}$ J), and *E. coli* had a value in between ($-6.71\times10^{-18}$ J and $-5.38\times10^{-18}$ J). Based on above discussion, in stationary state, *B. subtilis* should have the highest deposition coefficient values and *P. fluorescens* should have the least. The experimental results validated this prediction with a deposition coefficient value of 8.19 $hr^{-1}$, 3.87 $hr^{-1}$, and 1.44 $hr^{-1}$ for *B. subtilis*, *E. coli*, and *P. fluorescens*, respectively on silica gel. Similar results were observed for CRA with a deposition coefficient value of 7.44 $hr^{-1}$, 2.92 $hr^{-1}$, and 1.09 $hr^{-1}$ for *B. subtilis*, *E. coli*, and *P. fluorescens*, respectively. Also as discussed above, the $\Delta G_{132}^{TOT}$ values for the microorganisms for both silica gel and CRA decreased (increasing negatively) during stationary state would result in an increase in the deposition coefficient values. The experimental results validated this prediction with an increased of deposition coefficient from 6.90 $hr^{-1}$ to 8.19 $hr^{-1}$ for *B. subtilis* from logarithmic state to stationary state in silica gel column, 3.04 $hr^{-1}$ to 3.87 $hr^{-1}$ for *E. coli*, and 1.19 to 1.44 for *P. fluorescens*. Similar results were observed for CRA. Figure 2.3 (a) and (b) illustrated the relationship between deposition coefficient and $\Delta G_{132}^{TOT}$ for silica gel and CRA, respectively. As shown in Figure 2.3 (a) and (b), deposition coefficient displayed a linear relationship with $\Delta G_{132}^{TOT}$.

All three microorganisms had a larger deposition coefficient value for silica gel than CRA due to lower $\Delta G_{132}^{TOT}$ values (greater in negative) for silica gel, which was because

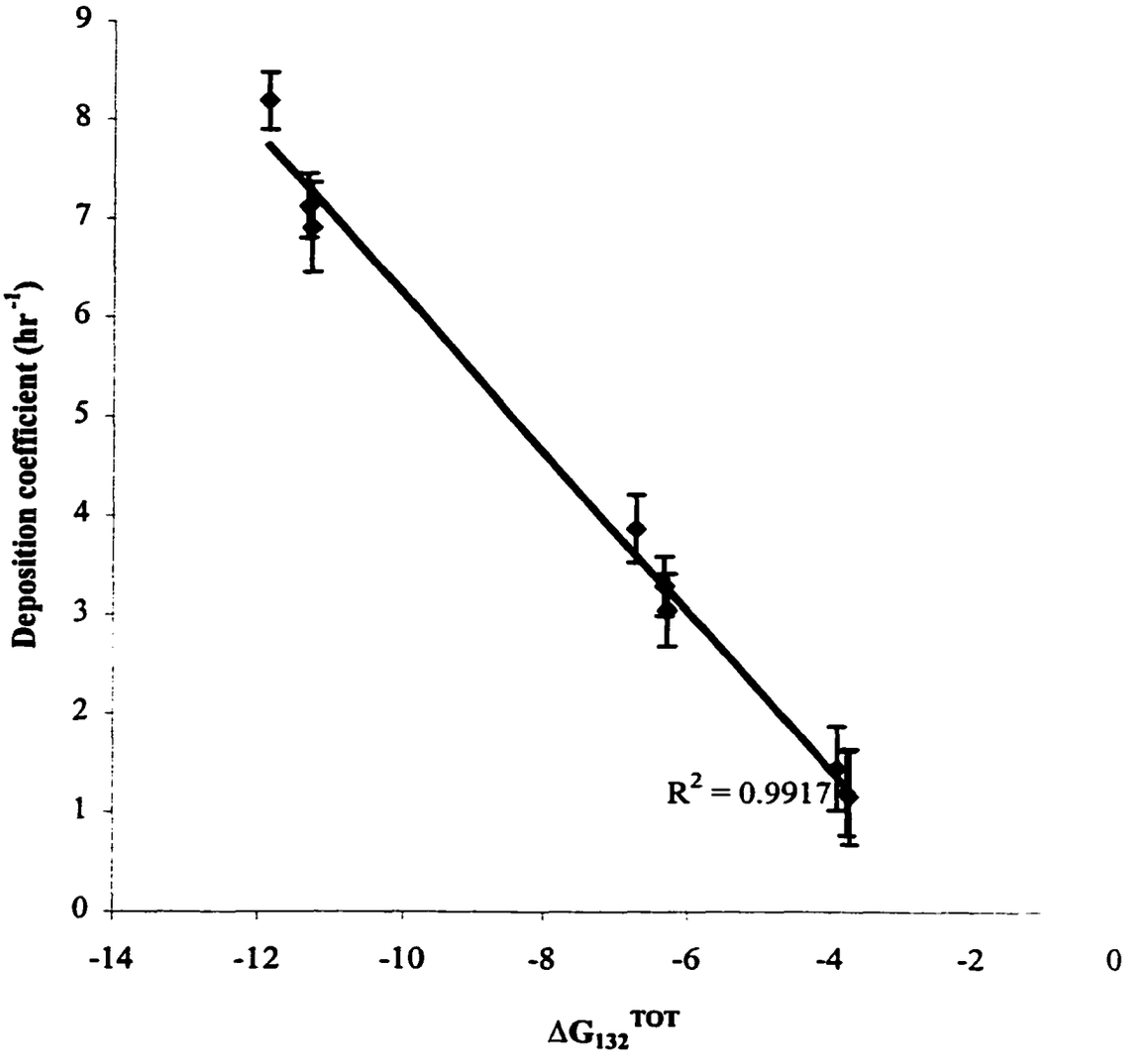


**Figure 2.3 (a)** Deposition coefficient as a function of $\Delta G_{132}^{TOT}$( $\times 10^{-18}$ J) for silica gel

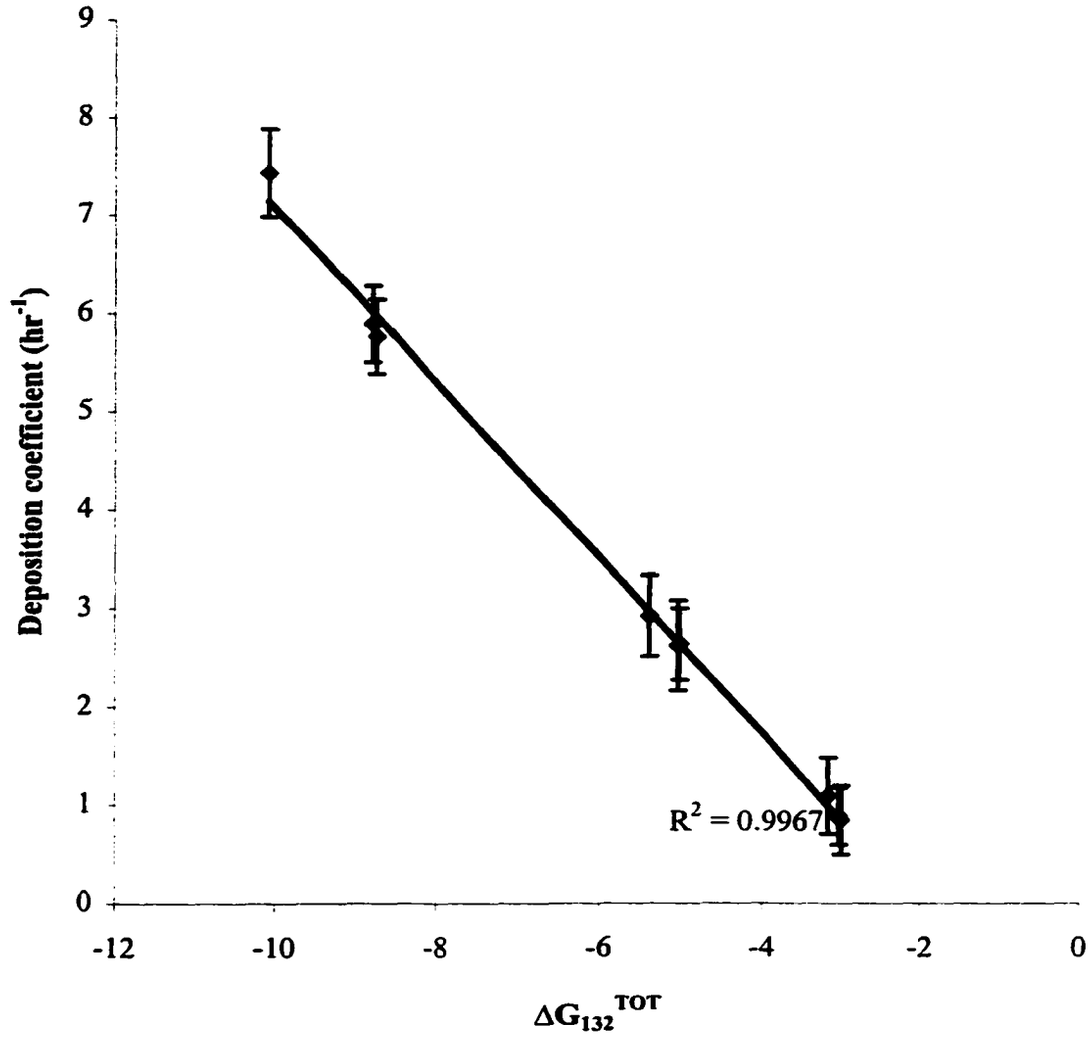


**Figure 2.3 (b)** Deposition coefficient as a function of $\Delta G_{132}^{TOT}$( $\times 10^{-18}$ J) for CRA

silica gel was more hydrophobic ($\Delta G_{232}^{TOT}$ = -32.84 mJ/m$^2$) than CRA ($\Delta G_{232}^{TOT}$ = -20.20 mJ/m$^2$). This is consistent with the fact that microorganisms deposit more on a more hydrophobic surface (Knox *et al.*, 1993).

## Conclusion

Summarizing, it can be concluded that $\Delta G_{132}^{TOT}$ is the determining factor for the deposition of the bacteria on the porous medium matrix and $\Delta G_{132}^{TOT}$ is mainly controlled by Lewis acid/base interaction between the bacteria and the medium matrix. Microorganisms in stationary state have a higher trend to deposit on the matrix than logarithmic and decay states, and microorganisms are easier to deposit on a more hydrophobic surface. By studying the surface thermodynamics of the microorganisms and the media, the transport of the microorganisms can be predicted, which will be a useful guild for field bacterial application such as *in-situ* remediation.

## Acknowledgements

The authors would like to thank Professor D. Grasso, Smith College, for helpful discussions on the development of microbial surface thermodynamic conceptual model used in this study. The work was support in part by National Science Foundation through Grant No. BES-9733969 to the University of Oklahoma.

## Notation

D average interstitial pore size (m)

fr fraction recovery

| | |
|---|---|
| G | Gibbs free energy ($mJ/m^2$) |
| h | height of capillary rise of liquid (m) |
| $K_c$ | deposition coefficient ($hr^{-1}$) |
| L | length of the column (m) |
| Pe | Peclet Number |
| R | radius of microorganism (m) |
| t | time (s) |
| V | interfacial velocity (m/s) |
| y | distance between the microorganism and the matrix (Å) |
| $y_0$ | distance of closest approach (Å) |

**Greek Letters**

| | |
|---|---|
| $\varepsilon$ | dielectric constant of the medium, 78.55 for water at 25 °C |
| $\varepsilon_0$ | dielectric permittivity of the medium in caccum, $8.854 \times 10^{-12}$ C/V·m |
| $\gamma$ | surface tension ($mJ/m^2$) |
| $\gamma^+$ | electron-acceptor parameter of Lewis acid/base component of the surface tension ($mJ/m^2$) |
| $\gamma^-$ | electron-donor parameter of Lewis acid/base component of the surface tension ($mJ/m^2$) |
| $1/\kappa$ | Debye-Hückel length (nm) |
| $\lambda$ | decay length of water (nm) |
| $\mu$ | viscosity of liquid ($N \cdot s/m^2$) |
| $\theta$ | contact-angle |

$\sigma$ standard deviation

$\tau$ measured average residence time (s)

$\psi$ potential measured at the particle's surface (mV)

$\zeta$ potential measured at the slipping plane by electrophoresis (mV)

**References**

1. Annable, M.D., Rao, P.S.C., Graham, W.D., Hatfield, K., and Wood, A.L. (1997) Use of Partitioning Tracer for Measuring Residual NAPL: Results from a Field-Scale Test, *J. Environ. Eng.*, 124: 498-504.

2. Barnes, R.B., Gore, R.C., Liddel, U. and Williams, V.Z. (1944) *Infrared Spectroscopy, Industrial Applications and Bibliography*, Reinhold Publishing Corporation, New York.

3. Bolster, C. H., Hornberger, G. M., Mills, A. L. and Wilson, J. L. (1998) A Method for Calculating Bacterial Deposition Coefficients Using the Fraction of Bacteria Recovered from Laboratory Columns, *Environ. Sci. Technol.*, 32:1329-1332.

4. Grasso, D., Smets, B. F., Strevett, K. A., Machinist, B. D., van Oss, C. J., Giese, R. F. and Wu, W. (1996) Impact of Physiological State on Surface Thermodynamics and Adhesion of Pseudomonas aeruginosa, *Environ. Sci. Technol.*, 30:3604-3608.

5. Jin, M., Delshad, M., Dwarakanath, V., McKinney, D.C., Pope, G.A., Sepehrnoori, K., Tiburg, C., and Jackson, R.E. (1995) Partitioning Tracer Test for Detection, Estimation, and Remediation Performance Assessment of Subsurface Phase Liquid, *Water Resour. Res.*, 31(5), 1201-1211.

6. Karapanagioti, Kleineidam, S., Ligouis, B., Sabatini, D. A. and Grathwohl, P. (1999) Phenanthrene Sorption with Heterogeneous Organic Matter in a Landfill Aquifer Material, *Physics and Chemistry of the Earth.* 24:535-541.

7. Knox, R.C., Sabatini, D.A. and Canter, L.W. (1993) *Subsurface Transport and Fate Processes*, Lewis Publishers, New York.

8. Ku, C., Joseph, D. H. Jr., Ranjani, S. and Lloyd, R. (1985) Particle Transfer from a Continuous Oil to a Dispersed Water Phase: Model Particle Study, *J. Colloid Interface Sci.*, 106:377-387.

9. Meinder, J. M., van der Mei, H. C. and Busscher, H. J. (1995) Deposition Efficient and Reversibility of Bacterial Adhesion under Flow, *J. Colloid Interface Sci.*, 176:329-341.

10. Marshall, K. C., Breznak, J. A., Calleja, G. B., Mcfeters, G. A. and Rutter, P. R. (1984) *Microbial Adhesion and Aggregation*, Springer-Verlag, New York.

11. Mercer, R. J., Ford, M. R., Stitz, L. J. and Bradbeer, C. (1993) Growth Rate Effect on Fundamental Transport Properties of Bacterial Populations, *Biotech. Bioeng.*, 42:1277-1286.

12. Singleton, P. (1997) *Bacteria in Biology, Biotechnology and Medicine*, John Wiley & Sons, New York.

13. Stenstrom, A. T. (1989) Bacterial Hydrophobicity, an Overall Parameter for the Measurement of Adhesion Potential to Soil Particles, *Appl. Environ. Micobiol.*, 55:142-147.

14. van der Mei, H. C., Cowan, M. M. and Busscher, H. J. (1991) Physicochemical and Structural Studies on Acinetobacter calcoaceticus RAG-1 and MR-481--Two Standard Strains in Hydrophobicity Tests, *Curr. Microbiol.*, 23:337-341.

15. van Loosdrecht, M. C. M., Lyklema, J., Norde, W., Schraa, G. and Zhender, A. J. B. (1987) The Role of Bacterial Cell Wall Hydrophobicity in Adhesion, *Appl. Environ. Micobiol.*, 53:1893-1897.

16. van oss, C. J. (1994) *Interfacial Forces in Aqueous Media*, Marcel Dekker, New York.

17. Wålinder, M. E. and Gardner, D. J. (1999) Factors Influencing Contact-angle Measurements on Wood particles by Column Wicking, *J. Adhesion Sci. Technol.*, 13:1363-1374.

# CHAPTER 3

# IMPACT OF CARBON AND NITROGEN CONDITIONS ON *E. coli* GROWTH AND SURFACE THERMODYNAMICS


## Abstract

*E. coli* cultured under different carbon and nitrogen conditions was measured for growth and surface thermodynamics to examine the impact of C/N ratio on *E. coli* growth and its surface thermodynamics. Among the three carbon sources, glucose grown cultures had the greatest specific growth rate (0.67 and 0.44 $hr^{-1}$ with ammonia and nitrate serving as the nitrogen source, respectively, and no carbon or nitrogen limitation), and yielded the least hydrophilic surface (31.49 and 22.23 $mJ/m^2$ of the total intrafacial interaction free energy); propionate grown cultures had the greatest stoichiometric yield coefficient (0.61and 0.49 g biomass per g substrate), lipopolysaccharide production efficiency (0.161and 0.149 g per g biomass), and yielded the most hydrophilic surface (46.32 and 39.32 $mJ/m^2$ of the total intrafacial interaction free energy). For the same carbon source, ammonia-grown cultures yielded a greater specific growth rate, growth yield and lipopolysaccharide production efficiency, and a more hydrophilic surface than nitrate grown cultures. In carbon-limited cultures, a smaller specific growth rate and lipopolysaccharide production efficiency and greater growth yield were observed as compared to cultures grown with no carbon and nitrogen limitation. In addition, under carbon-limited growth, the cells exhibited a less hydrophilic surface. When nitrogen was the limiting factor, *E. coli* displayed a smaller specific growth rate and growth yield, greater lipopolysaccharide production efficiency and a more hydrophilic surface as compared to cultures grown with no carbon and nitrogen limitation.

Key words: carbon, nitrogen, carbon and nitrogen conditions, growth, surface thermodynamics, and *E. coli.*

**Introduction**

Microbial anabolism depends upon a stoichiometric ratio of carbon and inorganic elements (nutrients) such as nitrogen, phosphors, sulfur, potassium, calcium, and magnesium as well as an energy source to synthesize new cellular materials (Tchobanoglous and Burton, 1991). Carbon and energy sources are commonly referred to as substrates. For heterotrophic microorganisms, organic compounds are the most common substrate. Nitrogen is needed for protein synthesis and accounts for about 12-16% of dry mass. Carbon and nitrogen are two essential components of a microbe and a proper carbon to nitrogen ratio (C/N) is required for microbial growth.

In a batch culture, if one of the essential requirements for growth (substrates or nutrients) is limited, it will be depleted first and the growth will cease; while in a continuous culture, the growth will be limited. Experimentally, the effect of a limiting substrate or nutrient has often be adequately described by the Monod equation (Monod, 1949):

$$\mu = \mu_{max} \frac{S}{K_s + S} \qquad (1)$$

where $\mu$ is specific growth rate ($hr^{-1}$); $\mu_{max}$ maximum specific growth rate ($hr^{-1}$); S growth-limiting substrate or nutrient concentration (mg $l^{-1}$); $K_s$ half-velocity constant, which equals to the substrate or nutrient concentration at one-half of the maximum growth rate (mg $l^{-1}$). As shown in equation (1), if the substrate or nutrient is limited, the microbial specific growth rate will be smaller than the maximum specific growth rate;

while when there is no substrate or nutrient limitation, the microbes will grow at the maximum specific growth rate.

Both, McEldowney and Fletcher (1986) and Quagliano and Miyazaki (1997) reported that carbon and nitrogen limitated microbial growth. Ellwood and Tempest (1972) showed that different growth conditions resulted in changes in the physico-chemistry of the bacterial surfaces, due to the fact that macromolecular components of the bacterial surfaces, e.g. lipo-polysaccharide, protein and exopolymers, varied in quantity with growth conditions. Similarly, Quagliano and Miyazaki (1997) observed that the yield of bacterial polyester poly-β-hydroxybutyrate (PHB) relative to the amount of glucose consumed increased with the C/N ratio (a maximum of 0.16 g PHB per g glucose consumed with a C/N ratio of 137.7). The extent of changes of the macromolecular components of the bacterial surfaces due to different growth conditions are reflected by the change of the bacterial surface thermodynamics, a reflection of the bacterial physico-chemical characteristics. In *E. coli*, the outer membrane surface is largely occupied by lipopolysaccharides (Nikaido and Yaara, 1985). Therefore, the change of quantity in lipopolysaccharides on *E. coli*'s surface will be demonstrated by the change of *E. coli*'s surface thermodynamics.

The objective of this research was to investigate the impact of carbon and nitrogen conditions on *E. coli* growth and lipopolysaccharide productions, and subsequent impact on the membrane surface thermodynamic properties. The understanding of the impact of carbon and nitrogen conditions on bacterial surface thermodynamics is critical in *in-situ*

bioremediation because the transport of the bacteria will be retarded by the interactions between the bacteria and the medium matrix (e.g., aquifer material), which is determined by the surface thermodynamics of the bacteria and the medium matrix.

**Materials**

*Bacterial strain* The pure culture used in this study was *E. coli* k12, obtained from ATCC (catalog No. 29181). After inoculated with 1 ml (1.0%) stationary phase culture, *E. coli* was grown in 250 Erlenmeyer flasks containing 100 ml media described below. The flasks were continuously trembled at 150 rpm on a Gyrotory Water Bath (Model G76, New Brunswick Scientific Co. Inc., Edison, NJ) at 37°C until late logarithmic phase that was determined by Adenosine Triphosphate (ATP) analysis.

*Media* The minimal media used in this research contained 5.44 g $KH_2PO_4$ and 6 ml salt solution consisting of 10 g $MgSO_4 \cdot 7H_2O$, 1.0 g $MnCl_2 \cdot 4H_2O$, 0.4 g $FeSO_4 \cdot 7H_2O$ and 0.1 g $CaCl_2 \cdot 2H_2O$ per liter in 1 liter distilled water. Glucose, lactate (sodium salt) or propionate (sodium salt) served as the carbon source and ammonia or nitrate served as the nitrogen source. The combination of each of the carbon and nitrogen sources at different C/N ratios formed 18 different medium formations (Table 3.1). Initial pH of the media was adjusted to 7.4 with 1 N HCl or 1 N NaOH and the lactate and propionate media were sterilized by autoclaving (121°C and 1 atm) for 20 min. Glucose was filter-sterilized and aseptically added to the autoclaved minimal media.

**Table 3.1 Carbon and nitrogen sources in different medium formations**

| Media | C source | N source | C:N ($g\ g^{-1}$) | Limitation |
|---|---|---|---|---|
| 1 | Glucose 0.2 g | $NH_4Cl$ 0.06 g | 5 : 1 | |
| 2 | Glucose 0.2 g | $NH_4Cl$ 0.01 g | 30 : 1 | N |
| 3 | Glucose 0.2 g | $NH_4Cl$ 0.16 g | 1 : 1.5 | C |
| 4 | Glucose 0.2 g | $NaNO_3$ 0.1 g | 5 : 1 | |
| 5 | Glucose 0.2 g | $NaNO_3$ 0.016 g | 30 : 1 | N |
| 6 | Glucose 0.2 g | $NaNO_3$ 0.73 g | 1 : 1.5 | C |
| 7 | Sodium lactate 0.25 g | $NH_4Cl$ 0.06 g | 5 : 1 | |
| 8 | Sodium lactate 0.25 g | $NH_4Cl$ 0.01 g | 30 : 1 | N |
| 9 | Sodium lactate 0.25 g | $NH_4Cl$ 0.46 g | 1 : 1.5 | C |
| 10 | Sodium lactate 0.25 g | $NaNO_3$ 0.01 g | 5 : 1 | |
| 11 | Sodium lactate 0.25 g | $NaNO_3$ 0.016 g | 30 : 1 | N |
| 12 | Sodium lactate 0.25 g | $NaNO_3$ 0.73 g | 1 : 1.5 | C |
| 13 | Sodium propionate 0.26 g | $NH_4Cl$ 0.07 g | 5 : 1 | |
| 14 | Sodium propionate 0.26 g | $NH_4Cl$ 0.012 g | 30 : 1 | N |
| 15 | Sodium propionate 0.26 g | $NH_4Cl$ 0.6 g | 1 : 1.5 | C |
| 16 | Sodium propionate 0.26 g | $NaNO_3$ 0.12 g | 5 : 1 | |
| 17 | Sodium propionate 0.26 g | $NaNO_3$ 0.02 g | 30 : 1 | N |
| 18 | Sodium propionate 0.26 g | $NaNO_3$ 0.89 g | 1 : 1.5 | C |

**Experiment protocols**

*Physiological state and growth rate determination* Late logarithmic phase was quantified through biochemical assay using ATP analysis. After inoculated on the Gyratory Water Bath Shaker at 37°C (Model G76, New Brunswick Scientific Co. Inc., Edison, NJ), 50 μl of the *E. coli* culture from different medium formations was sampled every 30 minutes for up to 60 hours. The light emission produced by the reaction of ATP extracted from cells with luciferase as measured by a luminometer (TD-20/20, Turner Design, Sunnyvale, CA) was compared to an ATP standard ($2.5 \times 10^{-8}$ g $ml^{-1}$ ATP which is equivalent to $5 \times 10^{7}$ bacteria per ml) (10 μg $ml^{-1}$ ATP in HEPES buffer, Turner Design, Sunnyvale, CA) to determine the viable bacterial cell numbers. Growth curves of the viable cell number versus time were thus obtained, which were used as the reference in determining the late logarithmic phase for *E. coli* in different medium formations. *E. coli* was cultured until late logarithmic phase as determined by its viable cell numbers before it was collected for the measurement of surface thermodynamics and extraction of lipopolysaccharides.

The growth rate was also measured by ATP analysis. After inoculation, 50 μl of the *E. coli* growing cultures was sampled every 30 minutes until it was collected. The results were converted to biomass based on the pre-determined relationship between the ATP values and biomass values, which was then used for the calculation of the growth rate.

*Measurement of surface thermodynamics* Surface thermodynamics of *E. coli* was measured by contact angle measurements (Contact Angle Meter, Tantec, Schaumburg,

IL) following the method described by Grasso *et al.* (1996). *E. coli* collected from different medium formations at late logarithmic phase (determined by ATP analysis) was vacuum filtered on silver metal membrane filters (0.45 μm, Osmonic, Inc., Livermore, CA) and air-dried for 30 minutes before being used for contact angle measurements. The amount of cells on the silver membrane filter was approximately 13 mg, which ensured a multi-layer coverage of the membrane. The moisture content was kept in the range of 25% to 30%. One apolar liquid, diiodomethane and two polar liquids, glycerol and water whose surface thermodynamics are known were used for the measurements. The results were fit in Young-Dupré's equation (2) to estimate the bacterial surface thermodynamics.

$$(1+\cos\theta)\gamma_L = 2(\sqrt{\gamma_S^{LW}\gamma_L^{LW}} + \sqrt{\gamma_S^{+}\gamma_L^{-}} + \sqrt{\gamma_S^{-}\gamma_L^{+}}) \qquad (2)$$

where $\theta$ is the measured contact angle (degree); $\gamma_L$ surface tension of the liquid used for the measurements (mJ $m^{-2}$); $\gamma^{LW}$ the Liftshitz-van der Waals component of surface tension (subscript "S" for solid, "L" for liquid) (mJ $m^{-2}$); and $\gamma^{+}$, $\gamma^{-}$ the electron-acceptor and electron-donor parameter of Lewis acid/base component of the surface tension (subscript "S" for solid, "L" for liquid) (mJ $m^{-2}$).

*Extraction of polysaccharides* Lipopolysaccharide extraction followed a method modified from Hancock and Poxton (1988). The collected *E. coli* was first washed free from medium components with phosphate-buffered saline (pH 7.0) and freeze-dried. The lyophilized cells were then resuspended in distilled water at a concentration of 5% (W/V) and mixed with equal volume of 90% (W/W) aqueous phenol at 67°C for 15 minutes. The mixture was transferred to centrifuge tubes and cooled in ice until phase separation occurred. The tubes were then centrifuged at 5000 *g* for 15 minutes. The upper

(aqueous) phase, containing the lipopolysaccharides, was dialyzed against running tap water for at least 18 hrs, until the smell of phenol cannot be detected. The dialyzed extract was then transferred to a round bottom flask connected to a rotoevaporator. The evaporation process was allowed to proceed until the precipitation turned to a honey-color, viscous consistency, which was then freeze dried.

*Analysis of glucose* Glucose was analyzed using a HPLC (Water Associates, Milford, MA) equipped with a Supercogel Pb column (30 cm × 7.8 cm) from Supelco (Bellefonte, PA). The mobile phase was 75% acetonitrile mixed with 25% nanopure DI water (v/v) (Barnstead Thermodyne, Debuque, IO) and the flow rate was 0.6 ml $min^{-1}$. The glucose concentration was quantified using a refractive index detector (Water Associates, Milford, MA) against external glucose standards with an injection of 10 μL.

*Analysis of lactate and propionate* Lactate and propionate were analyzed using a HPLC (Dionex Corporation, Sunnyvale, CA) equipped with an IonPac AS11 analysis column (4 mm) from Dionex. The eluents included: E1, degassed type 1 reagent grade water; E2, 1.0 mM NaOH; and E3, 100 mM NaOH. The gradient program of the eluents was as following: equilibration (5 min), 80% E1, 20% E2, and 0% E3; analysis (5 min), 85% E1, 20% E2, and 0% E3; analysis (10 min) 85% E1, 0% E2, and 15% E3; and regeneration (10 min), 65% E1, 0% E2, and 35% E3. The eluents were at a flow rate of 1.0 mL $min^{-1}$ and the injections were 10 μL. The lactate and propionate concentrations were quantified using a pulsed electrochemical detector (Dionex Corporation, Sunnyvale, CA) against external lactate and propionate standards.

**Results**

Carbon and nitrogen depletion was monitored through the course of the experiments. Carbon or nitrogen limitation was determined by comparing the residual carbon or nitrogen concentration to the predetermined half-velocity constant, $K_s$ (data not shown). The specific growth rate $\mu$ was determined by normalizing the biomass increment within a specific period of time. To examine the impact of carbon and nitrogen conditions on *E. coli* growth, the specific growth rate, $\mu$; stoichiometric yield coefficient, Y; lipopolysaccharide production efficiency, $Y_p$ were measured for each combination of different carbon and nitrogen sources. The *E. coli* growth experiments were performed in triplicate and the experimental variability inconsistency was within 5% (95% CI, t-test). *E. coli* had a greater growth rate when there was no carbon or nitrogen limitation. In addition, less biomass was produced when nitrogen was limited than when there was no carbon and nitrogen limitation or carbon limited. A representative growth curve under different growth conditions with ammonia or nitrate serving as the nitrogen source is illustrated in Figure 3.1 and Figure 3.2 respectively. The electron-acceptor and electron-donor parameters of Lewis acid/base component of surface tension, $\gamma^+$ and $\gamma^-$, and Lifshitz-van der Waals component of surface tension, $\gamma^{LW}$ were measured for surface thermodynamics. Each contact angle measurement was repeated 30 times and the average contact angle values were fit in equation (2).

Under conditions when there was no carbon or nitrogen limitation, different carbon sources (same nitrogen source) yielded different cell growth and surface thermodynamic properties (Table 3.2). Among the three carbon sources, glucose had the greatest specific

**Table 3.2 Summary of the growth and surface thermodynamic properties of *E. coli* cultured under different medium formations**

| Medium Formation* | C:N ($g\ g^{-1}$) | $\gamma^+$ ($mJ\ m^{-2}$) | $\gamma^-$ ($mJ\ m^{-2}$) | $\gamma^{LW}$ ($mJ\ m^{-2}$) | $\Delta G_{131}^{TOT}$ ($mJ\ m^{-2}$) | $\mu$ ($h^{-1}$) | Y (g biomass per g substrate) | $Y_p$ (g per g biomass) |
|---|---|---|---|---|---|---|---|---|
| Glu + $NH_4^+$ | 5 : 1 | 0.438 | 53.16 | 44.23 | 31.49 | 0.67±0.02 | 0.52±0.01 | 0.157±0.004 |
| Glu + $NH_4^+$ | 30 : 1 | 0.294 | 57.23 | 42.04 | 38.76 | 0.31±0.01 | 0.33±0.05 | 0.214±0.002 |
| Glu + $NH_4^+$ | 1 : 1.5 | 0.597 | 50.22 | 45.03 | 26.52 | 0.21±0.01 | 0.56±0.01 | 0.120±0.003 |
| Glu + $NO_3^-$ | 5 : 1 | 0.668 | 48.08 | 47.17 | 22.23 | 0.44±0.02 | 0.46±0.04 | 0.132±0.008 |
| Glu + $NO_3^-$ | 30 : 1 | 0.406 | 53.23 | 45.03 | 31.30 | 0.27±0.01 | 0.24±0.06 | 0.164±0.010 |
| Glu + $NO_3^-$ | 1 : 1.5 | 0.458 | 47.29 | 48.35 | 21.53 | 0.23±0.01 | 0.48±0.07 | 0.090±0.004 |
| Lac + $NH_4^+$ | 5 : 1 | 0.198 | 56.40 | 42.49 | 38.47 | 0.50±0.06 | 0.44±0.05 | 0.150±0.006 |
| Lac + $NH_4^+$ | 30 : 1 | 0.214 | 58.28 | 41.09 | 41.36 | 0.27±0.02 | 0.23±0.03 | 0.196±0.005 |
| Lac + $NH_4^+$ | 1 : 1.5 | 0.146 | 55.52 | 44.23 | 36.99 | 0.17±0.05 | 0.46±0.07 | 0.117±0.001 |
| Lac + $NO_3^-$ | 5 : 1 | 0.348 | 53.24 | 44.64 | 31.99 | 0.33±0.02 | 0.32±0.02 | 0.127±0.003 |
| Lac + $NO_3^-$ | 30 : 1 | 0.322 | 56.36 | 42.49 | 37.22 | 0.30±0.01 | 0.19±0.02 | 0.151±0.005 |
| Lac + $NO_3^-$ | 1 : 1.5 | 0.356 | 52.16 | 45.03 | 30.36 | 0.28±0.01 | 0.34±0.03 | 0.080±0.004 |
| Pro + $NH_4^+$ | 5 : 1 | 0.156 | 61.62 | 40.61 | 46.32 | 0.30±0.02 | 0.61±0.03 | 0.161±0.007 |
| Pro + $NH_4^+$ | 30 : 1 | 0.185 | 62.85 | 38.60 | 48.41 | 0.27±0.02 | 0.41±0.04 | 0.224±0.009 |
| Pro + $NH_4^+$ | 1 : 1.5 | 0.387 | 57.57 | 41.57 | 38.62 | 0.27±0.03 | 0.65±0.07 | 0.124±0.010 |
| Pro + $NO_3^-$ | 5 : 1 | 0.321 | 57.91 | 42.04 | 39.32 | 0.28±0.01 | 0.49±0.01 | 0.149±0.005 |
| Pro + $NO_3^-$ | 30 : 1 | 0.168 | 60.29 | 41.09 | 44.32 | 0.22±0.01 | 0.35±0.03 | 0.187±0.006 |
| Pro + $NO_3^-$ | 1 : 1.5 | 0.337 | 56.70 | 42.49 | 37.50 | 0.19±0.02 | 0.50±0.04 | 0.104±0.012 |

* Glu, glucose; Lac, sodium lactate; Pro, sodium propionate.

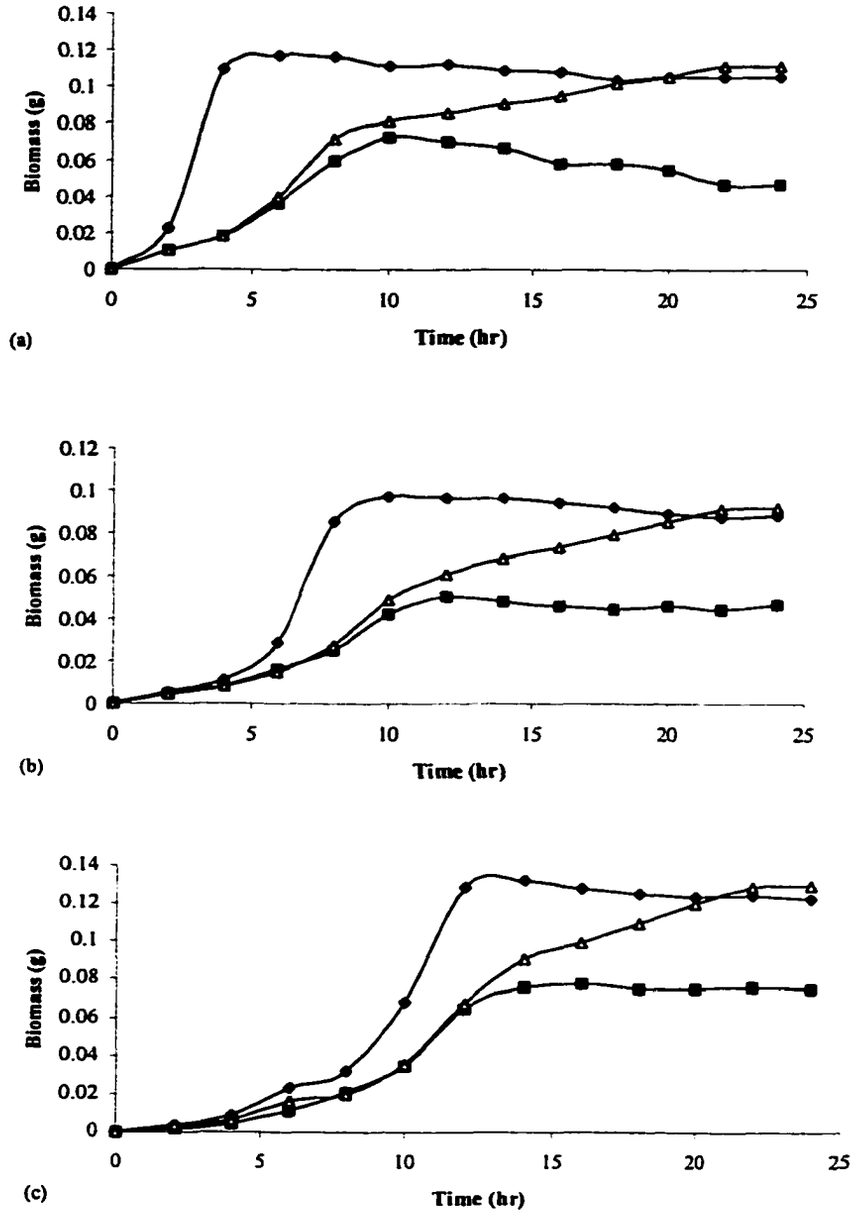


**Figure 3.1** *E. coli* growth under different carbon and nitrogen conditions with (a) glucose, (b) lactate, and (c) propionate serving as the carbon source and ammonia serving as the nitrogen source ◆ no carbon or nitrogen limitation, ■ nitrogen limited, Δ carbon limited.

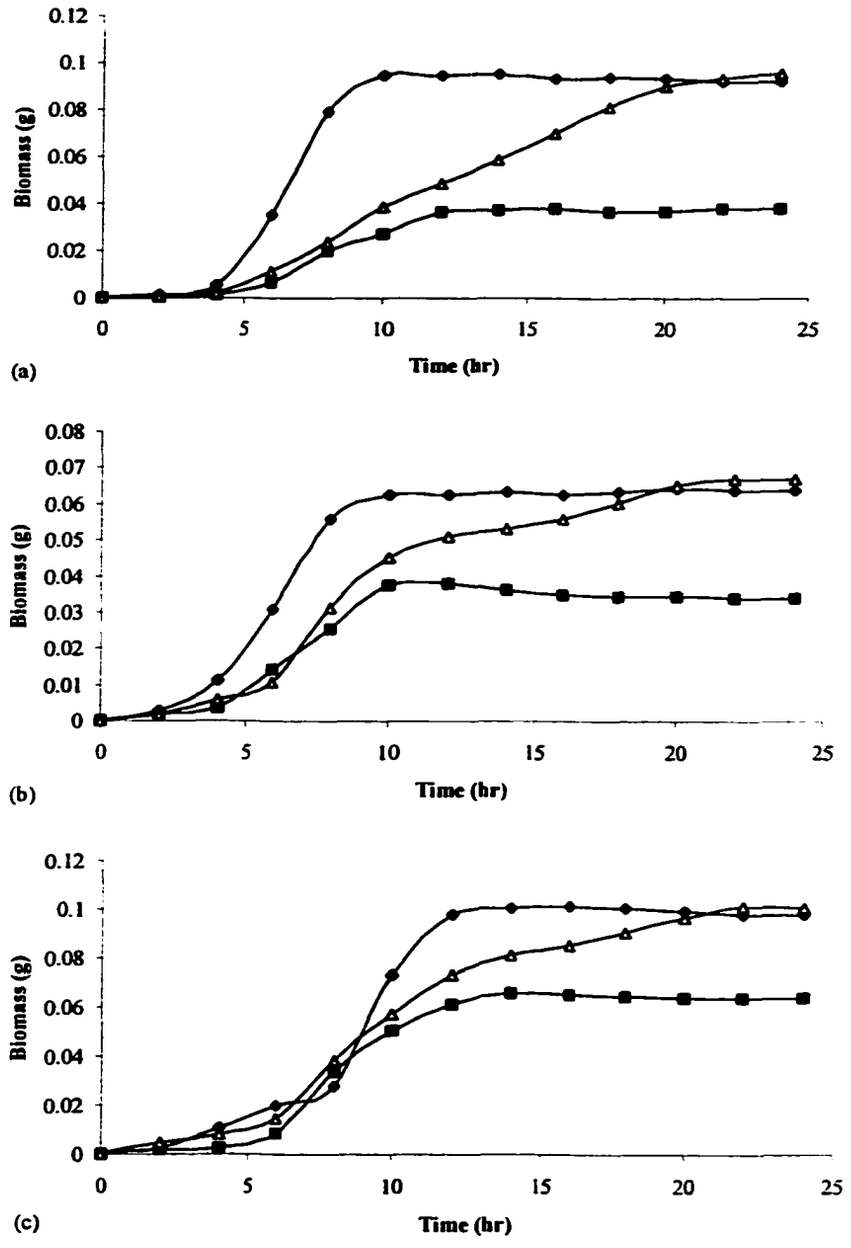


**Figure 3.2** *E. coli* growth under different carbon and nitrogen conditions with (a) glucose, (b) lactate, and (c) propionate serving as the carbon source and nitrate serving as the nitrogen source ◆ no carbon or nitrogen limitation, ■ nitrogen limited, Δ carbon limited.

growth rate $\mu$ (0.67 and 0.44 $hr^{-1}$ with ammonia and nitrate serving as the nitrogen source respectively) and van der Waals component of surface tension $\gamma^{LW}$ (44.23 and 47.17 mJ $m^{-2}$); propionate had the greatest stoichiometric yield coefficient Y (0.61and 0.49 g biomass per g substrate), lipopolysaccharide production efficiency $Y_p$ (0.161and 0.149 g per g biomass) and electron-donor parameter of Lewis acid/base component of surface tension, $\gamma^-$ (61.62 and 57.91 mJ $m^{-2}$). For the same carbon source, ammonia yielded greater $\mu$, Y, $Y_p$ and $\gamma^-$ for *E. coli*; while nitrate yielded greater $\gamma^{LW}$. For example, when glucose served as the carbon source, *E. coli* had a $\mu$ of 0.67 $hr^{-1}$, a Y of 0.52 g biomass per g substrate, a $Y_p$ of 0.157 g per g biomass, and a $\gamma^-$ of 53.16 mJ $m^{-2}$ with ammonia serving as the nitrogen source; while 0.44 $hr^{-1}$, 0.46 g biomass per substrate, and 0.132 g per g biomass, respectively with nitrate serving as the nitrogen source.

When carbon was limited, *E. coli* had smaller $\mu$, $Y_p$ and $\gamma^-$, but greater Y and $\gamma^{LW}$ than that when there was no substrate or nutrient limitation. For instance, when carbon was limited, $\mu$, Y, $Y_p$, $\gamma^-$ and $\gamma^{LW}$ of *E. coli* using glucose and ammonia as carbon and nitrogen sources were 0.21 $hr^{-1}$, 0.56 g biomass per g substrate, 0.120 g per g biomass, 50.22 mJ $m^{-2}$, and 45.03 mJ $m^{-2}$, respectively as compared to 0.67 $hr^{-1}$, 0.52 g biomass per g substrate, 0.157 g per g biomass, 53.16 mJ $m^{-2}$, and 44.23 mJ $m^{-2}$ when there was no carbon or nitrogen limitation.

When nitrogen was the limiting factor, *E. coli* had smaller $\mu$ , Y and $\gamma^{LW}$, but greater $Y_p$ and $\gamma^-$. Using glucose and ammonia as carbon and nitrogen sources, $\mu$, Y, $Y_p$, $\gamma^-$ and $\gamma^{LW}$

of *E. coli* were 0.31 $hr^{-1}$, 0.33 g biomass per g substrate, 0.214 g per g biomass, 57.23 mJ $m^{-2}$, and 42.04 mJ $m^{-2}$, respectively when nitrogen was limited; while when there was no carbon or nitrogen limitation, the corresponding values were 0.67 $hr^{-1}$, 0.52 g biomass per g substrate, 0.157 g per g biomass, 53.16 mJ $m^{-2}$, and 44.23 mJ $m^{-2}$.

**Discussion**

Impact of carbon and nitrogen sources on microbial cell growth According to McCarty (1975), and Faust and Hunter (1971), the energy that the bacteria obtain from respiratory oxidation must balance their need to synthesize new cells. Consequently,

$$\varepsilon A \Delta G_r + \Delta G_s = 0 \qquad (3)$$

where ε is the efficiency of energy transfer to or from the energy carrier (e.g., ATP) and McCarty (1975) assumed it to be 0.6; $\Delta G_r$ free energy released per electron equivalent (eeq) (amount of the substrate that releases 1 mole $e^-$ during a specified oxidation reaction) of electron-donor substrate converted for energy (e.g., respiration); $\Delta G_s$ carrier (ATP) energy required to synthesize 1 eeq of cells which includes energy loss incurred in using the energy carrier (e.g., ATP); and A the balance ratio between $\Delta G_r$ and $\Delta G_s$. For heterotrophic growth with ammonia as nitrogen source, A can be estimated by equation (4):

$$A = \frac{\frac{-\Delta G_p}{\varepsilon^m} - \Delta G_c}{\varepsilon \Delta G_r} \qquad (4)$$

where $\Delta G_p$ is the free energy required (or evolved) in conversion of the carbon source to pyruvate (kcal per eeq pyruvate); $\Delta G_c$ ATP energy required to form 1 eeq cells from pyruvate and ammonia which is assumed to be 7.5 kcal by McCarty (1975); m = +1 when

$\Delta G_p > 0$ and m = -1 when $\Delta G_P < 0$. For heterotrophic growth with nitrate as the nitrogen source, as nitrate needs to be converted to ammonia first before it can be used for synthesis, A is estimated by equation (5):

$$A = \frac{\frac{-\Delta G_p}{\varepsilon^m} - \frac{5}{7}\Delta G_c - 0.89}{\varepsilon \Delta G_r} \qquad (5)$$

Stoichiometric yield coefficient Y can be estimated using equation (6) (McCarty, 1975):

$$Y = \frac{\alpha}{\beta(1+A)} \text{ (g biomass formed per g substrate used)} \qquad (6)$$

where $\alpha$ is the mole weight of 1 eeq biomass which equals to 5.65 g for ammonia served as the nitrogen source and 4.04 g for nitrate as the nitrogen source if the biomass has a formula of $C_5H_7O_2N$, and $\beta$ is the mole weight of 1 eeq substrate which equals to 7.50 g, 7.42 g and 5.21g for glucose, lactate and propionate, respectively.

The maximum specific growth rate can be estimated by:

$$\mu_{max} = Yk \qquad (7)$$

where k is the maximum specific utilization rate (g substrate used per g biomass per day) when ignoring decay or maintenance. McCarty (1975) asserted that the rate of electron transfer in energy-yielding reactions (e.g., respiration) was relatively constant (per g biomass per day) varying between 0.5 and 2.0 among many types of microorganisms — including heterotrophs, autotrophs, aerobes, and anaerobes. Based on this assertion, the maximum specific utilization rate is

$$k = \frac{\beta(0.5 \sim 2.0)(1+A)}{A} \qquad (8)$$

Half reactions of the oxidation of glucose, lactate and propionate as well as the biomass cells, including the half reaction free energy values, are listed in Table 3.3. The theoretically estimated stoichiometric yield coefficient Y, which was obtained based on the assumption that the ATP energy required to form 1 eeq cells from pyruvate and ammonia is always 7.5 kcal regardless of the carbon to nitrogen ratio in the cells (McCarty, 1975), as well as the maximum specific growth rate $\mu_m$ values are also included in Table 3.3.

When there is no carbon or nitrogen limitation, *E. coli* should grow at the maximum specific growth rate. Similarly, based on the theoretical half reaction free energy values, propionate should have the greatest Y values, followed by glucose and lactate; glucose has the biggest $\mu_{max}$ values, followed by lactate and propionate for either ammonia or nitrate serving as the nitrogen source. According to equation (4) and (5), nitrate results in smaller A values than that of ammonia. As the $\alpha$ plays a more important role in determining Y and $\mu_{max}$ than A, nitrate yields smaller Y and $\mu_{max}$ values because *E. coli* has a smaller $\alpha$ value (4.04 g) with nitrate serving as nitrogen source than that of ammonia (5.65 g). The experimental results were consistent with these predictions.

Theoretically, propionate, glucose and lactate should have a Y value of 0.64, 0.54 and 0.49 g biomass per g substrate, and a $\mu_{max}$ value of 0.17 ~ 0.67, 0.31 ~ 1.24 and 0.22 ~ 0.87 $hr^{-1}$ respectively under the condition that ammonia serves as the nitrogen source and

**Table 3.3 Summary of the free energy values of the half reactions and theoretically calculated growth parameters**

| Reactions for Electron Donors | $\Delta G^0(w)$ kcal $eeq^{-1}$ |
|---|---|
| Glucose:<br>$1/24\ C_6H_{12}O_6 + 1/4\ H_2O = 1/4\ CO_2 + H^+ + e^-$ | -10.0 |
| Lactate:<br>$1/12\ CH_3CHOHCOO^- + 1/3\ H_2O = 1/6\ CO_2 + 1/12\ HCO_3^- + H^+ + e^-$ | -7.87 |
| Propionate:<br>$1/14\ CH_3CH_2COO^- + 5/14\ H_2O = 1/7\ CO_2 + 1/14\ HCO_3^- + H^+ + e^-$ | -6.66 |
| Pyruvate:<br>$1/10\ CH_3COCOO^- + 2/5\ H_2O = 1/5\ CO_2 + 1/10\ HCO_3^- + H^+ + e^-$ | -8.84 |

| | Ammonia as nitrogen source | | Nitrate as nitrogen source | |
|---|---|---|---|---|
| | Y (g biomass per g substrate) | $\mu_{max}$ ($hr^-$) | Y (g biomass per g substrate) | $\mu_{max}$ ($hr^-$) |
| Glucose | 0.54 | 0.31 ~ 1.24 | 0.41 | 0.27 ~ 1.09 |
| Lactate | 0.49 | 0.22 ~ 0.87 | 0.37 | 0.18 ~ 0.73 |
| Propionate | 0.64 | 0.17 ~ 0.67 | 0.48 | 0.13 ~ 0.54 |

no carbon or nitrogen limitation. The experimental results are either significantly close to the theoretical prediction (0.61, 0.52 and 0.44 g biomass per g substrate of Y) or within the theoretically predicted range (0.30, 0.67 and 0.50 $hr^{-1}$ of $\mu_{max}$). Similar observation was made for nitrate serving as the nitrogen source (0.49, 0.46 and 0.32 g biomass per g substrate of Y, and 0.28, 0.44 and 0.33 $hr^{-1}$ of $\mu_{max}$ as compared to theoretically calculated 0.48, 0.41 and 0.37 g biomass per g substrate of Y, and 0.13 ~ 0.54, 0.27 ~ 1.09 and 0.18 ~ 0.73 $hr^{-1}$).

When carbon or nitrogen is limited, the *E. coli* specific growth rate will be lower than that of $\mu_{max}$ according to the Monod equation. In the excess of nitrogen, carbon is completely used up, which results in higher Y values than that of no carbon or nitrogen limitation because Y is based on carbon consumption. So at the expense of excess nitrogen, carbon can be used more efficiently. Conversely, in the excess of carbon, nitrogen is used more efficiently, which results in smaller Y values as compared to that of no carbon or nitrogen limitation. As observed in the experiment, glucose grown cultures (with ammonia serving as the nitrogen source) had a Y value of 0.56 g biomass per g substrate under nitrogen limitation and 0.33 g biomass per g substrate under carbon limitation as compared to 0.52 g biomass per g substrate with no carbon or nitrogen limitation.

*Lipopolysaccharide production* Nikaido and Yaara (1985) showed that the outer surface of the membrane in *E. coli* was largely occupied by lipopolysaccharide, while phospholipid made up the inner leaflet. Sutherland and Wilkinson (1965) declared that

different *E. coli* species had the same lipopolysaccharide composition, which was 31.2% ~ 32.8% fucose, 16.3% ~ 19.6% glucose, 25.4% ~ 33.0% glucuronic acid, 0 ~ 9% nitrogen and 0 ~ 3% phosphorus. As in a bacterium, wall material is shed by turnover, the total amount of lipopolysaccharides present is the sum of those present in the cells and those present in the medium. According to Pooley (1976), and Hancock and Poxton (1988), the rate constants for lipopolysaccharide synthesis in the cells and in the medium have a fixed a ratio. In this research, the cell-bounded lipopolysaccharide production efficiency $Y_p$ was chosen as the parameter in describing lipopolysaccharide formation.

$Y_p$ is determined by Y but it is also impacted by the carbon source. Taking into consideration of the energy requirement for the conversion of carbon from pyruvate to lipopolysaccharide components of glucose, fucose and glucuronic acid, etc., $Y_p$ should be proportional to Y (Hancock and Poxton, 1988):

$$Y_p = \frac{\delta}{1+B} Y \qquad (8)$$

where $\delta$ is weight ratio of lipopolysaccharide to the cell; B amount of eeq carbon needed for energy to convert 1 eeq carbon from pyruvate to lipopolysaccharide components. B usually is small and can be neglected. For example, the B value for lactate (to form glucose) is 0.18. Therefore, when there is no carbon or nitrogen limitation, $Y_p$ should follow the same trend as Y, e.g., propionate has the greatest $Y_p$ followed by glucose and lactate either with ammonia or nitrate serving as the nitrogen source, and ammonia yields greater $Y_p$ for *E. coli* than nitrate.

The synthesis of lipopolysaccharides incorporates little nitrogen but increased carbon requirement (Hancock and Poxton, 1988). Therefore, when nitrogen is limited and excess carbon is available, cell synthesis will be limited by nitrogen limitation and the energy produced from the oxidation of excess carbon will go to lipopolysaccharide synthesis. Therefore, when nitrogen is limited, more lipopolysaccharides will be produced and *E. coli* will have a greater $Y_p$, which will result in a higher carbon to nitrogen ratio in the cells. On the contrary, when carbon is limited, less lipopolysaccharides will be produced. *E. coli* will have a smaller $Y_p$ and a smaller carbon to nitrogen ratio in the cells. This assumption is consistent with the observations by Goldman and Mark (2000). Goldman and Mark (2000) found that the carbon to nitrogen ratio in the bacteria varied from ~ 4.5 : 1 (by atoms) when carbon limited the growth to ~ 8 : 1 when nitrogen limited the growth. Also, in this research, *E. coli* was found to have a greater $Y_p$ with excess of carbon. For instance, glucose, Lactate, and propionate had a $Y_p$ of 0.214, 0.196, and 0.224 g per g biomass respectively when nitrogen was limited (with ammonia serving as the nitrogen source); while the corresponding $Y_p$ values were 0.157, 0.150, and 0.161 g per g biomass when there was no carbon or nitrogen limitation and 0.120, 0.117, and 0.124 g per g biomass when carbon was limited.

*Surface thermodynamics* The *E. coli* hydrophilicity was evaluated using the total free energies of the interactions, $\Delta G_{131}^{TOT}$ between the cells,1, immersed in water, 3, based on equations (9) to (11) (van Oss, 1994):

$$\Delta G_{131}^{TOT} = \Delta G_{131}^{LW} + \Delta G_{131}^{AB} \quad (9)$$

$$\Delta G_{131}^{LW} = -2(\sqrt{\gamma_3^{LW}} - \sqrt{\gamma_1^{LW}})^2 \quad (10)$$

$$\Delta G_{131}^{AB} = -4(\sqrt{\gamma_1^+} - \sqrt{\gamma_3^+})(\sqrt{\gamma_1^-} - \sqrt{\gamma_3^-}) \quad (11)$$

where $\Delta G_{131}{}^{LW}$ is the free energy of the van der Waals interactions between the cells (mJ $m^{-2}$) and $\Delta G_{131}{}^{AB}$ the free energy of the Lewis acid/base interactions between the cells (mJ $m^{-2}$) in water. The interactions between the *E. coli* cells were assumed as a semi-infinite flat parallel slabs configuration and were evaluated at the distance of closest approach (assumed to be 1.57 Å by van Oss, 1994) where physical "contact" can occur. At this distance, the electrostatic interactions can be neglected compared with Lifshitz-van deer Waals and Lewis acid/base interactions (Loosdrecht *et al.*, 1989). Based on van Oss (1994), a bacterial surface is classified hydrophilic when $\Delta G_{131}{}^{TOT}$ is greater than zero and the hydrophilicity increases with the increase of the $\Delta G_{131}{}^{TOT}$ value. *E. coli* cultured under all the medium formations had positive $\Delta G_{131}{}^{TOT}$ values (Table 3.2), therefore, *E. coli* exhibited a hydrophilic surface. According to the $\Delta G_{131}{}^{TOT}$ values, propionate yielded the most hydrophilic surface for *E. coli*, followed by lactate and glucose; and ammonia yielded a more hydrophilic surface than nitrate. Also, *E. coli* had a more hydrophilic surface when nitrogen was limited, and a less hydrophilic surface when carbon was limited than that of no carbon or nitrogen limitation.

According to van Oss (1994), Gram-negative bacterial surface thermodynamics is mainly determined by the outer surface of the bacterial membrane. As the outer surface of the

membrane in *E. coli* is largely occupied by lipopolysaccharides (Nikaido and Yaara, 1985), lipopolysaccharides play an important role in determining *E. coli*'s surface thermodynamics. Nikaidoand Yaara (1985) have also declared that one of the important functions of the outer membrane is to endow the bacterial surface with strong hydrophilicity, which is the result of lipopolysaccharides, the characteristic component of the outer membrane. Therefore, $\Delta G_{131}^{TOT}$ should be related to lipopolysaccharide production. As shown in Table 3.2, high $\Delta G_{131}^{TOT}$ values corresponded to high lipopolysaccharide production efficiency values.

**Conclusion**

Recent interest in predicting the fate and transport of bacteria in the subsurface area has drawn more and more attention by either a concern that microbes can contaminate drinking water supplies or their role in bioremediation (Fontes *et al.*, 1991). The fate and transport of bacteria in the subsurface area are determined by their interactions with the medium matrix, which are impacted by the bacterial surface thermodynamics. Altering carbon and nitrogen conditions of the bacterial growth can thus control the fate and transport of bacteria in the subsurface. The impact of C/N ratio on *E. coli* growth and surface thermodynamics was investigated in this research and a quantitative correlation between C/N conditions and microbial growth and surface thermodynamics was established, which is of significant importance for the field application of bioremediation. Under nitrogen excess and carbon limited environments, bacteria exhibit a more hydrophilic surface that will enhance the bacterial transport. Conversely, under carbon

excess and nitrogen limited environments, bacteria exhibit a less hydrophilic surface that retards their transport.

**Acknowledgements**

The work was support in part by National Science Foundation through Grant No. BES-9733969 to the University of Oklahoma.

**References**

1. Ellwood, D.C. and Tempest, D.W. (1972) Effects of Environment on Bacterial Wall Content and Composition. *Adv. Microb. Physiol.*, 7:43-47.

2. Faust, S.D. and Hunter, J.V. (1971) *Organic Compounds in Aquetic Environment*, Marcel Dekker, Inc., New York.

3. Fontes, D.E., Mills, A.L., Hornberger, G.M. and Herman, J.S. (1991) Physical and Chemical Factors Influencing Transport of Microorganisms through Porous Media, *Appl. Environ. Microbiol.*, 57:2473-2481.

4. Goldman, J.C. and Mark, R.D. (2000) Growth of Marine Bacteria in Batch and Continuous Culture under Carbon and Nitrogen Limitation, *Limn. Ocean.*, 45: 789-801.

5. Grasso, D., Smets, B. F., Strevett, K. A., Machinist, B. D., van Oss, C. J., Giese, R. F. and Wu, W. (1996) Impact of Physiological State on Surface Thermodynamics and Adhesion of Pseudomonas aeruginosa, *Environ. Sci. Technol.*, 30:3604-3608.

6. Hancock, I. and Poxton, I. (1988) *Bacterial Cell Surface Techniques*, John Wiley & Sons, New York.

7. Loosdrecht, M.C.M., Lyklema, J., Norde, W. and Zehnder, A.J.B. (1989) Bacterial Adhesion: a Physicochemical Approach, *Microb. Ecol.*, 17:1-15.

8. McCarty, P.L. (1975) Stoichiometry of Biological Reactions, *Progr. Water Technol.*, 7: 157-172.

9. McEldowney, S. and Fletcher, M. (1986) Effect of Growth Conditions and Surface Characteristics of Aquatic Bacteria on Their Attachment to Solid Surfaces, *J. Gen. Microbiol.* , 132:513-523.

10. Monod, J. (1949) The Growth of Bacterial Cultures, *Ann. Rev. Microbiol.*, 3: 371-394.

10. Nikaido, H. and Yaara, M. (1985) The Molecular Basis of Bacterial Outer Membraane Permeability, *Microbiol. Rev.* 49:1-32.

11. Pooley, H.M. (1976) Turnover and Spreading of Old Wall during Surface Growth of Bacillus subtilis, *J. Bacteriol.* 125:1127-1138.

12. Quagliano, J.C. and Miyazaki, S.S. (1997) Effect of Aeration and Carbon/Nitrogen Ratio on the Molecular Mass of the Biodegradation Polymer Poly-β-Hydroxybutyrate Obtained from *Azotobacter chroococcum* 6B, *Appl. Microbiol. Biotechnol.* 48:662-664.

13. Sutherland, I.W. and Wilkinson, J.F. (1965) Depolymerase for Bacterial Expolysaccharides Obtained from Phage-Infected bacteria, *J. Gen. Microbiol.*, 39:373-383.

14. Tchobanoglous, G. and Burton, F.L. (1991*) Wastewater Engineering, Treatment, Dispsal, and Reuse*, Third Eddition, Metcalf & Eddy, Inc., New York.

15. van Oss, C.J. (1994) *Interfacial Forces in Aqueous Media*, Marcel Dekker, New York.

# CHAPTER 4

# SURFACE FREE ENERGY RELATIONSHIPS USED TO EVALUATE MICROBIAL TRANSPORT


## Abstract

A microbial transport study of *Escherichia coli*, *Pseudomonas fluorescens*, and *Pseudomonas aeruginosa* through model media of silica gel and alluvial loam from Central Oklahoma Aquifer (COA) demonstrated that the retardation factor and deposition coefficient were related to the free energy of surface interactions between the bacteria and the media at different distances, which were determined by the radius and the surface thermodynamics of the microorganisms and the surface thermodynamics of the media. A combined model that incorporated the Deep-Bed Filtration Model into a simple Convection-Dispersion Model was used in evaluating the microbial transport. The Deposition coefficient, which described irreversible adsorption, was a function of the free energy of the surface interactions at the closest approach (1.57 Å) where Lewis acid/base interactions dominated. However, the retardation factor, which described reversible adsorption of bacterial transport, was a function of the free energy of the surface interactions at the last inflection point where van der Waals interactions dominated (~ 10 μm in this study).



Key words: retardation factor, deposition coefficient, free energy, van der Waals interactions, Lewis acid/base interactions, electrostatic interactions, and microbial transport.

## Introduction

Recent interest in predicting the fate and transport of bacteria in the subsurface area is motivated by either a concern that microbes can contaminate drinking water supplies or their role in bioremediation (Fontes *et al.*, 1991). Two types of models are often used to describe the transport of micro-size particles (colloids or biocolloids) in porous media: the Deep-Bed Filtration Model and the Convection-Dispersion Model (Rajagopalan and Tien, 1976). The Deep-Bed Filtration Model describes a process in which colloidal particles present in the flowing suspension are deposited within the porous media. The deposition of the colloids is considered to be irreversible and no consideration is given to hydrodynamic forces that may remove the particles from the surface and suspend them again in the flowing fluid (Ouyang *et al.*, 1996). The Convection-Dispersion Model describes the movement and spreading of the colloids during transport based on the assumption that given long enough time, all the particles transported can be recovered. Each model has its own parameter for describing the transport. The Deep-Bed Filtration Model utilizes the deposition coefficient, a parameter that describes irreversible adsorption (i.e., deposition) of the colloids on the media; while the Convection-Dispersion Model uses the retardation factor, a parameter that describes reversible adsorption (i.e., retardation) of the colloids when passing through the media.

As both deposition and retardation occur during bacterial transport, the deposition coefficient (Bolster *et al.*, 1998; Powelson and Mills, 1998; Gamerdinger *et al.*, 1994; Hornberger *et al.*, 1992; Harvey and Garabedian, 1991; Gannon *et al.*, 1991; and Elimelech and O'Melia, 1991) and retardation factor (Dohse and Lion, 1994; Bellin and

Rao, 1993; Bürgisser *et al.*, 1993; Jenkins and Lion, 1993; Magee *et al.*, 1991; and Nkedi-Kizza *et al.*, 1987) have been widely used individually in describing the transport of bacteria through porous media. Rijnaarts *et al.* (1996) published the collision efficiency of *P. putida* deposited on PFA of $0.82 \pm 0.03$. Jenkins and Lion (1993) observed the consistency of the retardation factor values for the transport of the bacterial strains through the porous media, which was obtained using the first temporal moment of the breakthrough curves (BTCs). It has been demonstrated that a combination of both parameters is required to accurately describe microbial transport in porous media (Rijnaarts *et al.*, 1996). Using a combined model that incorporated the Deep-Bed Filtration Model into a simple Convection-Dispersion Model, Harvey and Garabedian (1991) observed a good fit of model simulations to BTCs for concentrations of both bromide and bacteria in effluent from sand columns. Though the retardation factor and deposition coefficient can describe the bacterial transport, a mechanistic understanding of these two parameters (viz., the driving forces, the impact of the radius of the colloids and the media, etc.) has not been precisely explained, which is essential in developing a predictive model.

One of the primary processes affecting microbial transport is the propensity of cells to adhere to surfaces of porous media, which determines the microbial fate in porous media and groundwater (Smets *et al.*, 1999 and Karickhoff *et al.*, 1979). Theoretically, both deposition and retardation should be related to bacterial adhesion, which is due to the interfacial forces between the bacteria and the media. Winget *et al.* (2000) demonstrated that the partition coefficient was related to the difference between the standard-state free

energies of transfer of the solute into the two phases. Goss and Schwarzenbach (2001) recently also published their discovery of the relationship between the equilibrium portioning constant and the surface interaction free energy. Chen and Strevett (2001) illustrated that bacterial deposition on the porous media was related to the surface free energy of the interactions between the bacteria and the media at the closest approach. Based on van Oss' theory (1994), the bacteria-media interactions that should be considered in aqueous media are: apolar, or Lifshitz-van der Waals (LW) interactions; polar, electron-donor/electron-acceptor interactions, or Lewis acid-base (AB) interactions; and electrostatic (EL) interactions. Deposition of the bacteria on the media and retardation of the bacteria by the media are determined by these interactions.

The objective of this study was to relate deposition and retardation to surface interactions between the bacteria and the media. Specifically, (1) to verify that the deposition of the bacteria on the media is determined by the free energy of the surface interactions at the closest approach where Lewis acid/base interactions dominate and the retardation of the bacteria by the media is by the free energy of the surface interactions at the last point of inflection where van der Waals interactions dominate, and (2) to relate these interfacial forces obtained, based on independently determined surface thermodynamic properties of the bacteria and the media, to the experimental observations.

**Model Development**

Harvey and Garabedian (1991) incorporated the colloid filtration model into a simple transport model to explain the movement, losses and retardation due to adsorption and

spreading of bacteria in porous media. A one-dimensional equation for the transport of bacteria, which contains terms for storage, reversible and irreversible adsorption, dispersion, and advection can be written as:

$$\theta\frac{\partial C}{\partial t}+(1-\theta)\rho_b\frac{\partial S}{\partial t}=D\theta\frac{\partial^2 C}{\partial x^2}-v\theta\frac{\partial C}{\partial x}-\theta k_c C \qquad (1)$$

where $\theta$ is the porosity ($m^3/m^3$); C the concentration of bacteria in solution (number of cells/$m^3$); t the elapsed time from the initial injection of bacteria (sec); $\rho_b$ the sediment bulk density ($g/m^3$); S the concentration of reversibly adsorbed bacteria on the porous media (cells/g); D the hydrodynamic dispersion coefficient ($m^2$/sec); v the interstitial pore water velocity (m/sec); x the longitudinal coordinate (m); and $k_c$ the deposition coefficient that indicates the rate of irreversible adsorption of bacteria on the porous media($sec^{-1}$).

If reversible adsorption of bacteria onto the porous media is justified to behave according to a linear isotherm, and the adsorption is rapid with respect to advection, the time variation of bacteria on the solid and in solution can be modeled as (Knox *et al.*, 1993):

$$\frac{\partial S}{\partial t}=\frac{\partial S}{\partial C}\frac{\partial C}{\partial t}=\left[\frac{k_s}{k_d}\frac{\theta}{\rho_b(1-\theta)}\right]\frac{\partial C}{\partial t}=K_p\frac{\partial C}{\partial t} \qquad (2)$$

where $k_s$ is the first order adsorption rate constant ($sec^{-1}$); $k_d$ first order desorption rate constant ($sec^{-1}$); and $K_p$ the linear equilibrium distribution coefficient of the microorganisms between the aqueous phase and the porous medium ($m^3/g$).

By substituting equation (2) into equation (1), the one-dimension transport can be expressed as:

$$[1+\frac{\rho_b(1-\theta)}{\theta}K_p]\frac{\partial C}{\partial t}=D\frac{\partial^2 C}{\partial x^2}-v\frac{\partial C}{\partial x}-k_c C \tag{3}$$

where $[1+\rho_d\cdot(1-\theta)\cdot K_p/\theta]$ is defined as retardation factor (R), which is the average transport velocity of bacteria ($v_{av}$) relative to that of water ($v_w$), or $R = v_w/v_{av}$. By dividing equation (3) by R,

$$\frac{\partial C}{\partial t}=D^*\frac{\partial^2 C}{\partial x^2}-v^*\frac{\partial C}{\partial x}-k_c^* C \tag{4}$$

where $D^* = D/R$ is referred to as the effective hydrodynamic dispersion coefficient; $v^* = v/R$ the effective interstitial velocity; and $k_c^* = k_c/R$ the effective deposition coefficient. Therefore, the retardation factor is an indicator of the "lag" of the bacterial transport due to reversible adsorption. As the retardation factor is calculated based on the relative velocity of bacteria to that of water, which is obtained based on the assumption that local equilibrium (equation (2)) is reached, for a pulse input in a column experiment, the retardation factor can be estimated using the first temporal moment of the bacterial BTCs, i.e. (Dohse and Lion, 1994):

$$R=\frac{\int_0^\infty \frac{C}{C_0}\vartheta d\vartheta}{\int_0^\infty \frac{C}{C_0}d\vartheta}-\frac{\vartheta_p}{2} \tag{5}$$

where $\vartheta$ is the pore volume; and $\vartheta_p$ the pulse width or pulse duration in pore volumes as defined by Dohse and Lion (1994) which equals to 0.13 in this study.

The deposition coefficient describes the deposition of bacteria on the media during transport. As the deposition of the bacteria refers to the portion that cannot be recovered in the effluent, it reflects the irreversible adsorption during transport. According to Unice and Logan (2000), dispersion can be neglected in calculating particle collision efficiencies in both laboratory and field experiments. The deposition coefficient can be described by the colloid filtration model that is used to explain the removal of colloidal-sized materials during filtration in packed-bed systems (Harvey and Garabedian, 1991):

$$k_c = \frac{3}{2}\frac{(1-\theta)}{d_g}\alpha\eta v \tag{6}$$

where $d_g$ is the diameter of the porous medium grain (m); $\alpha$ the collision efficiency; and $\eta$ the single-collector efficiency. Disregarding the effects of gravitational forces in deposition (an assumption that should be true for bacterial cells because the density of the cells is close to that of water) and also disregarding the effects of straining (an assumption that should also be valid because the bacterial cells are so much smaller than the medium grain, Rijnaarts *et al.*, 1996), $\eta$ is given by (Tien *et al.*, 1979):

$$\eta = 4A_s^{(1/3)}N_{Pe}^{(-2/3)} \tag{7}$$

where

$$A_s = 2(1-p^5)/(2-3p+3p^5-2p^6) \tag{8}$$

$$N_{Pe} = 3\pi\mu d_p d_g v/(kT) \tag{9}$$

Here $p=(1-\theta)^{1/3}$; $\mu$ fluid viscosity ($1.002 \times 10^{-3}$ N· s/m$^2$ for water at 20°C); $d_p$ bacterial diameter (m); k the Boltzmann constant ($1.38048 \times 10^{-23}$ J/K); and T absolute temperature (K).

The deposition coefficient can be calculated based on equation (10) where the negligible dispersion is also taken into consideration (Bolster *et al.*, 1998):

$$k_c = \frac{v}{L}\{-Ln(fr) + \frac{[Ln(fr)]^2}{Pe}\} \tag{10}$$

where L is the length between the injection and where the bacteria are collected (m); *fr* bacterial fraction recovery; *Pe* Peclet number, which can be determined by studying the BTCs from a conservative tracer based on the following equation (Annable *et al.*, 1997 and Jin *et al.*, 1995):

$$\sigma^2 = \tau^2 \cdot [\frac{2}{Pe} - \frac{2}{Pe^2} \cdot (1 - e^{-Pe})] \tag{11}$$

where $\sigma$ is the standard deviation and $\tau$ the measured average residence time for the tracer in the reactor (sec), determined by:

$$\tau = \frac{\int_0^\infty t \cdot C(t)dt}{\int_0^\infty C(t)dt} \tag{12}$$

$$\sigma^2 = \frac{\int_0^\infty C(t)(t-\tau)^2 dt}{\int_0^\infty C(t)dt} = \frac{\int_0^\infty \tau^2 \cdot C(t)dt}{\int_0^\infty C(t)dt} - \tau^2 \tag{13}$$

In equations (12) and (13), C is the measured concentration of the tracer at the outlet of the column ($g/m^3$) and t the elapsed time from the initial injection of the tracer (sec).

In equation (6), the level of $\alpha$ is controlled by cell-solid interactions and by the amount of previously attached bacteria (Rijnaarts *et al.*, 1996). For this study, as the mean grain diameter of the media was three orders in magnitude greater than that of the bacteria and

the ratio of the bacteria to the medium grains was in the range of 1 to 10, the fractional surface coverage of the bacteria on the media was very small. The blocking function was thus minimal (Johnson and Elimelech, 1995) and straining was excluded (Rijnaarts *et al.*, 1996). Therefore, $\alpha$ is solely determined by cell-solid interactions and can be calculated by:

$$\alpha = \frac{2d_g[-Ln(fr) + \frac{Ln^2(fr)}{Pe}]}{3(1-\theta)\eta L} \tag{14}$$

**Materials**

The bacteria selected for this study included *Escherichia coli, Pseudomonas fluorescens,* and *P. aeruginosa*, which are typical representatives of rod-shaped bacteria *Enterobacteriaceae* and *Pseudomonadaceas*. The *E. coli* strain used in this research was JM109, a gift from the Department of Botany and Microbiology at the University of Oklahoma. It was cultured on Nutrient Broth (Difco 0003) at 37°C. *P. fluorescens* (P-17) and *P. aeruginosa* were obtained from ATCC (Catalog No. 17559 and 15152) and grown on Nutrient Broth (Difco 0003) at 26°C and 30°C, respectively. The physiological states of the bacteria were quantified through a biochemical assay using Adenosine Triphosphate (ATP) analysis (Turner Design, Sunnyvale, CA). After inoculation, the cultures were placed on the Gyrotory Water Bath Shaker (Model G76, New Brunswick Scientific Co. Inc., Edison, NJ) at 150 RPM. 50 µl of cultures were sampled for light emission at a time interval of 30 minutes. The light emission produced by the reaction of ATP extracted from cells with luciferase as measured by a luminometer (TD-20/20,

Turner Design, Sunnyvale, CA) was compared to an ATP standard ($2.5 \times 10^{-8}$ g/ml ATP which is equivalent to $5 \times 10^{7}$ bacteria per ml) (10 μg/ml ATP in HEPES buffer, Turner Design, Sunnyvale, CA) to determine the number of viable bacterial cells. Thus, the number of viable bacterial cells versus time curves were obtained, which were used as the reference for the determination of stationary state for different bacterial strains. For column experiments, bacterial solutions collected in the stationary phase of growth (predetermined by ATP assay) were centrifuged at 2500 RPM (Damon/IEC Divison, Needham Heights, MA) and washed twice with sterilized nano-pure deionized water (NPDI) before they were resuspended in the sterilized NPDI to make a bacterial solution. After this process, exopolysaccharide (if any) was stripped off the bacteria (Hancock and Poxton, 1988). During the transport process, the growth of the bacteria was assumed to be minimal due to the lack of substrate or nutrient. Therefore, the bacterial surface property should remain unchanged during the transport and could be described by their surface thermodynamics. The concentration of the solution was measured by ATP analysis (around $5 \times 10^{7}$ cell/ml).

Porous media used for this research included silica gel from Fisher Scientific (Lot No. 995627, 100 mesh) and alluvial loam from the Central Oklahoma Aquifer (COA) (Norman, Oklahoma). The median grain radius of silica gel was assumed to be 100 μm according to U.S. standard sieve sizes and their corresponding open dimension (Holtz and Kovacs, 1981). Before being packed in the column, it was sterilized at 121°C for 20 min. The median grain radius size of COA was 65 μm with 38% passing a 200 sieve. The organic fraction and hydraulic conductivity were reported to be $0.340 \pm 0.20$ and ($8.2 \pm$

1.3) × $10^{-5}$ cm/s (Karapanagioti et al., 1999). Due to concerns about structural and chemical alterations, COA was not sterilized. Instead, it was air dried and stored desiccated to minimize the presence of an active bacterial population.

**Experiment Protocol**

The surface free energies of the media, silica gel and COA, were studied using the wicking method (Wålinder and Gardner, 1999 and Ku *et al.*, 1985). As capillary rise velocity measurements of a liquid in the column can also yield the contact angle of the liquid with respect to the particles' surface, this method determined the contact angle ($\cos\beta$) by measuring the velocity of capillary rise through a porous layer based on the Washburn equation:

$$h^2 = (R_e \cdot t \cdot \gamma_L \cdot \cos\beta) \cdot (2 \cdot \mu)^{-1} \qquad (15)$$

where h is the height (m) of capillary rise of the wicking liquid at time t (sec); $\gamma_L$ the total surface tension of the wicking liquid (mJ/m$^2$); $\mu$ the viscosity of the liquid (N·s/m$^2$) and $R_e$ the average interstitial pore size (m). By using a liquid with low surface tension, such as methanol ($\gamma$ = 22.5 mJ/m$^2$) or hexane ($\gamma$ = 18.4 mJ/m$^2$), the average interstitial pore size $R_e$ can be obtained from equation (15) since methanol or hexane is expected to spread over the solid surface during the wicking measurement resulting in $\cos\beta$=1. Once $R_e$ was determined, an apolar liquid, diiodomethane and two polar liquids, glycerol and water were applied to estimate their respective $\cos\beta$ values. The cosine of contact angle $\beta$ is a measure of the resultant of the energy of cohesion of the liquid and the energy of adhesion between liquid and solid, which can be used to calculate the solid surface thermodynamic properties.

The surface thermodynamic properties of the microorganisms were estimated by contact angle measurements (Contact Angle Meter, Tantec, Schaumburg, IL) following the method described by Grasso *et al.* (1996). Bacterial strains collected in stationary state (as determined by ATP analysis) were vacuum filtered on silver metal membrane filters (0.45 μm, Osmonic, Inc., Livermore, CA) and air-dried for about 30 minutes before the contact angle measurements. The amount of cells on the silver filter was approximately 13 mg to ensure a multi-layer covering of the membrane, and the moisture content was kept in the range of 25% to 30%. Diiodomethane, glycerol and water were used for the contact angle measurements to span a range of polarities.

Each contact angle measurement was repeated 30 times and the surface thermodynamic parameters were estimated by the van Oss-Chaudhury-Good equation (van Oss, 1994) using the average results.

$$(1+\cos\beta)\gamma_L = 2(\sqrt{\gamma_S^{LW}\gamma_L^{LW}} + \sqrt{\gamma_S^+\gamma_L^-} + \sqrt{\gamma_S^-\gamma_L^+}) \qquad (16)$$

where $\gamma_L$ is the surface tension of the liquid that is used for the measurements ($mJ/m^2$) which can be calculated by:

$$\gamma_L = \gamma_L^{LW} + 2\sqrt{\gamma_L^-\gamma_L^+} \qquad (17)$$

Here $\gamma^{LW}$ is the Liftshitz-van der Waals component of surface tension (subscript S for solid and L for liquid) ($mJ/m^2$); $\gamma^+$ the electron-acceptor parameter and $\gamma^-$ the electron-donor parameter of Lewis acid/base component of the surface tension (subscript S for solid and L for liquid) ($mJ/m^2$).

The Lifshitz-van der Waals and Lewis acid-base interactions between the microorganisms 1 and the matrix media 2, immersed in water 3 were then estimated by equation (18) and (19) (Meinders *et al.*, 1995):

$$\Delta G(y)_{132}^{LW} = 2\pi\Delta G_{y_0 132}^{LW}\frac{y_0^2 R}{y} \tag{18}$$

$$\Delta G(y)_{132}^{AB} = 2\pi \mathrm{R} y_0 \Delta G_{y_0 132}^{AB} e^{(y_0 - y)/\lambda} \tag{19}$$

where $\Delta G_{y0132}{}^{LW}$ and $\Delta G_{y0132}{}^{AB}$ are the Gibbs energy of two parallel plates, 1 and 2, immersed in water 3 at a distance of closest approach, $y_0$ (minimum equilibrium distance and assumed to be 1.57 Å by van Oss, 1994), which can be obtained from equations (20) and (21) (Meinders *et al.*, 1995):

$$\Delta G_{y_0\ 132}^{LW} = -2(\sqrt{\gamma_3^{LW}} - \sqrt{\gamma_2^{LW}})(\sqrt{\gamma_3^{LW}} - \sqrt{\gamma_1^{LW}}) \tag{20}$$

$$\Delta G_{y_0\ 132}^{AB} = 2\sqrt{\gamma_3^+}(\sqrt{\gamma_1^-} + \sqrt{\gamma_2^-} - \sqrt{\gamma_3^-}) + 2\sqrt{\gamma_3^-}(\sqrt{\gamma_1^+} + \sqrt{\gamma_2^+} - \sqrt{\gamma_3^+}) - 2\sqrt{\gamma_1^+\gamma_2^-} - 2\sqrt{\gamma_1^-\gamma_2^+} \tag{21}$$

where y is the distance between the microorganisms (sphere) and the matrix (flat plate) measured from the outer edge of the sphere (m); R the radius of the microorganism (m); $\lambda$ the decay length of water, assumed to be 0.6 nm for pure water (van Oss, 1994). In equations (18) and (19), the microorganisms are modeled as a sphere having a radius at least one order of magnitude less than that of the soil matrix. Therefore, a sphere-flat plate interaction is adopted to simplify the interactions between the microorganisms and the matrix.

The electrostatic interactions $\Delta G_{132}^{EL}$ can be evaluated by (constant potential approach) (valid for $\kappa y > 10$, van Oss, 1994):

$$\Delta G(y)_{132}^{EL} = \pi\varepsilon\varepsilon_0 R[2\psi_{01}\psi_{02}Ln(\frac{1+e^{-\kappa y}}{1-e^{-\kappa y}}) + (\psi_{01}^2 + \psi_{02}^2)Ln(1-e^{-2\kappa y})] \quad (22)$$

where $\varepsilon$ and $\varepsilon_0$ are the relative dielectric permittivity of water (78.55 for water at 25°C) and permittivity under vaccum (8.854 x $10^{-12}$ C/V·m) respectively; $1/\kappa$ the Debye-Hückel length and an estimation of the effective thickness of the electrical double layer (Marshall *et al.*, 1984) which equals 100 nm for DI water; $\psi_{01}$, $\psi_{02}$ potentials at the surfaces of the microorganisms and the matrix, which can be calculated based on the following equation (van Oss, 1994):

$$\psi_0 = \zeta(1 + z/a)\exp(\kappa z) \quad (23)$$

where $\zeta$ is the zeta potential measured at the slipping plate; z the distance from the particle surface to the slipping plate that is generally on the order of 5 Å (van Oss, 1994); and a the radius of the particle. $\zeta$-potentials of the bacteria and the media were measured by suspending in a NPDI solution using Lazer Zee Meter (Model 501, Pen Kem, Inc., Bedford Hills, NY).

The transport of three bacterial strains through the porous media was evaluated in column experiments, which were conducted using a column from Kimble-Kontes (Vineland, NJ) with 2.5-cm ID × 15-cm length (Table 4.1). The media used for the column experiments, silica gel and COA were initially saturated with 10 pore volumes of sterilized NPDI, which was introduced at the inlet of the column by a peristaltic pump (Masterflex, Cole-Parmer, Vernon Hills, IL) at a flow rate of 0.03 ml/sec. A conservative pulse tracer

**Table 4.1 Summary of the Parameters Used in Column Experiment**

| Microorganisms | Radius |
|---|---|
| *E. coli* | 0.5 μm |
| *P. fluorescens* | 0.3 μm |
| *P. aeruginosa* | 0.3 μm |

| Porous Media | Radius | Porosity | Density |
|---|---|---|---|
| Silica gel | ~ 100 μm | 0.51 | 2.65 g/cm$^3$ |
| COA | ~ 65 μm | 0.48 | 2.62 g/cm$^3$ |

| Column Experiment | |
|---|---|
| Column | 2.5-cm ID x 15-cm Length |
| Flow Rate | 0.03 ml/sec |
| Pe | 13.9 (silica gel) and 76.4(COA) |
| Pulse Width | 0.133 pore volumes |

(chloride) BTC was determined separately before the introduction of bacteria. The conductivity (μmhos) of the tracer was measured and used in equations (11) to (13) to estimate *Pe*. For each run, 10 ml of bacterial solution (concentration predetermined by ATP analysis) was injected via a syringe using an injection port. The column was continuously flushed with sterilized NPDI until a background ATP signal was detected from the elution collected by a fraction collector. The concentration of ATP was then used to generate BTCs for each bacterium (Figure 4.1). After each run, mass balance was performed. Bacterial contents inside the column were measured by making the media a suspended solution to perform an ATP measurement.

**Results and Discussion**

Each run was done in triplicate, and the inconsistency of BTCs was within 5% (95% CI). A representative BTC for each bacterium is illustrated in Figure 4.1. A fitting of the model

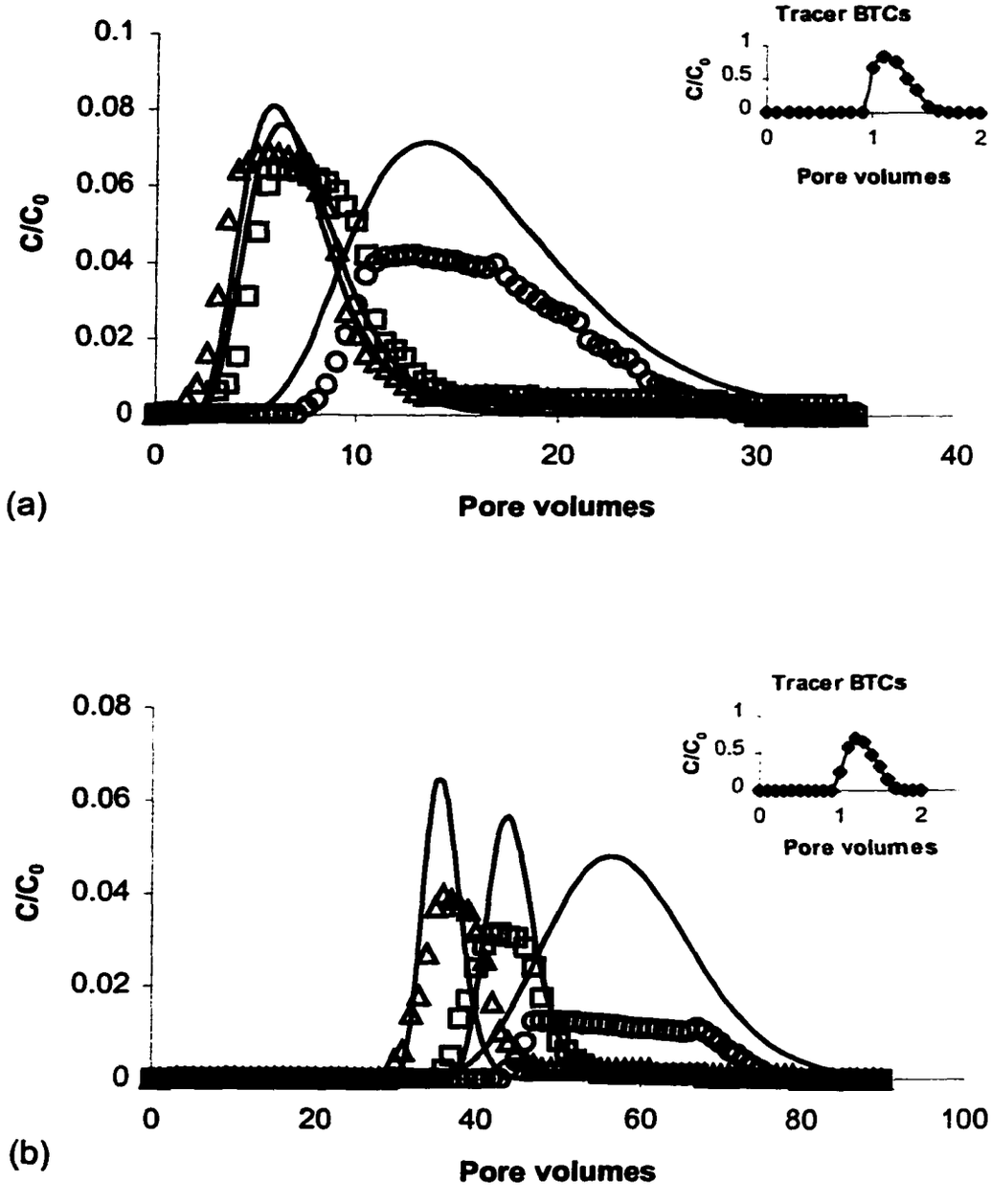


**Figure 4.1** BTCs of the bacteria on (a) silica gel and (b) COA Δ —— *P. fluorescens*; □ —— *P. aeruginosa*; O —— *E. coli*; —— Theoretical simulations

proposed in equation (1) is also shown in Figure 4.1 using the following theoretical solution for equation (1):

$$\frac{C(t)}{C_0} = \frac{V_0}{A[4\pi D^* t]^{1/2}} \exp[-\frac{(x - v^* t)^2}{4D^* t} - k_c^* t] \quad (24)$$

where $V_0$ is the initial injection volume; A the cross-sectional area of flow through the porous media. As bacteria are colloids, not soluble substances, the falling limb of the BTCs was not as significant as soluble compounds. Thus the proposed model fitted the BTCs. The fractional recovery values were obtained by numerically integrating the measured BTCs of the bacteria and then dividing by the input values. Mass balance showed that the loss of the bacteria (not contained in the column or collected in the effluent) was less than 6% (95% CI).

The existence of van der Waals interactions was first postulated by van der Waals as early as 1873 and they are well recognized as a weak force. Van der Waals interactions comprise three different, but closely related phenomena: 1. Randomly orienting dipole-dipole or Keesom interaction; 2. Randomly orienting dipole-induced dipole or Debye interaction; and 3. Fluctuating dipole-induced dipole or London interaction, of which van der Waals-London interaction is of preponderant importance (van Oss, 1994). Electrostatic interactions are also well known due to the fact that very few biological macromolecules or particles (or indeed any inorganic or organic surfaces) are completely devoid of electrical surface charge. Therefore, the traditional DLVO theory (a theory of colloidal stability put forward by Derjaguin, Landau, Verwey and Overbeek) only includes van der Waals and electrostatic interactions. Now the so-called extended DLVO

theory includes Lewis acid-base interactions, a polar interaction that are also called electron-acceptor-electron-donor interactions. These interactions, which are of polar, but not of eletrodynamic (dipole-dipole, dipole-induced dipole, or fluctuating dipole-induced dipole interactions) or electrostatic (electrostatic interactions) origin represent energies that may be up to two decimal orders of magnitude higher than van der Waals and electrostatic interactions. Lewis acid/base interactions between polar moieties in polar media (such as water) are at the origin of virtually all the anomalies that have beset the interpretation of interfacial interactions in polar media (van Oss, 1994).

The total free energy and the free energies of van der Waals, Lewis acid/base and electrostatic interactions between *E. coli* and silica gel were calculated using their surface thermodynamic properties (Table 4.2). The total free energy at a distance smaller than 5 nm was dominated by the free energy of Lewis acid/base interactions, at a distance greater than 5 μm was by the free energy of van der Waals interactions (Figure 4.2). The free energy of electrostatic interactions only existed at a distance between 10 nm to 10 μm. This is easily explained because when the distance between the bacteria and the matrix is smaller than 5 nm, Lewis acid/base interactions show an exponential increase with the decrease of the distance, which result in interactions one order greater in magnitude than those of van der Waals interactions. Electrostatic interactions are neglected at this distance because of the superimposition of the double layers. When the bacteria and the matrix are at a distance greater than 5 μm, Lewis acid/base interactions exhibit a zero value owing to the fact that they are short-range forces, and electrostatic interactions can be neglected because there is little interaction occurring at a distance

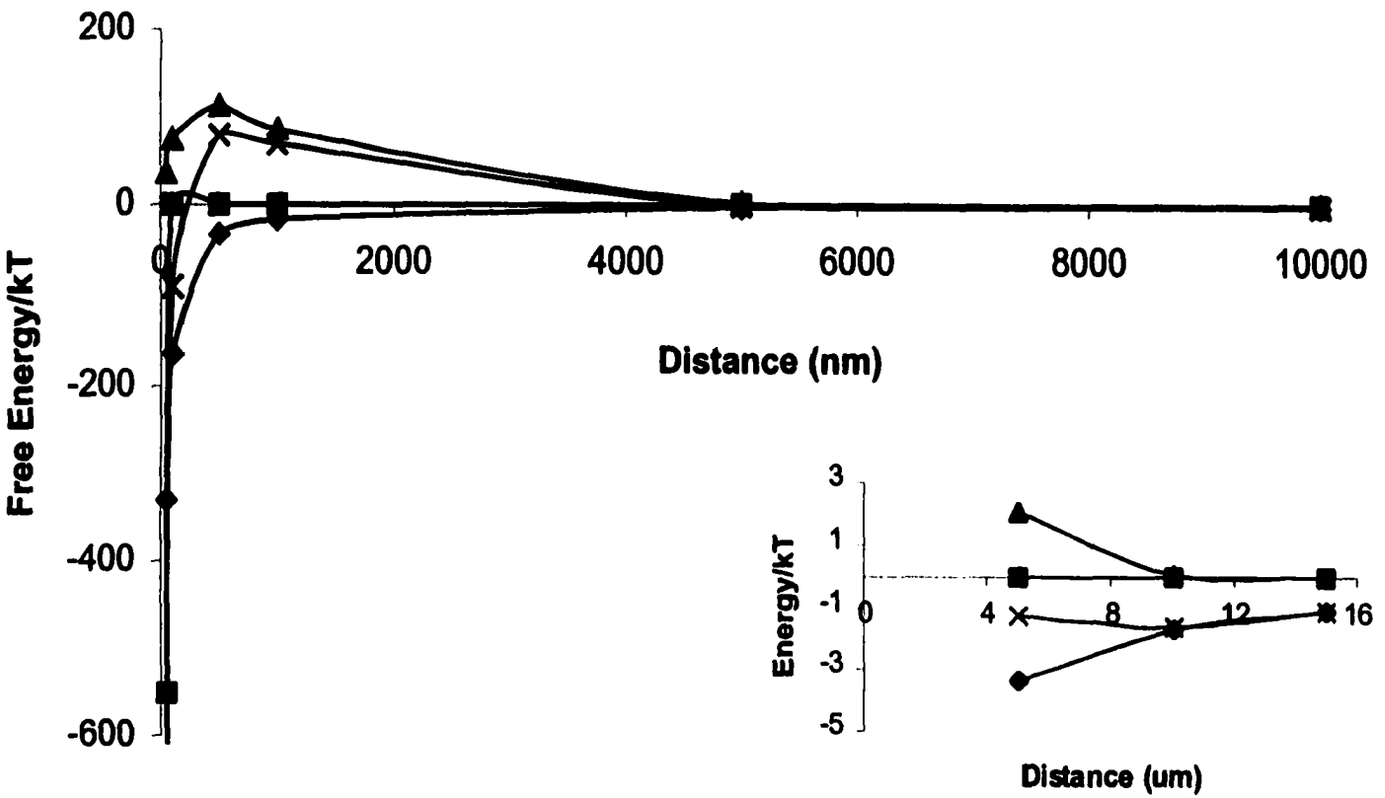


**Figure 4.2** Free energies between *E. coli* and silica gel with respect to distance × Total free energy, ▲ Free energy of electrostatic interactions, ■ Free energy of Lewis acid/base interactions, ◆ Free energy of van der Waals interactions.

**Table 4.2 Surface Thermodynamic Properties of the Microorganisms and the Media**

| Stain | ζ-potential (mV) | $\gamma^{LW}$ (mJ/m$^2$) | $\gamma^+$ (mJ/m$^2$) | $\gamma^-$ (mJ/m$^2$) |
|---|---|---|---|---|
| *E. coli* | -10.6±0.3 | 33.2 | 2.25 | 54.9 |
| ***P. fluorescens*** | -12.4±0.2 | 35.4 | 1.51 | 56.7 |
| *P. aeruginosa* | -14.7±0.4 | 36.5 | 0.96 | 59.2 |

| Porous Medium | ζ-potential (mV) | $\gamma^{LW}$ (mJ/m$^2$) | $\gamma^+$ (mJ/m$^2$) | $\gamma^-$ (mJ/m$^2$) |
|---|---|---|---|---|
| Silica gel | -27.0±0.8 | 25.7 | 0.00 | 11.7 |
| COA | -42.5±0.6 | 27.4 | 0.03 | 13.7 |

much greater than the thickness of the double layer. For the distances in between, electrostatic interactions exist because the distance is in the same range as the thickness of the double layer, which results in strong electrostatic interactions. The last inflection point of the interactions occurred at a distance around 10 μm (Figure 4.2), which also applied to the other microorganisms with the two porous media. Thus 10 μm was chosen as the reference distance for the calculation of van der Waals interactions. The existence of van der Waals interactions at this distance was not unique. Mahanty and Ninham (1976) demonstrated that the decrease of the interaction energy of dispersion forces slowed down at large distances by giving the full numerical methods for calculating retardation. The existence of van der Waals forces for the microorganisms at these distances was due to their unique surface properties (i.e., a much greater $\gamma^{LW}$ value than other colloids). Similar graphs were observed for the free energies versus distance of the interactions between all the three microorganisms studied and the two porous media.

The total free energy of the interactions at a distance smaller than 5 nm and greater than 5 μm was found to be negative, i.e., attractive; while in between was positive, i.e., repulsive. The process of the bacteria passing by a clean medium particle can thus be assumed by five steps: (1) Due to hydrodynamic dispersion or molecular diffusion, the bacteria approach the medium particle within the range of the last inflection point of the interactions between the bacteria and the media, and van der Waals (attractive) interactions begin to behave. (2) When van der Waals interactions balance hydrodynamic dispersion or molecular diffusion at the last interaction inflection point, the bacteria will remain "still" or be adsorbed to the media particle (initial adsorption). (3) This initial adsorption is not stable and the surface shear forces may break the balance as van der Waals interactions are a weak interaction, which results in desorption (Absolom *et al.*, 1983). When the balance is broken, the bacteria either leave the medium particle, or come closer to the medium particle. (4) If the bacteria get closer to the particle, electrostatic (repulsive) interactions begin to behave, and only the bacteria having enough energy to overcome the electrostatic interactions may pass this distance, resulting in enhanced Lewis acid/base (attractive) interactions. (5) The bacteria are dragged onto the surface of the medium particle because the attractive forces (Lewis acid/base interactions) tend to increase dramatically compared to the repulsive forces (electrostatic interactions) with the decrease of the distance, which results in the final deposition. This assumption is consistent with that proposed by Loosdrecht *et al.* (1989). They demonstrated that Gibbs free energy of Lewis acid/base interactions was responsible for irreversible adhesion, and the Gibbs free energy of van der Waals interactions was responsible for reversible adhesion.

*Deposition coefficient*

The deposition coefficient describes irreversible adsorption of the bacteria on the porous media. As discussed previously, with a smaller (negatively greater) free energy value, Lewis acid/base interactions can balance electrostatic interactions at a distance farther away from the closest approach. Therefore, the collision efficiency $\alpha$ and thus deposition coefficient $k_c$ should be a function of the free energy of Lewis acid/base interactions at the closest approach.

Calculations indicated that greater $\alpha$ values corresponded to smaller $\Delta G_{132}^{AB}$ values (Table 4.3). For example, *E. coli* had a $\alpha$ value of 0.222 and a $k_c$ value of 6.07 $hr^{-1}$ on COA that corresponded to a $\Delta G_{132}^{AB}$ value of $-6.63 \times 10^{-15}$ J; while *P. fluorescens* had a $\alpha$ value of 0.114 and a $k_c$ value of 1.87 $hr^{-1}$ on silica gel that corresponded to a $\Delta G_{132}^{AB}$ value of $-3.65 \times 10^{-15}$ J. To eliminate the impact of the sizes from the bacteria and the media on bacterial deposition, the depositions of dimensionally similar strains *P. fluorescens* and *P. aeruginosa* on the same media were compared. *P. aeruginosa* had greater $\alpha$ (0.126 on silica gel and 0.144 on COA) and $k_c$ (2.07 $hr^{-1}$ and 5.54 $hr^{-1}$) values than *P. fluorescens* (0.114 and 0.132, 1.87 $hr^{-1}$ and 5.08 $hr^{-1}$, respectively) with corresponding smaller $\Delta G_{132}^{AB}$ values ($-3.90 \times 10^{-15}$ J on silica gel and $-4.38 \times 10^{-15}$ J on COA) than those of *P. fluorescens* ($-3.65 \times 10^{-15}$ J and $-4.11 \times 10^{-15}$ J). Though the differences of the $\alpha$ values were not significant, they showed the same tendency that

**Table 4.3 The Deposition Coefficient $k_c$ and Collision Efficiency $\alpha$ as a Function of Lewis Acid/Base Free Energy at the Closest Approach $\Delta G_{132}^{AB}$ and Retardation Factor R as a Function of van der Waals Free Energy at the Last Interaction Inflection Point $\Delta G_{132}^{LW}$**

| Strain/Medium | $\Delta G_{132}^{AB}$ ($\times 10^{-15}$ J) | $k_c$ ($hr^{-1}$) | $\alpha$ | | $\Delta G_{132}^{LW}$ ($\times 10^{-21}$ J) | R |
|---|---|---|---|---|---|---|
| *E. coli* / Silica gel | -5.92 | 2.28 ± 0.10 | 0.195 ± 0.009 | | -6.79 | 16.19 |
| *P. fluorescens* / Silica gel | -3.65 | 1.87 ± 0.14 | 0.114 ± 0.008 | | -4.79 | 8.17 |
| *P. aeruginosa* / Silica gel | -3.90 | 2.07 ± 0.08 | 0.126 ± 0.005 | | -5.13 | 10.13 |
| *E. coli* / COA | -6.63 | 6.07 ± 0.11 | 0.222 ± 0.004 | | -9.57 | 61.27 |
| *P. fluorescens* / COA | -4.11 | 5.08 ± 0.04 | 0.132 ± 0.001 | | -6.73 | 15.97 |
| *P. aeruginosa* / COA | -4.38 | 5.54 ± 0.15 | 0.144 ± 0.004 | | -7.21 | 18.15 |

greater $\alpha$ values corresponded to smaller $\Delta G_{132}^{AB}$ values. These differences of the collision efficiency, $\alpha$ and the deposition coefficient, $k_c$ were totally due to the differences of the bacterial surface thermodynamic properties.

For the same strain, COA was found to have greater $\alpha$ values than silica gel. For instance, the $\alpha$ values for *E. coli* on silica gel and COA were 0.195 and 0.222 respectively. The consequential $\Delta G_{132}^{AB}$ values at the closest approach were $-5.92 \times 10^{-15}$ J and $-6.63 \times 10^{-15}$ J respectively. Similar observations were made for *P. fluorescens* and *P. aeruginosa*.

*Retardation factor*

Retardation factor is an indicator of the "lag" of the bacterial transport in the porous media, which describes the reversible adsorption. By definition, it is a function of the distribution coefficient of the microorganisms between the media and the aqueous phase. According to van Oss (1994), the distribution coefficient can be related to the free energy of the interactions between the microorganisms and the media. The free energy of van der Waals interactions at the last inflection point of the interactions is the actual driving force, thus

$$\frac{\Delta G_{132}^{LW}}{kT} = -\phi Ln[\rho_b \frac{(1-\theta)}{\theta} K_p] \qquad (25)$$

where $\phi$ is the correction factor. $\Delta G_{132}^{LW}/kT$ versus $Ln[\rho_b(1-\theta)/\theta K_p]$, which equals $Ln(R+1)$, had a linear relationship with $\Delta G_{132}^{LW}/kT$ (Figure 4.3), indicating that retardation

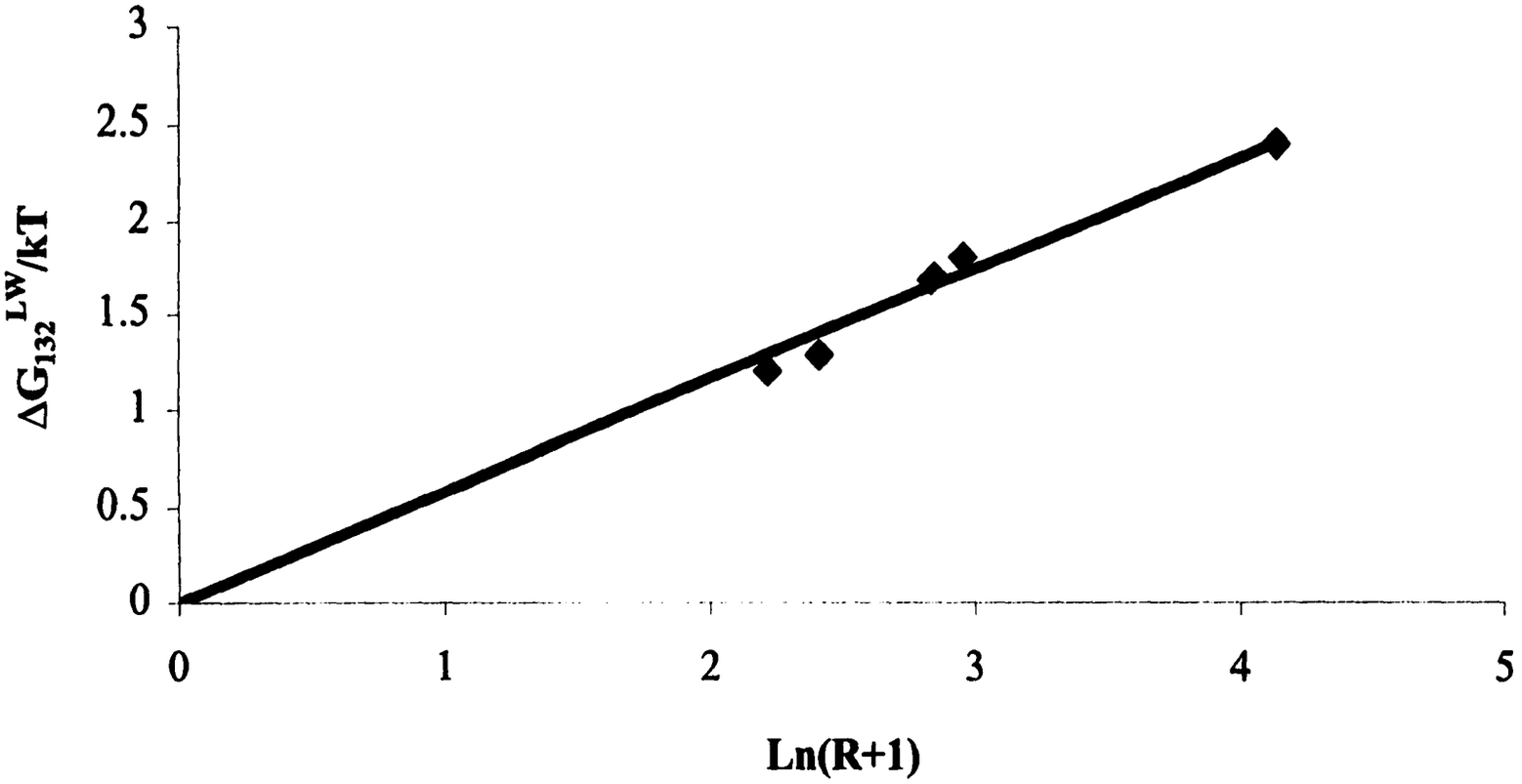


**Figure 4.3** The retardation factor R as a function of the free energy of van der Waals interactions at the last inflection point

factor R is a function of the free energy of van der Waals interactions at the last interaction inflection point.

Study of the BTCs found that on the same media, *E. coli* was retarded most, followed by *P. aeruginosa* and *P. fluorescens*. This result was consistent with the van der Waals interaction free energy $\Delta G_{132}^{LW}$ values at the last interaction inflection point (Table 4.3). For example, $\Delta G_{132}^{LW}$ values at the last interaction inflection point between the bacteria and silica gel were $-6.79 \times 10^{-21}$ J for *E. coli*, $-5.13 \times 10^{-21}$ J for *P. aeruginosa*, and $-4.79 \times 10^{-21}$ J for *P. fluorescens*. According to equation (18) and (20), for the same media, $\Delta G_{132}^{LW}$ at the last interaction inflection point was determined by $\gamma^{LW}$ and the radius of the microorganisms. It seemed that the radius of microorganisms played a more important role than that of $\gamma^{LW}$. This is why, though *P. aeruginosa* (R = 0.3 μm) had a smaller $\Delta G_{yo132}^{LW}$ value (-1.10 mJ/m$^2$) than *E. coli* (-0.88 mJ/m$^2$), its $\Delta G_{132}^{LW}$ value at the last interaction inflection point was greater than that of *E. coli* (R = 0.5 μm). For the same-sized microorganisms, a greater $\gamma^{LW}$ value corresponded to a smaller $\Delta G_{132}^{LW}$ value and thus a greater retardation factor value, which can be seen by comparing *P. aeruginosa* and *P. fluorescens*.

Compared with silica gel, COA showed greater retardation for the same microorganism. The bacteria had a retardation factor value 1.8 to 3.8 times higher passing through COA than silica gel. Further investigation of the media's surface thermodynamics found that COA had a greater $\gamma^{LW}$ value (27.4 mJ/m$^2$) than that of silica gel (25.7 mJ/m$^2$).

According to equation (18) and (20), for the same microorganism, $\Delta G_{132}^{LW}$ at the last interaction inflection point was determined by the $\gamma^{LW}$ values of the media only.

**Acknowledgements**

The work was support in part by National Science Foundation through Grant No. BES-9733969 to the University of Oklahoma.

**References**

1. Absolom, D. R., Lamberti, F. V., Policova, Z., Zingg, W., van Oss, C. J. and Neumann, A. W. (1983) Surface Thermodynamics of Bacterial Adhesion, *Appl. Environ. Microbiol.* 46:90-97.

2. Annable, M. D., Rao, P. S. C., Hatfield, K., Graham, W. D., Wood, A. L., and Enfield, C. G. (1998) Partitioning Tracers for Measuring Residual NAPL: Field-Scale Test Results. *J. Environ. Eng.*, 124: 498-503.

3. Bellin, C. A. and Rao, P. S. C. (1993) Impact of Bacterial Biomass on Contaminant Sorption and Transport in Subsurface Soil, *Appl. Environ. Microbiol.*, 59:1813-1820.

4. Bolster, C. H., Hornberger, G. M., Mills, A. L. and Wilson, J. L. (1998) A Method for Calculating Bacterial Deposition Coefficients Using the Fraction of Bacteria Recovered from Laboratory Columns, *Environ. Sci. Technol.*, 32:1329-1332.

5. Bürgisser, C. S., ernik, M., Borkovec, M. and Sticher, H. (1992) Determination of Nonlinear Adsorption Isotherms from Column Experiments: An Alternative to Batch Studies, *Environ. Sci. Technol.*, 27: 943-948.

6. Chen, G. and Strevett, K. A. (2001) Impact of Surface Thermodynamics on Bacterial Transport, *Environ. Microbiol.*, 3: 237-245.

7. Dohse, D. M. and Lion, L. W. (1994) Effect of Microbial Polymers on the Sorption and Transport of Phenanthrene in a Low-Carbon Sand, *Environ. Sci. Technol.*, 4:541-548.

8. Elimelech, M. and O'Melia, C. R. (1990) Kinetic of Deposition of Colloidal Particles in Porous Media, *Environ. Sci. Technol.*, 24:1528-1536.

9. Fontes, D. E., Mills, A. L., Hornberger, G. M. and Herman, J. S. (1991) Physical and Chemical Factors Influencing Transport of Microorganisms through Porous Media, *Appl. Environ. Microbiol.*, 57:2473-2481.

10. Gamerdinger, A. P., van Rees, K. C. J., Rao, P. S. C. and Jessup, R. E. (1994) Evaluation of *in situ* Columns for Characterizing Organic Contaminant Sorption during Transport, *Environ. Sci. Technol.*, 28:376-382.

11. Gannon, J. T., Mingelgrin, U., Alexander, M. and Wagenet, R. J. (1991) Bacterial Transport through Homogeneous, *Soil Biol. Biochem.* 23:1155-1160.

12. Gooses, K. and Schwarzenbach, R. P. (2001) Linear Free Energy Relationship Used to Evaluate Equilibrium Partitioning of Organic Compounds, *Environ. Sci. Technol.* 35: 1-9.

13. Grasso, D., Smets, B. F., Strevett, K. A., Machinist, B. D., van Oss, C. J., Giese, R. F. and Wu, W. (1996) Impact of Physiological State on Surface Thermodynamics and Adhesion of Pseudomonas aeruginosa, *Environ. Sci. Technol.*, 30:3604-3608.

14. Hancock, I. And Poxton, I. (1988) *Bacterial Cell Surface Techniques*, John Wiley & Sons, New York.

15. Harvey, R. W. and Garabedian, S. P. (1991) Use of Colloid Filtration Theory in Modeling Movement of Bacteria through a Contaminated Sandy Aquifer, *Environ. Sci. Technol.*, 25:178-185.

16. Holtz, R. D. and Kovacs, W. D. (1981) *An Introduction to Geotechnical Engineering*, Prentice-Hall, Inc., Englewood Cliffs, NJ.

17. Hornberger, G. M., Mills, A. L. and Herman, J. S. (1992) Bacterial Transport in Porous Media: Evaluation of a Model Using Laboratory Observations, *Water Resources Research*, 28:915-938.

18. Jenkins, M. B. and Lion, L. W. (1993) Mobile Bacteria and Transport of Polynuclear Aromatic Hydrocarbons in Porous Media, *Appl. Environ. Microbiol.*, 59:3306-3313.

19. Jin, M., Delshad, M., Dwarakanath, V., McKinney, D. C., Pope, G. A., Sepehrnoori, K., Tiburg, C., and Jackson, R. E. (1995) Partitioning Tracer Test for Detection, Estimation, and Remediation Performance Assessment of Subsurface Phase Liquid, *Water Resour. Res.*, 31(5), 1201-1211.

20. Johnson, P. R. and Elimelech, M. (1995) Dynamics of Colloid Deposition in Porous Media: Blocking Based on Random Sequential Adsorption, Langmuir, 11: 801-812.

21. Karapanagioti, H. K., Kleineidam, S., Ligouis, B., Sabatini, D. A. and Grathwohl, P. (1999) Phenanthrene Sorption with Heterogeneous Organic Matter in a Landfill Aquifer Material, *Physics and Chemistry of the Earth*. 24:535-541.

22. Karickhoff, S. W., Brown, D. S. and Scott, T. A. (1979) Sorption of Hydrophobic Pollutants on Natural Sediments, *Water Res.* 13:241-248.

23. Knox, R. C., Sabatini, D. A. and Canter, L. W. (1993) *Subsurface Transport and Fate Processes*, Lewis Publishers, New York.

24. Ku, C., Joseph, D., Henry, Jr., Ranjani, S. and Lloyd, R. (1985) Particle Transfer from a Continuous Oil to a Dispersed Water Phase: Model Particle Study, *J. Colloid Interface Sci.*, 106:377-387.

25. Loosdrecht, M. C. M., Lyklema, J., Norde, W. and Zehnder, A. J. B. (1989) Bacterial Adhesion: A Physicochemical Approach, *Microbial Ecology*, 17:1-15.

26. Magee, B. R., Lion, L. W. and Lemley, A. T. (1991) Transport of Dissolved Organic Macromolecules and Their Effect on the Transport of Phenanthrene in Porous Media, *Environ. Sci. Technol.*, 25:323-331.

27. Mahanty, J. and Ninham, B. W. (1976) *Dispersion Forces*, Academic Press, New York.

28. Marshall, K. C., Breznak, J. A., Calleja, G. B., Mcfeters, G. A. and Rutter, P. R. (1984) *Microbial Adhesion and Aggregation*, Springer-Verlag, New York.

29. Meinders, J. M., van der Mei, H. C. and Bussher, H. J. (1995) Deposition Efficiency and Reversibility of Bacterial Adhesion under Flow, *Journal of Colloid and Interface Science*, 176:329-341.

30. Nkedi-Kizza, P., Rao, P. S. C. and Hornsby, A. G. (1987) Influence of Organic Cosolvents on Leaching of Hydrophobic Organic Chemicals through Soils, *Environ. Sci. Technol.*, 21:1107-1111.

31. Ouyang, Y., Shinde, D., Mansell, R. S. and Harris, W. (1996) Colloid-Enhanced Transport of Chemicals in Subsurface Environments: A Review, *Critical Reviews in Environmental Science and Technology*, 26(2):189-204.

32. Powelson, D. K. and Mills, A. L. (1998) Water Saturation and Surfactant Effects on Bacterial Transport in Sand Columns, *Soil Science*, 163:694-704.

33. van oss, C. J. (1994) *Interfacial Forces in Aqueous Media*, Marcel Dekker, New York.

34. Rajagopalan, R. and Tien, C. (1976) Trajectory Analysis of Deep Bed Filtration Using the Sphere in Cell Porous Media Model, *AIChE J.* 22: 523-533.

35. Rijnaarts, H. H. M., Norde, W., Bouwer, E. J., Lyklema, J. and Zehnder, A.J.B. (1996) Bacterial Deposition in Porous Media Related to the Clean-Bed Collision Efficiency and Substratum-Blocking by Attached Cells. *Envion. Sci. Technol.* 30:2869-2876.

36. Smets, B. F., Grasso, D., Engwall, M. A. and Machinist, B. J. (1999) Surface Physiochemical Properties of *Pseudomonas fluorescens* and Impact on Adhesion and Transport through Porous Media, *Colloid and Surfaces B: Biointerfaces* 14:121-139.

37. Tien, C., Turian, R. M. and Pandse, H. (1979) Simulation of the Dynamics of Deep Bed Filters, *AIChE J.*, 25: 385-395.

38. Unice, K. M. and Logan, B. E. (2000) Insignificant Role of Hydrodynamic Dispersion of Bacterial Transport, *J. Environ. Eng.*, 126: 491- 500.

39. Wålinder, M. E. and Gardner, D. J. (1999) Factors Influencing Contact Angle Measurements on Wood Particles by Column Wicking, *J. Adhesion Sci. Technol*, 13:1363-1374.

40. Winget, P., Cramer, C. J. and Truhlar, D. G. (2000) Prediction of Soil Sorption Coefficients Using a Universal Solvation Model, *Environ. Sci Technol.* 34:4733 – 4740.

# CHAPTER 5

# MICROBIAL DEPOSITION IN POROUS MEDIA: A SURFACE THERMODYNAMIC INVESTIGATION


## Abstract

A microbial transport study of *Echerichia coli*, *Pseudomonas aeruginosa*, *Pseudomonas fluorescens*, *Pseudomonas putida*, *Pseudomonas* sp. and *Bacillus subtilis* through a model medium of silica gel demonstrated that bacterial deposition in porous media was determined by interfacial interactions between bacteria and the medium as well as interfacial interactions between the deposited and suspended bacterial cells. The clean bed collision efficiency, $\alpha_0$ was an exponential function of $\Delta G_{132}^{TOT}$ (sum of $\Delta G_{132}^{LW}$, free energy of van der Waals interactions, $\Delta G_{132}^{AB}$, free energy of Lewis acid/base interactions and $\Delta G_{132}^{EL}$, free energy of electrostatic interactions between bacteria and the medium matrix at the equilibrium distance). The blocking factor, B that depicts the ratio of the blocked area to the geometric area of the medium surface, was an exponential function of $\Delta G_{131}^{TOT}$ (sum of $\Delta G_{131}^{LW}$, free energy of van der Waals interactions, $\Delta G_{131}^{AB}$, free energy of Lewis acid/base interactions and $\Delta G_{131}^{EL}$, free energy of electrostatic interactions between deposited and suspended bacterial cells at the equilibrium distance). Among the bacterial strains studied, *P. aeruginosa* had the greatest $\alpha_0$ (0.41) and *B. subtilis* had greatest B (13.7) because *P. aeruginosa* had the smallest $\Delta G_{132}^{TOT}$ (-983.8 kT) and *B. subtilis* had greatest $\Delta G_{131}^{TOT}$ (1574.9 kT).



Key words: Microbial deposition, free energy, van der Waals interactions, Lewis acid/base interactions, electrostatic interactions.

## Introduction

Interest in predicting the fate and transport of bacteria in the subsurface area is motivated by either a concern that microbes can contaminate drinking water supplies or their role in bioremediation (1). The transport of bacteria is retarded by their sorption on soil and subsurface materials, which can be described by the colloid filtration model (2-10). The removal of colloidal-sized bacteria during filtration in packed-bed systems (e.g., subsurface geological formations) is expressed as (11):

$$k_c = \frac{3}{2}\frac{(1-\theta)}{d_g}\alpha\eta v \qquad (1)$$

where $k_c$ is the deposition coefficient ($sec^{-1}$); $\theta$ medium porosity ($m^3/m^3$); $d_g$ diameter of the porous medium grain (m); $\alpha$ collision efficiency factor; $\eta$ single collector efficiency; and $v$ interstitial velocity (m/sec). The collision efficiency factor, $\alpha$, represents the probability of a particle to attach upon reaching the collector surface and is a function of the fraction of surface covered with cells, $\phi$ if monolayer sorption is assumed (12, 13):

$$\alpha = \alpha_0(1-B\phi) \qquad (2)$$

where $\alpha_0$ is the clean bed collision efficiency; B blocking factor; and $\phi$ fraction of surface covered with cells. Rijnaarts *et al.* (14) suggested that bacterial deposition in porous media can be determined by interactions between bacterial cells and the substratum. Specifically, $\alpha_0$ can be determined by cell-solid interactions and corresponds to a Gibbs energy barrier or activation energy for adhesion; while B should be strongly affected by cell-cell interactions. Whereas, an explicit description of the relationships between bacterial deposition and the interactions has not been outlined so far.

Therefore, this research is devoted to an experimental investigation of the role that the interactions between bacteria and medium matrix play in determining bacterial deposition. It is the goal of this study to depict and mechanistically derive an expression for the relationships of cell-solid and cell-cell interactions with deposition parameters. The understanding of these relationships is of significant importance in predicting the fate and transport of bacteria in the subsurface area.

**Materials and Methods**

*Bacterial strains and growth conditions.* The bacteria selected for this study were typical representatives of rod-shaped bacterial strains of *Enterobacteriaceae*, *Pseudomonadaceas*, and *Bacillaceae*, which included *Echerichia coli* HB101 (ATCC 33694), *Pseudomonas aeruginosa* (ATCC 15152), *Pseudomonas fluorescens* (ATCC 17559), *Pseudomonas putida* (ATCC 12633), *Pseudomonas* sp. (ATCC 55648) and *Bacillus subtilis* (ATCC 6051a). *E. coli* HB101 was cultured on Luria-Bertani (LB) Broth (Sigama L-3522) at 37°C; *P. fluorescens*, *P.putida*, *P. aeruginosa*, *P.* sp. and *B. subtilis* were cultured on Nutrient Broth (Difco 0003) at 26°C 26°C, 30°C, 30°C and 30°C, respectively. All cultures were incubated until stationary state to maintain stable surface characteristics (15). For column experiments, the bacterial strains were centrifuged at 2500 RPM (Damon/IEC Divison, Needham Heights, MA) and washed twice with a sterilized buffer solution (potassium phosphate monobasic-sodium hydroxide buffer, Fisher Scitific, Pittsburgh, PA) before resuspended in an electrolyte solution to make a bacterial solution. The electrolyte solution was prepared using analytical reagent-grade NaCl (Fisher Scientific, Pittsburgh, PA) and Nano-pure

deionized water (NPDI, Barnstead, Dubuque, IA) at a concentration of $10^{-5}$ M. During the washing process, soluble exopolysaccharide (if any) was stripped off the bacteria (16), which was important for bacteria to maintain a constant surface property. When transported in the column, the growth of the bacteria was assumed to be minimal due to the lack of substrate or nutrient. This was validated by the insignificant change of the bacterial Adenosine Triphosphate (ATP) content for the duration of transport (17). Therefore, the bacterial surface property should remain unchanged during the transport and could be described by their surface thermodynamics. Bacterial concentrations were quantified by ATP analysis (17). Bacterial transport in column experiments was performed at a concentration of ~ $10^9$ cells per ml (predetermined by ATP analysis).

*Porous medium.* The porous medium used in this research was silica gel from Fisher Scientific (100 mesh). The median grain radius size of silica gel was 100 μm. Before being packed in the column, silica gel was sterilized at 121°C for 20 min.

*Physiological state determination.* Physiological states of the bacteria were quantified through biochemical assay using ATP analysis (17). After inoculation, the cultures were placed on the Gyrotory Water Bath Shaker (New Brunswick Scientific Co. Inc. Model G76) at 150 RPM. 50 μl of cultures was sampled at a time interval of 30 minutes. The light emission produced by the reaction of ATP extracted from the cells with luciferase as measured by a luminometer (TD-20/20, Turner Design, Sunnyvale, CA) was compared to an ATP standard ($2.5 \times 10^{-8}$ g/ml ATP which is equivalent to $5 \times 10^7$ bacteria per ml, 10 μg/ml ATP in HEPES buffer, Turner Design, Sunnyvale, CA) to determine the number of

viable bacterial cells. Thus, curves of the number of viable bacterial cells versus time were obtained, which were used as the reference for the determination of stationary state for different bacterial strains.

*Measurement of surface thermodynamics.* Surface thermodynamics of the medium, silica gel, was studied using the wicking method (18, 19). This method determined the contact angle ($\cos\beta$) by measuring the velocity of capillary rise through a porous layer based on the Washburn equation:

$$h^2 = (R_e \cdot t \cdot \gamma_L \cdot \cos\beta) \cdot (2 \cdot \mu)^{-1} \qquad (3)$$

where h is the height (m) of capillary rise of the wicking liquid at time t (sec); $\gamma_L$ total surface tension of the wicking liquid ($mJ/m^2$); $\mu$ viscosity of liquid ($N \cdot s/m^2$) and $R_e$ average interstitial pore size (m). By using a liquid with low surface tension, such as methanol ($\gamma = 22.5$ $mJ/m^2$) or hexane ($\gamma = 18.4$ $mJ/m^2$), the average interstitial pore size $R_e$ can be obtained from equation 3 since methanol or hexane is expected to spread over the solid surface during the wicking measurement resulting in $\cos\beta=1$. Once $R_e$ was determined, an apolar liquid, diiodomethane and two polar liquids, glycerol and water were applied to estimate their respective $\cos\beta$ values.

Microbial surface thermodynamic properties were estimated by the contact angle measurement (Contact Angle Meter, Tantec, Schaumburg, IL) following the method described by Grasso *et al.* (15). Bacterial strains collected in stationary state (predetermined by ATP analysis) were vacuum filtered on silver metal membrane filters (0.45 μm, Osmonic, Inc., Livermore, CA) and air-dried for about 30 minutes before the

contact angle measurement. The amount of cells on the silver filter was approximately 13 mg to ensure a multi-layer covering of the membrane, and the moisture content was kept in the range of 25% to 30%. As described previously for the wicking method, diiodomethane, glycerol and water were used for the contact angle measurement.

Each measurement was repeated 30 times and the surface thermodynamic parameters were estimated by Young-Dupré equation 4 using the average results.

$$(1+\cos\beta)\gamma_L = 2(\sqrt{\gamma_S^{LW}\gamma_L^{LW}} + \sqrt{\gamma_S^{+}\gamma_L^{-}} + \sqrt{\gamma_S^{-}\gamma_L^{+}}) \qquad (4)$$

where $\gamma_L$ is the surface tension of the liquid that is used for the measurements ($mJ/m^2$) which can be calculated by:

$$\gamma_L = \gamma_L^{LW} + 2\sqrt{\gamma_L^{-}\gamma_L^{+}} \qquad (5)$$

Here $\gamma^{LW}$ is the Liftshitz-van der Waals component of surface tension (subscript S for solid and L for liquid) ($mJ/m^2$); $\gamma^+$ electron-acceptor parameter and $\gamma^-$ electron-donor parameter of Lewis acid/base component of surface tension (subscript S for solid and L for liquid) ($mJ/m^2$).

*Surface thermodynamic model development.* The Lifshitz-van der Waals and Lewis acid-base interactions between microorganisms 1 and the medium matrix 2, immersed in water 3 at the equilibrium distance or closest approach, $y_0$ (assumed to be 1.57 Å by van Oss (20)) were estimated by equations 6 and 7 assuming that the contact area is $2\pi Ry_0$ (21):

$$\Delta G(y)_{132}^{LW} = 2\pi R y_0 \Delta G_{y_0 132}^{LW} \quad (6)$$

$$\Delta G(y)_{132}^{AB} = 2\pi R y_0 \Delta G_{y_0 132}^{AB} \quad (7)$$

where R is the radius of the microorganism; $y_0$ equilibrium distance (assumed to be 1.57 Å by van Oss (19); $\Delta G_{y0132}{}^{LW}$ and $\Delta G_{y0132}{}^{AB}$ Gibbs energy of two parallel plates, 1 and 2, immersed in water 3 at the equilibrium distance and can be calculated using equations 8 and 9 (21):

$$\Delta G_{y_0\ 132}^{LW} = -2(\sqrt{\gamma_3^{LW}} - \sqrt{\gamma_2^{LW}})(\sqrt{\gamma_3^{LW}} - \sqrt{\gamma_1^{LW}}) \quad (8)$$

$$\Delta G_{y_0\ 132}^{AB} = 2\sqrt{\gamma_3^+}(\sqrt{\gamma_1^-} + \sqrt{\gamma_2^-} - \sqrt{\gamma_3^-}) + 2\sqrt{\gamma_3^-}(\sqrt{\gamma_1^+} + \sqrt{\gamma_2^+} - \sqrt{\gamma_3^+}) - 2\sqrt{\gamma_1^+\gamma_2^-} - 2\sqrt{\gamma_1^-\gamma_2^+} \quad (9)$$

In equations 6 and 7, the microorganisms are modeled as a sphere having a radius at least one order less than that of the medium matrix. Therefore, a sphere-plate interaction configuration is adopted to simplify the interactions between the microorganisms and the medium matrix. For interactions between the microorganisms, a sphere-sphere interaction configuration is assumed and thus the contact area is $\pi R y_0$ and the Gibbs energies can be calculated as:

$$\Delta G(y)_{131}^{LW} = \pi R y_0 \Delta G_{y_0 131}^{LW} \quad (10)$$

$$\Delta G(y)_{131}^{AB} = \pi R y_0 \Delta G_{y_0 131}^{AB} \quad (11)$$

where $\Delta G_{y0131}^{LW}$ and $\Delta G_{y0131}^{AB}$ are Gibbs energies of two plates immersed in water 3 at the equilibrium distance and can be calculated using equations 8 and 9 by substituting 2 for 1.

The electrostatic interaction free energy, $\Delta G_{131}^{EL}$ and $\Delta G_{132}^{EL}$ can be evaluated by (constant potential approach) (valid for $0.1 < \kappa y < 300$, van Oss (20)):

$$\Delta G(y)_{131}^{EL} = 0.5 \cdot \pi\varepsilon\varepsilon_0 R\psi_{01}^{\ 2} Ln(1+e^{-\kappa y})] \quad (12)$$

$$\Delta G(y)_{132}^{EL} = \pi\varepsilon\varepsilon_0 R\psi_{01}\psi_{02} Ln(1+e^{-\kappa y})] \quad (13)$$

where $\varepsilon$ and $\varepsilon_0$ are the relative dielectric permittivity of water (78.55 for water at 25°C) and permittivity under vacuum ($8.854 \times 10^{-12}$ C/V·m) respectively; $\psi_{01}$, $\psi_{02}$ potentials at the surfaces of the microorganisms and the medium matrix; $1/\kappa$ Debye-Hückel length and also an estimation of the effective thickness of the electrical double layer (98.15 nm for $10^{-5}$ M NaCl that was used in column experiments) (22). $\psi_{01}$, $\psi_{02}$ can be calculated based on the following equation:

$$\psi_0 = \zeta(1 + z/a)\exp(\kappa z) \quad (14)$$

where $\zeta$ is the zeta potential measured at the slipping plate; z distance from the particle surface to the slipping plate that is generally on the order of 5 Å (20); and *a* radius of the particle; . $\zeta$-potentials of the bacteria and the medium were measured by suspending in a $10^{-5}$ M NaCl solution using Lazer Zee Meter (Model 501, Pen Kem, Inc.).

*Column experiments*. The transport of six bacterial strains through the porous medium was conducted using a column from Kimble-Kontes (Vineland, NJ) with 2.5-cm ID × 15-

cm length (Table 5.1). The medium used for column experiments, silica gel was initially saturated with 10 pore volumes of sterilized $10^{-5}$ M NaCl. For each run, 30 ml of bacterial solution at a concentration of ~ $10^9$ cells per ml as predetermined by ATP analysis, was injected via a syringe using an injection port. The column was continuously flushed with sterilized $10^{-5}$ NaCl by a peristaltic pump (Masterflex, Cole-Parmer, Vernon Hills, IL) at a flow rate of 0.01 ml/sec until a background ATP signal was detected from the elution collected by a fraction collector. The ATP concentration was monitored and used to generate breakthrough curves (BTCs) for each bacterium. After each run, mass balance was performed. Bacterial contents inside the column were measured by making the medium a suspended solution to perform an ATP measurement. A conservative pulse tracer (chloride) BTC was determined separately before the introduction of bacteria to estimate the Peclet number using equations 20 to 22. Each run was done in triplicates.

**Table 5.1 Summary of the Parameters Used in Column Experiment**

| Microorganisms | Radius |
|---|---|
| *E. coli* | 0.5 μm |
| *P. aeruginosa* | 0.3 μm |
| *P. fluorescens* | 0.3 μm |
| *P. putida* | 0.3 μm |
| *P.* sp | 0.3 μm |
| *B. subtilis* | 1.0 μm |

| Porous Media | Radius | Porosity | Density |
|---|---|---|---|
| Silica gel | ~ 100 μm | 0.51 | 2.65 g/cm$^3$ |

| Column Experiment | |
|---|---|
| Column | 2.5-cm ID x 15-cm Length |
| Flow Rate | 0.03 ml/sec |
| Pe | 13.9 |

*Determination of η.* The single collector efficiency, η, represents the ratio of the rate at which particles strike a collector to the rate at which particles approach a collector. Disregarding the effects of gravitational forces in deposition (an assumption that should be true for bacterial cells because the density of the cells is close to that of water) and also disregarding the effects of straining (an assumption that should also be valid because the bacterial cells are so much smaller than the medium grain), η is given by (6, 23):

$$\eta = 4A_s^{(1/3)}N_{Pe}^{(-2/3)} \tag{15}$$

where

$$A_s = 2(1-p^5)/(2-3p+3p^5-2p^6) \tag{16}$$

$$N_{Pe} = 3\pi\mu\ d_p d_g v/(kT) \tag{17}$$

Here $p=(1-\theta)^{1/3}$; μ fluid viscosity ($1.002 \times 10^{-3}$ N· s/m$^2$ for water at 20°C); $d_p$ bacterial diameter (m); k Boltzmann constant ($1.38048 \times 10^{-23}$ J/K); and T absolute temperature (K).

*Determination of $\alpha_0$ and B.* For irreversible particle deposition occurring in a packed column of spherical collectors, the collector surface coverage θ may be obtained as a function of time from experimental particle breakthrough data according to the relationship (24):

$$\phi = \frac{\pi R_p^2 v R_c C_0 \int_0^t (1-C/C_0)dt}{3L(1-\theta)} \tag{18}$$

where $R_p$ is the particle radius; $R_c$ collector radius; $C_0$ column inlet particle number concentration; C column effluent particle number concentration corresponding to time t;

L length between the injection and where the bacteria are collected or packed bed column length (m).

The dynamics of particle deposition in porous media are perhaps best illustrated as the changing rate at which collector surfaces are covered by particles. Thus, $\alpha$ can be determined based on the fraction recovery in the effluent (2).

$$\alpha = \frac{2d_g\left[-\mathrm{Ln}\left(\int_0^t (C/C_0)dt + \frac{\mathrm{Ln}^2\left(\int_0^t (C/C_0)dt\right)}{Pe}\right)\right]}{3(1-\theta)\eta L} \tag{19}$$

where *Pe* is the Peclet number, which can be obtained from studying the BTCs of a conservative tracer based on equation 20 (25, 26):

$$\sigma^2 = \tau^2 \cdot \left[\frac{2}{Pe} - \frac{2}{Pe^2} \cdot (1 - e^{-Pe})\right] \tag{20}$$

where $\sigma$ is the standard deviation and $\tau$ measured average residence time for the tracer in the reactor (sec), determined by:

$$\tau = \frac{\int_0^\infty t \cdot C(t)dt}{\int_0^\infty C(t)dt} \tag{21}$$

$$\sigma^2 = \frac{\int_0^\infty C(t)(t-\tau)^2 dt}{\int_0^\infty C(t)dt} = \frac{\int_0^\infty \tau^2 \cdot C(t)dt}{\int_0^\infty C(t)dt} - \tau^2 \tag{22}$$

In equations 21 and 22, C is the measured concentration of the tracer at the outlet of the column ($g/m^3$) and t elapsed time from the initial injection of the tracer (sec).

Furthermore, $\phi$ and $\alpha$ with respect to elapsed time were determined using equations 18 and 19, based on which the relationship between $\phi$ and $\alpha$ was derived. By fitting the corresponding $\phi$ and $\alpha$ values into equation 2, $\alpha_0$ and B were obtained.

**Results**

For all the bacterial strains, the collision efficiency, $\alpha$ displayed a linear relationship with the cell surface coverage, $\phi$ (Figure 5.1). In Figure 5.1, the intercept is the clean bed collision efficiency, $\alpha_0$ and the blocking factor, B can be calculated by dividing the slope by $\alpha_0$. *P. aeruginosa* (Figure 5.1 b) had the greatest $\alpha_0$ (0.41) and *B. subtilis* (Figure 5.1 f) had greatest B (13.7) among the bacterial strains studied; while *P.* sp. (Figure 5.1 e) had both the smallest $\alpha_0$ (0.08) and the smallest B (1.0). Surface thermodynamics properties of the microorganisms and the medium are shown in Table 5.2. These surface thermodynamics properties were used to calculate the free energies of cell-solid and cell-cell interactions and are summarized in Table 5.3. Calculated values of $\alpha_0$ and B are also summarized in Table 5.3.

A lower total free energy, $\Delta G_{132}^{TOT}$ (sum of $\Delta G_{132}^{LW}$, free energy of van der Waals interactions, $\Delta G_{132}^{AB}$, free energy of Lewis acid/base interactions and $\Delta G_{132}^{EL}$, free energy of electrostatic interactions between bacteria and the medium matrix) value corresponded to a greater $\alpha_0$ value. *P. aeruginosa* had the greatest $\alpha_0$ (0.41) value among the microorganisms studied because it had the lowest $\Delta G_{132}^{TOT}$ value (-983.8 kT). *P.* sp had the smallest $\alpha_0$ (0.08) value among the microorganisms studied because it had the highest $\Delta G_{132}^{TOT}$ value (-677.2 kT).

**Table 5.2 Bacterial and Medium Surface Thermodynamic Properties**

| Stain/Medium | ζ-potential (mV) | $\gamma^{LW}$ ($mJ/m^2$) | $\gamma^{+}$ ($mJ/m^2$) | $\gamma^{-}$ ($mJ/m^2$) |
|---|---|---|---|---|
| *E. coli* | -10.6±0.4 | 39.1 | 0.59 | 58.9 |
| *P. aeruginosa* | -14.7±0.4 | 36.5 | 0.96 | 59.2 |
| *P. fluorescens* | -10.2±0.1 | 35.4 | 0.42 | 56.9 |
| *P. putida* | -10.6±0.2 | 34.8 | 0.62 | 55.4 |
| *P. sp* | -10.8±0.1 | 34.3 | 0.72 | 53.4 |
| *B. subtilis* | -14.7±0.4 | 44.6 | 0.08 | 59.9 |
| Silica gel | -27.0±0.8 | 25.7 | 0.00 | 11.7 |

**Table 5.3 Interaction Free Energies and Corresponding Clean Bed Collision Efficiency $\alpha_0$ and Blocking Factor B**

| Strain/Medium | $\Delta G_{132}^{TOT}$ (kT) | $\alpha_0$ | $\Delta G_{131}^{TOT}$ (kT) | B |
|---|---|---|---|---|
| *E. coli* / Silica gel | -948.1 | 0.34 | 1455.8 | 5.3 |
| *P. aeruginosa* / Silica gel | -983.8 | 0.41 | 1435.2 | 4.1 |
| *P. fluorescens* / Silica gel | -803.1 | 0.15 | 1475.9 | 9.1 |
| *P. putida* / Silica gel | -760.9 | 0.14 | 1371.9 | 2.9 |
| *P.* sp / Silica gel | -677.2 | 0.08 | 1280.1 | 1.0 |
| *B. subtilis* / Silica gel | -889.2 | 0.23 | 1574.9 | 13.7 |

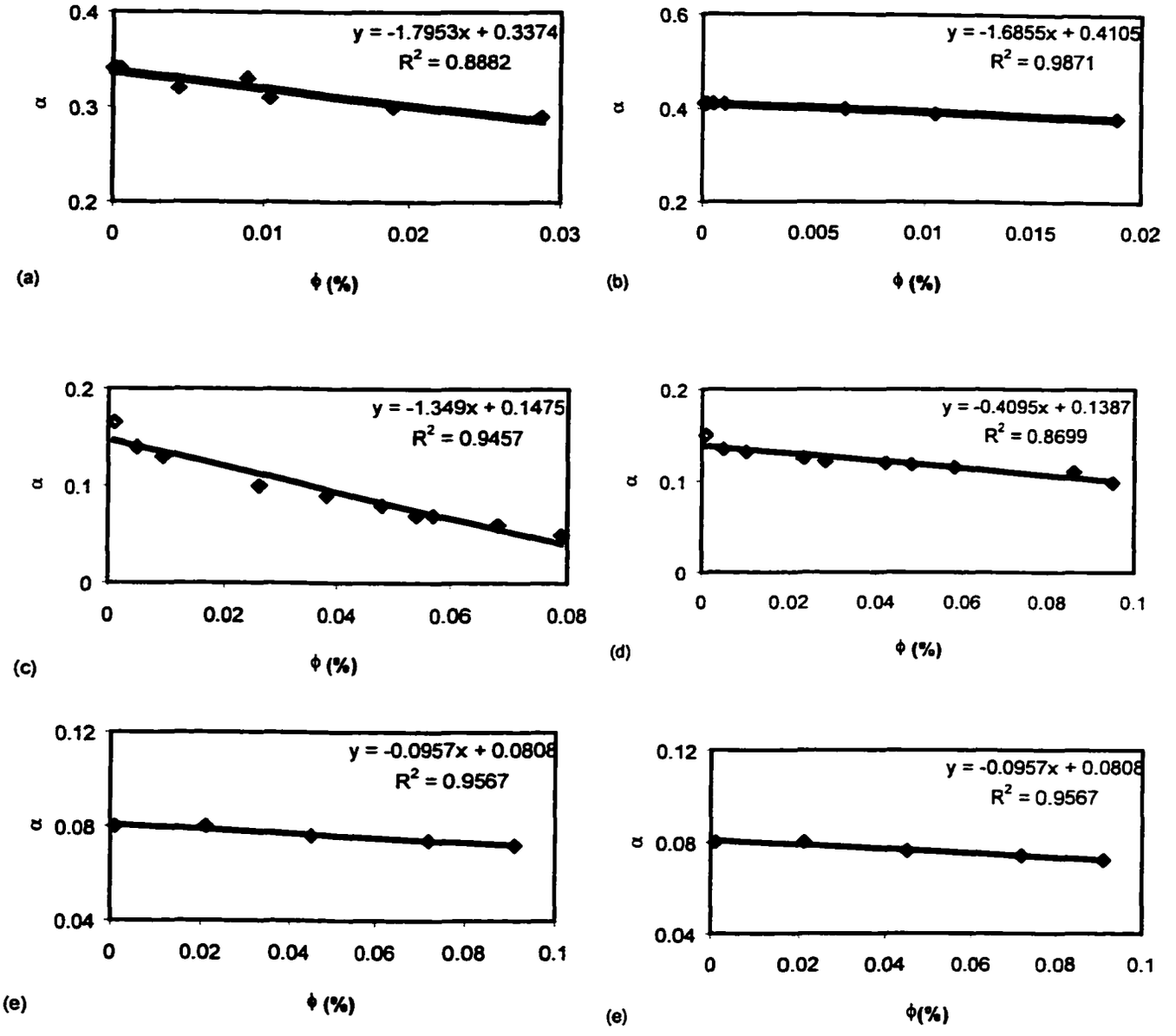


**Figure 5.1** Collision efficiency, $\alpha$ versus cell surface coverage, $\phi$ of (a) *E. coli*, (b) *P. aeruginosa*, (c) *P. fluorescens*, (d) *P. putida*, (e) *P.* sp., and (f) *B. subtilis*.

The blocking factor, B was a function of $\Delta G_{131}^{TOT}$ (sum of $\Delta G_{131}^{LW}$, free energy of van der Waals interactions, $\Delta G_{131}^{AB}$, free energy of Lewis acid/base interactions and $\Delta G_{131}^{EL}$, free energy of electrostatic interactions between deposited and suspended bacterial cells). Compared with other stains, *B. subtilis* showed the greatest B value (13.7) due to its greatest $\Delta G_{131}^{TOT}$ value (1574.9 kT) and *P.* sp. exhibited the smallest B value (1.0) as a result of its smallest $\Delta G_{131}^{TOT}$ value (1280.1 kT).

A smaller (negatively greater) $\Delta G_{132}^{TOT}$ value did not necessarily correspond to a greater $\Delta G_{131}^{TOT}$ value. As seen in Table 5.3, *P. aeruginosa* had a smaller $\Delta G_{132}^{TOT}$ value (-983.8 kT) than *P. fluorescens* (-803.1 kT), whereas, it had a smaller $\Delta G_{131}^{TOT}$ value (1435.2 kT) than that of *P. fluorescens* (1475.9 kT). Accordingly, *P. aeruginosa* had a greater $\alpha_0$ value (0.41) and smaller B value (4.1) than those of *P. fluorescens* (0.15 and 9.1, respectively).

**Discussion**

*Clean bed collision efficiency.* By definition, the clean bed collision efficiency, $\alpha_0$, is equal to the collision efficiency, $\alpha$ when there is no deposited cells on the media ($\theta = 0$), i.e., $\alpha_0 = \alpha$. Therefore, $\alpha_0$ describes the possibility of particles that strike the collector to attach on the media without the effect of the deposited cells. Rijnaarts *et al.* (14) identified that $\alpha_0$ was solely determined by cell-solid interactions, i.e., interactions between bacteria and the medium matrix and predicted that $\alpha_0$ corresponded to a Gibbs free energy of the interactions. According to traditional and extended DLVO theory, interactions between biotic and abiotic surfaces that should be considered in aqueous

media are: apolar, or Lifshitz-van der Waals (LW) interactions; polar, electron-donor/electron-acceptor, or Lewis acid-base (AB) interactions; and electrostatic (EL) interactions (20, 21, 27-29). Lifshitz van-der Waals interactions are initiated by the unevenness of the electron cloud surrounding the molecules or particles. The electron deficient part of a molecule or particle is the positive pole and the electron excess part is the negative pole. Lifshitz-van der waals interactions are thus electrostatic attractions between oppositely charged poles of two or more dipoles. Lewis acid-base interactions, a polar interaction, are initiated by interactions between Lewis acids, which are electron pair acceptors, and Lewis bases, which are electron pair donors, reacting to form adducts in which a coordinate covalent bond is formed. Electrostatic interactions occur between highly charged particles dispersed in electrolytes. Thus, van der Waals, Lewis acid/base and electrostatic interactions between bacteria and the medium matrix should play roles in determining bacterial deposition. Marmur (30) developed an equation to calculate the fraction of successful collisions out of the total collisions as a function of the interaction Gibbs free energy:

$$f = e^{-\Delta G_{132}^{TOT} / \phi kT} \qquad (23)$$

To examine that $\alpha_0$ is a function of $f$, logarithms of experimentally obtained $\alpha_0$ of different bacterial strains were plotted versus corresponding $\Delta G_{132}^{TOT}/1000kT$ in Figure 5.2. The linear relationship between $Ln\alpha_0$ and $\Delta G_{132}^{TOT}/1000kT$ indicated that $f$ depicted the role of the interaction Gibbs free energy played in determining microbial deposition in porous media.

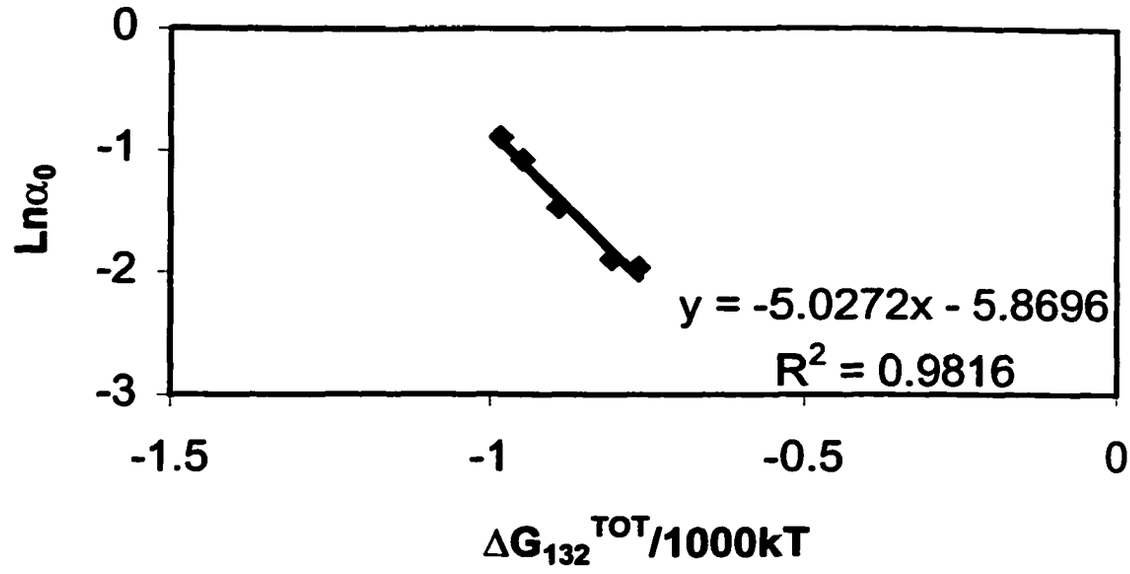


**Figure 5.2** $Ln\alpha_0$ versus $\Delta G_{132}^{TOT}/1000$ kT

*Blocking factor.* Cell-coating which is due to the deposited cells on substratum surface will alter the interactions between the microbes and the substratum by changing the substratum surface properties. This will accordingly impact the deposition of bacteria on the substratum. The change of the deposition of bacteria on the substratum surface is governed by the blocking factor, B. By definition, B is the screening of the medium surface by attached cells, i.e., the ratio of the blocked area to the geometric area of the medium surface (29). It is related to the maximum surface coverage $\theta_{max}$ for monolayer adhesion: $B = 1/\theta_{max}$ (4, 24, 32). When the linear relationship cannot hold, the Random Sequential Adsorption (RSA) dynamic blocking function should be followed (30) and equation 2 becomes:

$$\alpha = \alpha_0[1 - 4\phi + \frac{6\sqrt{3}}{\pi}\phi^2 + (\frac{40}{\sqrt{3}\pi} - \frac{176}{3\pi^2})\phi^2] \qquad (24)$$

For bacterial deposition, the linear blocking function seems sufficient and owing to repulsive cell-cell interactions, monolayer adhesion assumption is made (14). Rijnaarts

*et al.* (14) predicted that B, or reciprocal of the maximum surface coverage for monolayer adhesion, was determined by the cell-cell interactions. Analogous to $\alpha_0$, B can be a function of the total free energy of the cell-cell interactions as following:

$$g = \frac{1}{e^{\Delta G_{131}^{TOT} / \phi kT}} \tag{25}$$

Logarithms of experimentally obtained B of different bacterial strains were plotted versus corresponding $\Delta G_{131}^{TOT}/1000kT$ in Figure 5.3 and the linear relationship proved the role of the interaction free energy in the determination of B.

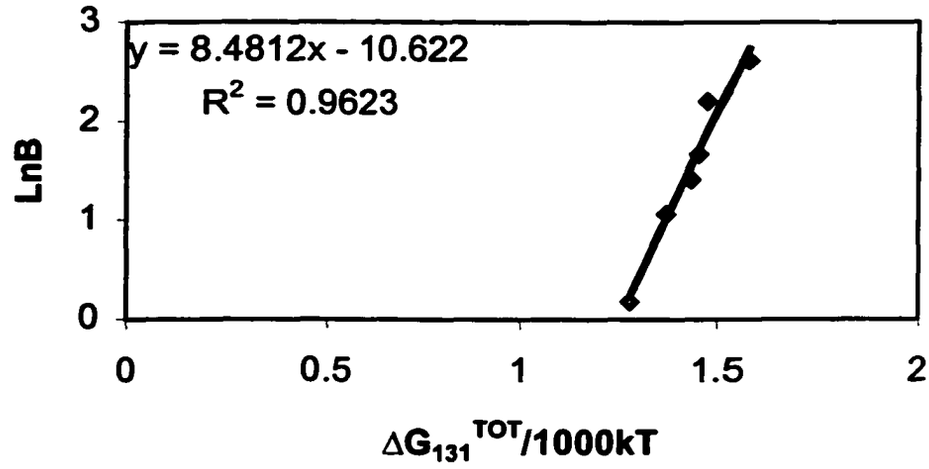


**Figure 5.3** LnB versus $\Delta G_{131}^{TOT}/1000$ kT

Among van der Waals, Lewis acid/base and electrostatic interactions, Lewis acid/base interactions dominate (Table 5.4). From equation 9, it can be seen that water mediated

**Table 5.4 van der Waals, Lewis acid/base and Electrostatic Interaction Free Energies**

| Strain | $\Delta G_{132}^{LW}$ (kT) | $\Delta G_{132}^{AB}$ (kT) | $\Delta G_{131}^{EL}$ (kT) | $\Delta G_{131}^{LW}$ (kT) | $\Delta G_{131}^{AB}$ (kT) | $\Delta G_{132}^{EL}$ (kT) |
|---|---|---|---|---|---|---|
| *E. coli* | -91.8 | -887.7 | 31.4 | -180.7 | 1620.8 | 15.7 |
| *P. aeruginosa* | -79.5 | -947.7 | 43.4 | -135.6 | 1549.1 | 21.7 |
| *P. fluorescens* | -74.3 | -758.9 | 30.1 | -118.0 | 1578.9 | 15.0 |
| *P. putida* | -71.4 | -720.8 | 31.3 | -109.5 | 1465.8 | 15.6 |
| *P.* sp | -68.7 | -640.4 | 31.9 | -101.4 | 1365.6 | 15.9 |
| *B. subtilis* | -116.6 | -816.0 | 43.4 | -291.4 | 1844.6 | 21.7 |

$\Delta G_{132}^{AB}$ is determined by $\gamma^+$ and $\gamma^-$ of both bacterial strains and the medium; while water mediated $\Delta G_{131}^{AB}$ is only determined by $\gamma^+$ and $\gamma^-$ of bacterial strains. To further understand Lewis acid/base interactions, equation 9 was rearranged as:

$$\Delta G_{y_0 132}^{AB} = 2[(\sqrt{\gamma_1^+} - \sqrt{\gamma_2^+})(\sqrt{\gamma_1^-} - \sqrt{\gamma_2^-}) - \frac{1}{2}\Delta G_{y_0 131}^{AB} - \frac{1}{2}\Delta G_{y_0 232}^{AB}] \quad (26)$$

Equation 26 shows that intramolecular Lewis acid/base interactions depends not only on the surface properties of bacterial strains ($\Delta G_{y0131}^{AB}$) and the medium ($\Delta G_{y0232}^{AB}$), it also depends on the relativity of electron-donor and electron-acceptor potentials of bacterial strains and the medium. This explains why smaller (negatively greater) $\Delta G_{132}^{TOT}$ value does not necessarily correspond to greater $\Delta G_{131}^{TOT}$ value, which leads to that greater $\alpha_0$ does not necessarily correspond to greater B.

**Conclusion**

Bacterial deposition in porous media was determined by interactions between bacteria and the medium as well as interactions between the deposited and suspended bacterial cells. The clean bed collision efficiency, $\alpha_0$ was a function of the total free energy of the cell-solid interactions at the equilibrium distance. The blocking factor, B was a function of the total free energy of the cell-cell interactions at the equilibrium distance. Explicit description of these functions was put forwards in this research, which will be of great importance in understanding the fate and transport of microbes in the subsurface, and in guidance of *in-situ* bioremediation.

**Acknowledgements**

The work was support in part by National Science Foundation through Grant No. BES-9733969 to the University of Oklahoma.

**References**

1. Fontes, D.E., Mills, A.L., Hornberger, G.M. and Herman, J.S. *Appl. Environ. Microbiol.* 1991, 57:2473-2481.

2. Bolster, C. H., Hornberger, G. M., Mills, A. L. and Wilson, J. L. *Environ. Sci. Technol.* 1998, 32:1329-1332.

3. Powelson, D.K. and Mills, A.L. *Soil Science* 1998, 163:694-704.

4. Johnson, P.R. and Elimelech, M. *Langmuir* 1995, 11: 801-812.

5. Gamerdinger, A.P., van Rees, K.C.J., Rao, P.S.C. and Jessup, R.E. *Environ. Sci. Technol.* 1994, 28:376-382.

6. Hornberger, G.M., Mills, A.L. and Herman, J.S. *Water Resources Research* 1992, 28:915-938.

7. Harvey, R.W. and Garabedian, S.P. *Environ. Sci. Technol.* 1991, 25:178-185.

8. Gannon, J.T., Mingelgrin, U., Alexander M. and Wagenet R.J. *Soil Biol. Biochem.* 1991, 23:1155-1160.

9. Elimelech, M. and O'Melia, C.R. *Environ. Sci. Technol.* 1990a, 24: 1528-1536.

10. Elimelech, M. and O'Melia, C.R. *Langmuir* 1990b, 6: 1153-1163.

11. Rajagopalan, R. and Tien, C. *AIChE J.* 1976, 22: 523-533.

12. Meinders, J. M., Noordmans, J., Busscher, H. J. *J. Colloid Interface Sci.* 1992, 152: 265 –280.

13. Dabros, T and van de Ven, T.G.M. *Colloids Polym. Sci.* 1983, 261: 694-707.

14. Rijnaarts, H. H. M., Norde, W., Bouwer, E. J., Lyklema, J. and Zehnder, A.J.B. *Environ. Sci. Technol.* 1996, 30: 2877 – 2883.

15. Grasso, D., Smets, B.F., Strevett, K.A. and Machinist, B.D., van Oss, C. J., Giese, R. F. and Wu, W. *Environ. Sci. Technol.* 1996, 30:3604-3608.

16. Hancock, I. And Poxton, I. (1988) *Bacterial Cell Surface Techniques*, John Wiley & Sons, New York.

17. Chen, G. and Strevett, K.A. *Environ. Microbiol.* 2001, 3: 237-245.

18. Wålinder, M.E. and Gardner, D.J. *J. Adhesion Sci. Technol.* 1999, 13:1363-1374.

19. Ku, C., Joseph, D. H. Jr., Ranjani, S. and Lloyd, R., *J. Colloid Interface Sci.* 1985, 106:377-387.

20. van Oss, C.J. (1994) *Interfacial Forces in Aqueous Media*, Marcel Dekker, New York.

21. Meinder, J. M., van der Mei, H. C. and Busscher, H. J *J. Colloid Interface Sci.* 1995, 176:329-341.

22. Marshall, K. C., Breznak, J. A., Calleja, G. B., Mcfeters, G. A. and Rutter, P. R. (1984) *Microbial Adhesion and Aggregation*, Springer-Verlag, New York.

23. Tien, C., Turian, R.M. and Pandse, H. *AIChE J.* 1979, 25: 385-395.

24. Liu, D., Johnson, P.R. and Elimelech, M. *Environ. Sci. Technol.* 1995, 29: 2963-2973.

25. Annable, M.D., Rao, P.S.C., Hatfield, K., Graham, W.D., Wood, A.L., and Enfield, C.G. *J. Environ. Eng.* 1998, 124: 498-503.

26. Jin, M., Delshad, M., Dwarakanath, V., McKinney, D.C., Pope, G.A., Sepehrnoori, K., Tiburg, C., and Jackson, R.E. *Water Resour. Res.* 1995, 31(5), 1201-1211.

27. Chattopadhyay, S. and Puls, R. W. *Environ. Sci. Technol.* 1999, 33: 3609 – 3614.

28. Smets, B. F., Grasso, D., Engwall, M. A. and Machinist, B. J. *Colloids Surf. B: Biointerfaces*, 1999, 14: 121 – 139.

29. Rijnaarts, H. H. M., Norde, W., Bouwer, E. J., Lyklema, J. and Zehnder, A. J. B. *Colloids Surf. B: Biointerfaces* 1995, 4: 5 – 22.

30. Marmur, A. *J Colloid Interface Sci.* 1979, 72: 41-48.

31. Schaaf, P. and Talbot, J. J. Chem. Phys. 1989, 91: 4401- 4409.

32. Rijnaarts, H. H. M., Norde, W., Bouwer, E. J., Lyklema, J. and Zehnder, A.J.B. *Envion. Sci. Technol.* 1996, 30:2869-2876.

# CHAPTER 6

# DETERMINATION OF MICROBIAL SORPTION ISOTHERMS FROM COLUMN EXPERIMENTS


## Abstract

Microbial sorption isotherms of *Pseudomonas fluorescens, Pseudomonas putida* and *Pseudomonas* sp. on an alluvial loam from Central Oklahoma Aquifer (COA) were achieved using column experiments, which cannot be obtained using the traditional batch methods due to the difficulty of distinguishing between reversible and irreversible sorption. All three bacterial strains had a concave isotherm on COA that can be described by the Freundlich expression. A surface thermodynamic explanation of the concave-shaped microbial sorption isotherms was reached in this study and the impact of transport velocity on the microbial BTCs was discussed. The high solid to solution ratio in column experiments is close to that is encountered in the natural system of interest, which makes this method more useful in guidance of *in-situ* bioremediation.



Key words: sorption isotherms, column experiments, *Pseudomonas fluorescens, Pseudomonas putida* and *Pseudomonas* sp.


## Introduction

Interest in predicting the fate and transport of microbes in the subsurface is motivated by either a concern that microbes can contaminate drinking water supplies or their role in bioremediation (Fontes *et al.*, 1991). Microbial transport is greatly impacted by their irreversible deposition (Bolster *et al.*, 1998; Powelson and Mills, 1998; Gamerdinger *et*

*al.*, 1994; Hornberger *et al.*, 1992; Harvey and Garabedian, 1991; Gannon *et al.*, 1991; and Elimelech and O'Melia, 1990) and reversible sorption (Dohse and Lion, 1994; Bellin and Rao, 1993; Bürgisser *et al.*, 1993; Jenkins *et al.*, 1993; Magee *et al.*, 1991; and Nkedi-Kizza *et al.*, 1987) on the medium matrix. The movement and spreading of microbes during transport can be described by a combined model that incorporates the Deep-Bed Filtration Model into a simple Convection-Dispersion Model (ignoring biodegradation) (Chen and Strevett, 2001; Harvey and Garabedian, 1991):

$$\theta\frac{\partial C}{\partial t}+(1-\theta)\rho_b\frac{dS}{dt}=D\theta\frac{\partial^2 C}{\partial x^2}-v\theta\frac{\partial C}{\partial x}-\theta k_c C \qquad (1)$$

where $\theta$ is the porosity ($m^3/m^3$); C microbial concentration in solution (number of cells/$m^3$); t elapsed time from the initial microbial injection (sec); $\rho_b$ sediment bulk density ($g/m^3$); S concentration of reversibly adsorbed microbes on the porous medium (cells/g); D hydrodynamic dispersion coefficient ($m^2$/sec); v interstitial pore water velocity (m/sec); x longitudinal coordinate (m); and $k_c$ deposition coefficient that indicates the rate of irreversible adsorption of microbes on the porous medium ($sec^{-1}$). Using this model, Harvey and Garabedian (1991) observed a good fit of model simulations to breakthrough curves (BTCs) for concentrations of both bromide and bacteria in effluent from sand columns.

The reversible sorption of bacteria onto the porous medium can be expressed in term of solution concentration (Knox *et al.*,1993):

$$\frac{dS}{dt}=\frac{\partial S}{\partial C}\frac{\partial C}{\partial t} \qquad (2)$$

By substituting equation (2) into equation (1) and rearranging, a one-dimension transport can be expressed as:

$$(1+\frac{1-\theta}{\theta}\rho_b\frac{dS}{dC})\frac{\partial C}{\partial t} = D\frac{\partial^2 C}{\partial x^2} - v\frac{\partial C}{\partial x} - k_c C \qquad (3)$$

where $1+\frac{1-\theta}{\theta}\rho_b\frac{dS}{dC}$ is defined as retardation factor, R, and is the average transport velocity of bacteria ($v_{av}$) relative to that of water ($v_w$), such that $R = v_{av}/ v_w$. The reversible microbial sorption on the porous medium is determined by their sorption isotherms. Due to the difficulty of distinguishing between reversible and irreversible sorption, microbial sorption isotherms cannot be achieved in batch experiments. Column experiments for the determination of sorption parameters, which borrows the idea from nonlinear chromatography, have been developed (Bürglsser et al, 1993).

In the case of linear adsorption isotherms, such that $\frac{dS}{dC} = K_p$, where $K_p$ is the microbial distribution coefficient between the aqueous phase and the porous medium ($m^3/g$), R will be a constant and independent of microbial solution concentration. Accordingly, equation (3) can be easily solved and used to fit the microbial transport BTCs. While for nonlinear isotherms, R will depend on the microbial solution concentration and equation (3) will be a non-linear differential equation and can only be solved using numerical methods.

The objectives of this study were to characterize microbial sorption isotherms on an alluvial loam from Central Oklahoma Aquifer (COA) from column experiments. The validity of the isotherms was established by fitting into the microbial transport BTCs

using numerical methods. A surface thermodynamic explanation of the isotherms was reached through the investigation of the interfacial interaction free energies.

**Materials and Methods**

*Bacterial strains and growth conditions* Three bacteria, *Pseudomonas fluorescens, Pseudomonas putida* and *Pseudomonas* sp. were selected for this study, which were typical representatives of microorganisms used in bioremediation of contaminated soil and associated groundwater. They were all obtained from ATCC (17559, 12633 and 55648) and grown on Nutrient Broth (Difco 0003) at 26°C, 26°C, and 30°C, respectively until stationary state. Before column experiments, the bacterial strains were centrifuged at 2500 RPM (Damon/IEC Divison, Needham Heights, MA) and washed twice with a sterilized buffer solution (potassium phosphate monobasic-sodium hydroxide buffer, Fisher Scitific, Pittsburgh, PA) and then resuspended in sterilized nano-pure deionized water (NPDI, Barnstead, Dubuque, IA) to make a bacterial solution. After the washing process, soluble exopolysaccharide (if any) was stripped off the bacteria (Hancock and Poxton, 1988). During transport in the column, the growth of the bacteria was assumed to be minimal due to the lack of substrate or nutrient and short retention time. Therefore, the bacterial surface property should remain unchanged during transport and could be described by their surface thermodynamics. Bacterial concentrations were quantified by Adenosine Triphosphate (ATP) analysis.

*Porous medium* The porous medium used in this research was an alluvial loam from the Central Oklahoma Aquifer (COA) (Norman, Oklahoma). The median grain radius size of

COA was 65 μm with 38% passing a 200 sieve. The organic fraction and hydraulic conductivity were reported to be 0.340 ± 0.20 and (8.2 ± 1.3) × $10^{-5}$ cm/s (Karapanagioti et al., 1999). Due to concerns about structural and chemical alterations, COA was not sterilized. Instead, it was air dried and stored desiccated to minimize the presence of an active bacterial population.

*Physiological state determination* Stationary state of the bacteria was quantified through biochemical assay using ATP analysis. After inoculation, the cultures were placed on the Gyrotory Water Bath Shaker (New Brunswick Scientific Co. Inc. Model G76) at 150 RPM. 50 μl of cultures was sampled at a time interval of 30 minutes. The light emission produced by the reaction of ATP extracted from the cells with luciferase as measured by a luminometer (TD-20/20, Turner Design, Sunnyvale, CA) was compared to an ATP standard ($2.5 \times 10^{-8}$ g/ml ATP which is equivalent to $5 \times 10^{7}$ bacteria per ml, 10 μg/ml ATP in HEPES buffer, Turner Design, Sunnyvale, CA) to determine the number of viable bacterial cells. Thus, curves of the number of viable bacterial cells versus time were obtained, which were used as the reference for the determination of stationary state for different bacterial strains.

*Measurement of surface thermodynamics* Surface thermodynamics of the medium, COA, was studied using the wicking method (Wålinder and Gardner, 1999 and Ku *et al.*, 1985). This method determined the contact angle (cosβ) by measuring the velocity of capillary rise through a porous layer based on the Washburn equation:

$$h^2 = (R_e \cdot t \cdot \gamma_L \cdot \cos\beta) \cdot (2 \cdot \mu)^{-1} \qquad (4)$$

where h is the height (m) of capillary rise of the wicking liquid at time t (sec); $\gamma_L$ total surface tension of the wicking liquid ($mJ/m^2$); $\mu$ viscosity of the wicking liquid ($N \cdot s/m^2$) and $R_e$ average interstitial pore size (m). By using a liquid with low surface tension, such as methanol ($\gamma = 22.5$ $mJ/m^2$) or hexane ($\gamma = 18.4$ $mJ/m^2$), the average interstitial pore size $R_e$ can be obtained from equation (4) since methanol or hexane is expected to spread over the solid surface during the wicking measurement resulting in $\cos\beta=1$. Once $R_e$ was determined, an apolar liquid, diiodomethane and two polar liquids, glycerol and water were applied to estimate their respective $\cos\beta$ values.

Microbial surface thermodynamic properties were estimated by the contact angle measurement (Contact Angle Meter, Tantec, Schaumburg, IL) following the method described by Grasso *et al.* (1996). Bacterial strains collected in stationary state (predetermined by ATP analysis) were vacuum filtered on silver metal membrane filters (0.45 μm, Osmonic, Inc., Livermore, CA) and air-dried for about 30 minutes before the contact angle measurement. The amount of cells on the silver filter was approximately 13 mg to ensure a multi-layer covering of the membrane, and the moisture content was kept in the range of 25% to 30%. As described previously for the wicking method, diiodomethane, glycerol and water were used for the contact angle measurement.

Each measurement was repeated 30 times and the surface thermodynamic parameters were estimated by Young-Dupré equation (5) using the average results.

$$(1+\cos\beta)\gamma_L = 2\left(\sqrt{\gamma_S^{LW}\gamma_L^{LW}} + \sqrt{\gamma_S^{+}\gamma_L^{-}} + \sqrt{\gamma_S^{-}\gamma_L^{+}}\right) \quad (5)$$

where $\gamma_L$ is the surface tension of the liquid that is used for the measurement ($mJ/m^2$) which can be calculated by:

$$\gamma_L = \gamma_L^{LW} + 2\sqrt{\gamma_L^- \gamma_L^+} \quad (6)$$

where $\gamma^{LW}$ is the Liftshitz-van der Waals component of surface tension (subscript S for solid and L for liquid) ($mJ/m^2$); $\gamma^+$ electron-acceptor parameter and $\gamma^-$ electron-donor parameter of Lewis acid/base component of surface tension (subscript S for solid and L for liquid) ($mJ/m^2$).

*Surface thermodynamic model development* The Lifshitz-van der Waals and Lewis acid-base interactions between microbes 1 and medium matrix 2, immersed in water 3 were then estimated by equation (7) and (8) (Meinders *et al.*, 1995):

$$\Delta G(y)_{132}^{LW} = 2\pi R \frac{y_0^2}{y} \Delta G_{y_0 132}^{LW} \quad (7)$$

$$\Delta G(y)_{132}^{AB} = 2\pi R y_0 e^{(y_0 - y)/\lambda} \Delta G_{y_0 132}^{AB} \quad (8)$$

where $\lambda$ is the decay length of water, assumed to be 0.6 nm for pure water (van Oss, 1994); y distance between the microbes (sphere) and the medium matrix (flat plate) measured from the outer edge of the sphere (m); $y_0$ equilibrium distance that is assumed to be 1.57 Å by van Oss, 1994; R radius of the microbes (m); $\Delta G_{y0132}^{LW}$ and $\Delta G_{y0132}^{AB}$ Gibbs energies of two parallel plates, 1 and 2, immersed in water 3 at the distance of $y_0$, which can be obtained from equations (9) and (10) (Meinders *et al.*, 1995):

$$\Delta G^{LW}_{y_0\ 132} = -2(\sqrt{\gamma_3^{LW}} - \sqrt{\gamma_2^{LW}})(\sqrt{\gamma_3^{LW}} - \sqrt{\gamma_1^{LW}}) \quad (9)$$

$$\Delta G^{AB}_{y_0\ 132} = 2\sqrt{\gamma_3^+}(\sqrt{\gamma_1^-} + \sqrt{\gamma_2^-} - \sqrt{\gamma_3^-}) + 2\sqrt{\gamma_3^-}(\sqrt{\gamma_1^+} + \sqrt{\gamma_2^+} - \sqrt{\gamma_3^+}) - 2\sqrt{\gamma_1^+\gamma_2^-} - 2\sqrt{\gamma_1^-\gamma_2^+} \quad (10)$$

In equations (7) and (8), microbes are modeled as a sphere having a radius at least one order of magnitude less than that of the medium matrix. Therefore, a sphere-flat plate interaction is adopted to simplify the interactions between microorganisms and the medium matrix.

When the medium surface is occupied by deposited bacterial cells, the interactions between bacterial cells in solution and deposited cells on the medium surface will impact the interactions between the microbes in solution and the medium matrix:

$$\Delta G(y)^{LW}_{131} = \pi R \frac{y_0^2}{y} \Delta G^{LW}_{y_0 131} \quad (11)$$

$$\Delta G(y)^{AB}_{131} = \pi R y_0 e^{(y_0 - y)/\lambda} \Delta G^{AB}_{y_0 131} \quad (12)$$

where $\Delta G_{y0131}{}^{LW}$ and $\Delta G_{y0131}{}^{AB}$ are Gibbs energies of interactions between spheres 1, immersed in water 3 at the distance of $y_0$ and can be calculated using equations (9) and (10) by substituting 1 for 2.

The electrostatic interaction free energies, $\Delta G_{131}{}^{EL}$ and $\Delta G_{132}{}^{EL}$ can be evaluated by (constant potential approach) (valid for $0.1 < \kappa y < 300$, van Oss, 1994):

$$\Delta G(y)^{EL}_{131} = 0.5 \cdot \pi \varepsilon \varepsilon_0 R \psi_{01}{}^2 Ln(1 + e^{-\kappa y})] \quad (13)$$

$$\Delta G(y)^{EL}_{132} = \pi \varepsilon \varepsilon_0 R \psi_{01} \psi_{02} Ln(1 + e^{-\kappa y})] \quad (14)$$

where ε and $\varepsilon_0$ are the relative dielectric permittivity of water (78.55 for water at 25°C) and permittivity under vaccum (8.854 x $10^{-12}$ C/V·m) respectively; $\psi_{01}$, $\psi_{02}$ potentials at the surfaces of the microbes and the medium matrix; 1/κ Debye-Hückel length and also an estimation of the effective thickness of the electrical double layer (Marshall *et al.*, 1984). $\psi_{01}$, $\psi_{02}$ can be calculated based on the following equation:

$$\psi_0 = \zeta(1 + z/a)\exp(\kappa z) \qquad (15)$$

where $\zeta$ is the zeta potential measured at the slipping plate; z distance from the particle surface to the slipping plate that is generally on the order of 5 Å (van Oss, 1994); and *a* radius of the particle; . $\zeta$-potentials of the bacteria and the medium were measured by suspending in a $10^{-5}$ M NaCl solution using Lazer Zee Meter (Model 501, Pen Kem, Inc.).

*Bacterial transport parameter determination* The deposition coefficient $k_c$ that describes the microbial irreversible sorption in porous media can be measured using equation (16) (Bolster *et al.*, 1998):

$$k_c = \frac{v}{L}\{-\mathrm{Ln}(fr) + \frac{[\mathrm{Ln}(fr)]^2}{Pe}\} \qquad (16)$$

where L is the length between the injection and where the bacteria are collected or packed bed column length (m); *fr* microbial fraction recovery; *Pe* Peclet number, which can be obtained from studying the BTCs of a conservative tracer based on equation (17) (Annable *et al.*, 1997 and Jin *et al.*, 1995):

$$\sigma^2 = \tau^2 \cdot [\frac{2}{Pe} - \frac{2}{Pe^2} \cdot (1 - e^{-Pe})] \qquad (17)$$

where σ is the standard deviation and τ measured average residence time for the tracer in the reactor (sec), determined by:

$$\tau = \frac{\int_0^\infty t \cdot C(t)dt}{\int_0^\infty C(t)dt} \tag{18}$$

$$\sigma^2 = \frac{\int_0^\infty C(t)(t-\tau)^2 dt}{\int_0^\infty C(t)dt} = \frac{\int_0^\infty t^2 \cdot C(t)dt}{\int_0^\infty C(t)dt} - \tau^2 \tag{19}$$

In equations (18) and (19), C is the measured concentration of the tracer at the outlet of the column ($g/m^3$) and t elapsed time from the initial injection of the tracer (sec).

*Column experiments* The transport of three bacterial strains through the porous medium of COA was evaluated in column experiments, which were conducted using a column from Kimble-Kontes (Vineland, NJ) with 2.5-cm ID × 15-cm length (Table 6.1). COA was initially saturated with 10 pore volumes of sterilized NPDI, which was introduced at the inlet of the column by a peristaltic pump (Masterflex, Cole-Parmer, Vernon Hills, IL) at flow rates of 0.06 ml/sec and 0.1 ml/sec. A conservative pulse tracer (chloride) BTC was determined separately before the introduction of bacteria. The conductivity (μmhos) of the tracer was measured and used in equations (17) to (19) to estimate *Pe*. For each run, 10 ml of bacterial solution (concentration predetermined by ATP analysis) was injected via a syringe using an injection port. The column was continuously flushed with sterilized NPDI until a background ATP signal was detected from the elution collected by

**Table 6.1 Summary of the Parameters Used in Column Experiment**

| Microorganisms | Diameter |
|---|---|
| *P. fluorescens* | ~ 0.6 μm |
| *P. putida* | ~ 0.6 μm |
| *P.* sp | ~ 0.6 μm |

| Porous Media | Radius | Porosity | Density |
|---|---|---|---|
| COA | ~ 65 μm | 0.48 | 2.62 g/cm$^3$ |

| Column Experiment | |
|---|---|
| Column | 2.5-cm ID x 15-cm Length |
| Flow Rate | 0.06 ml/sec and 0.1 ml/sec |
| *Pe* | 152.8 (0.06 ml/sec) and 254.6 (0.1 ml/sec) |

a fraction collector. The concentrations of ATP were then used to generate BTCs for each bacterium. For each bacterial strain at one flow rate, three runs were performed, and the inconsistency of BTCs was within 5% (95% CI). A representative BTC for each bacterium at each flow rate is illustrated in Figure 6.1. After each run, mass balance was performed. Bacterial contents inside the column were measured by making the medium a suspended solution to perform an ATP measurement. Relative parameters used in column experiments are listed in Table 6.1.

**Results**

All the BTCs (Figure 6.1) had a diffuse front upon a step concentration increase and a self-sharpening front in the case of step decrease. This behavior demonstrated that the retention of the microbes on the medium increased with the increasing concentration in solution, which led to a broad, diffuse front. In the case of step decrease (desorption), the retention time decreased in time and led to the development of a narrow, self-sharpening front (Bürglsser et al., 1993). What was more, the BTCs of the relative microbial

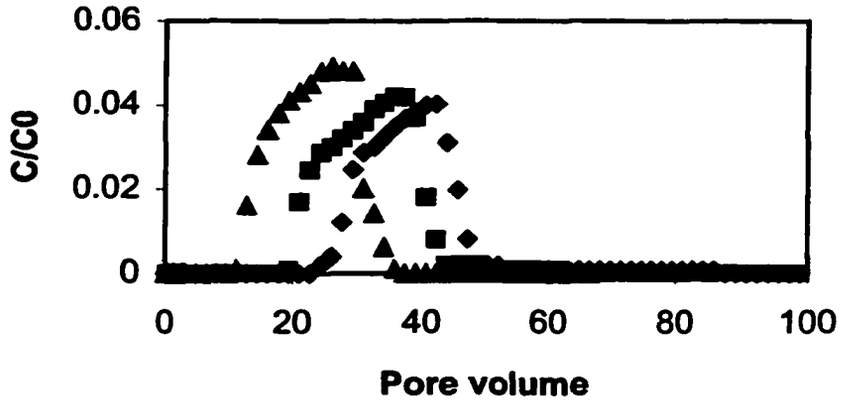


**Figure 6.1** BTCs of the microbes on COA O — *P. fluorescens*; — *P. putida*; Δ — *P.* sp.

concentration versus pore volume of the same microbes at different pore velocities nearly superimposed.

Bürglsser et al. (1993) developed a method that allowed rapid measurements of an entire, possibly nonlinear sorption isotherm by a simple integration of the diffuse front of the BTCs. Based on this method, the concentration of reversibly adsorbed bacteria on the porous medium, S, can be obtained by integrating the experimental record of the retention time t(c) if the dispersion term in equation (3) is neglected (D = 0):

$$S = \frac{\theta}{\rho_b(1-\theta)} \int_0^c \left(\frac{t(c')}{t_0} - 1\right) dc' - \int_0^c t(c') k_c dc' \qquad (20)$$

where $t_0 = L/v$ and is the average microbial travel time in the column. The insignificant role of hydrodynamic dispersion on microbial transport has been proven by Unice and Logan (2000). Schweich and Sardin (1981) also demonstrated that hydrodynamic dispersion can be neglected for Pe > 100. For this research, all the column experiments were performed with Pe > 100, thus equation (20) can be used to determine the microbial isotherms.

The microbial isotherms (Figure 6.2) were obtained using equation (20) from the microbial BTCs. Since the BTCs of each bacterium at different flow rates superimposed, the isotherms were unique for each bacterium. In other words, microbial sorption isotherms were not impacted by the flow rate. All the three bacterial strains had a concave isotherm on COA. The microbial sorption isotherms can be described by the Freundlich expression:

$$S = K_{fr} C_e^N \qquad (21)$$

where $K_{fr}$ is the Freundlich partition coefficient $[(m^3/g)^N]$; N Freundlich exponent coefficient. $K_{fr}$ and N values for the microbes are listed in Figure 6.2, which were obtained using numerical simulation.

**Discussion**

The underlying principle behind the isotherms resulted from some forms of bonding between the microbes and sorption receptor sites on the solid. The amount of sorption

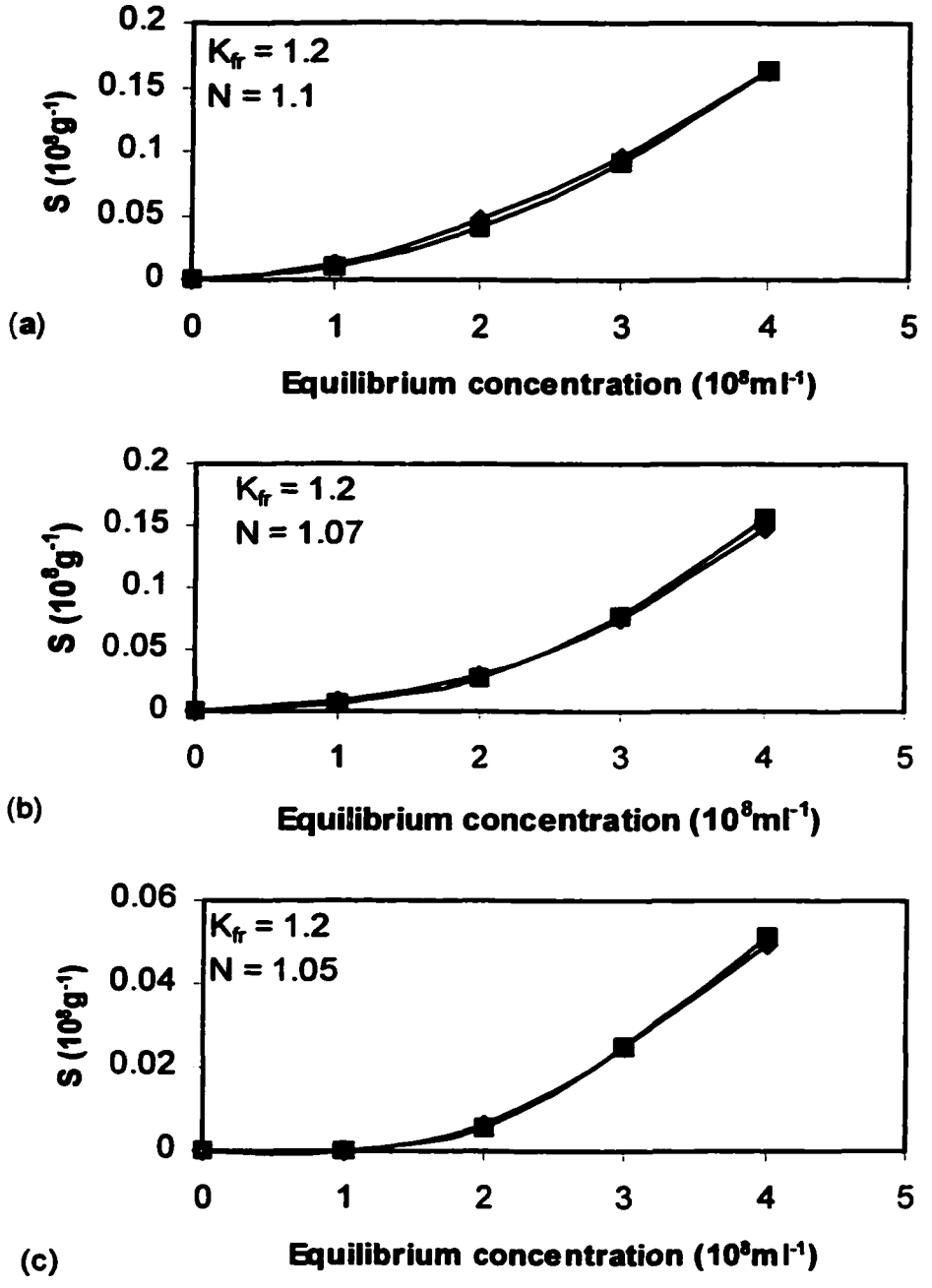


**Figure 6.2** Microbial sorption isotherms (a) *P. fluorescens*; (b) *P. putida*; (c) *P.* sp.;

**Table 6.2 Bacterial and Medium Surface Thermodynamic Properties**

| Stain/Medium | ζ-potential (mV) | $\gamma^{LW}$ ($mJ/m^2$) | $\gamma^{+}$ ($mJ/m^2$) | $\gamma^{-}$ ($mJ/m^2$) |
|---|---|---|---|---|
| *P. fluorescens* | -10.2±0.1 | 35.4 | 0.42 | 56.9 |
| *P. putida* | -10.6±0.2 | 34.8 | 0.62 | 55.4 |
| *P.* sp | -10.8±0.1 | 34.3 | 0.72 | 53.4 |
| COA | -42.5±0.6 | 27.4 | 0.03 | 13.7 |

**Table 6.3 Interaction Free Energies at a Secondary Maximum**

| Strain/Medium | *P. fluorescens* | *P. putida* | *P.* sp |
|---|---|---|---|
| $\Delta G_{131}^{LW}$ (kT) | -7.42 | -6.84 | -6.37 |
| $\Delta G_{131}^{AB}$ (kT) | -1.97 | -1.83 | -1.70 |
| $\Delta G_{131}^{EL}$ (kT) | 11.09 | 11.97 | 12.43 |
| $\Delta G_{131}^{TOT}$ (kT) | 1.70 | 3.30 | 4.36 |
| $\Delta G_{132}^{LW}$ (kT) | -6.54 | -6.28 | -6.06 |
| $\Delta G_{132}^{AB}$ (kT) | -0.56 | -0.53 | -0.48 |
| $\Delta G_{132}^{EL}$ (kT) | 92.46 | 96.11 | 97.81 |
| $\Delta G_{132}^{TOT}$ (kT) | 85.36 | 89.30 | 91.27 |

that occurred was dependent on the surface characteristics of the microbes and porous medium. More generally, interfacial interactions between the microbes and the porous medium were thought to be the driving force. To develop a surface thermodynamic explanation of the isotherms, interfacial interactions of suspended bacterial cells in the solution with the medium matrix as well as with deposited cells on the medium surface were investigated. Loosdrecht et al. (1989) and Chen and Strevett (2001) discovered that microbial reversible sorption was a function of the total free energy of the interactions between bacterial cells and the medium matrix at the secondary maximum.

During the transport, deposited cells (due to irreversible sorption) on the medium surface, cell-coating, altered the interactions between suspended bacterial cells in the solution and the medium by changing the medium surface properties. Based on the surface thermodynamic properties of the microbes and the medium (Table 6.2), the interaction free energies between the microbes and the medium at the secondary maximum were calculated (Table 6.3). As the total free energy of attractive cell-cell (between suspended and deposited bacterial cells on the medium surface) interactions of $\Delta G_{131}^{TOT}$ at the secondary maximum (1.70kT, 3.30 kT and 4.36 kT for *P. fluorescens*, *P. putida* and *P.* sp. respectively) was smaller (negatively greater) than that of the cell-solid (between suspended bacterial cells and the medium surface) interactions (85.36 kT, 89.30 kT and 91.27 kT), suspended bacterial cells in the solution had a greater potential to partition on the medium surface covered with deposited cells. This led to an increase in bacterial reversible adsorption with the increase of microbial solution concentration as deposited cells on the medium surface increased accordingly. Since the more the medium surface

is covered with deposited cells, the more impact cell-cell interactions will have on the microbial reversible adsorption, which leads to a concave isotherm.

Bacterial isotherms were verified in the column experiments. The microbial sorption isotherms $s = k_{fr} c_e^N$ was incorporated into equation (3) (assuming equilibrium was reach during the microbial transport inside the column):

$$(1+\frac{1-\theta}{\theta}\rho_p N K_{fr} C^{N-1})\frac{\partial C}{\partial t} = D\frac{\partial^2 C}{\partial x^2} - v\frac{\partial C}{\partial x} - k_c C \qquad (22)$$

Equation (22) was then solved using numerical methods with the following initial and boundary conditions:

$C=C_0$ x=0 t=0 (22a)

C=0 x=L t=0 (22b)

where $C_0$ is the initial injected microbial concentration. The simulated results were compared against experimental observations and the experimental results were successfully represented by this numerical model (Figure 6.3). The fitness of the model simulation and experimental observation also confirmed that the Convection-Dispersion Model incorporated with Filtration Model to account for irreversible soprtion could be sued to describe microbial transport in porous media.

Theoretically, reversible sorption of the microbes on the porous medium that is determined by microbial sorption isotherms should not be impacted by the transport

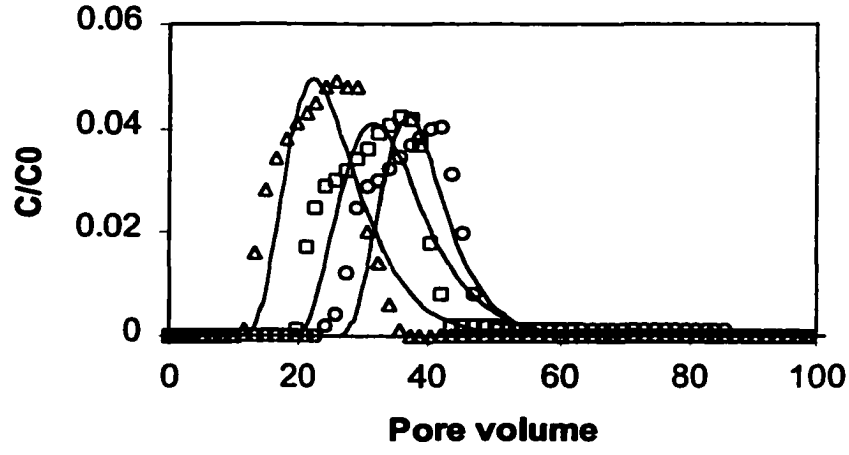


**Figure 6.3** Theoretical simulations of the microbial BTCs on COA

O — *P. fluorescens*; — *P. putida*; Δ — *P.* sp.; — Theoretical simulations.

velocity as long as the equilibrium is reached (Dohse and Lion, 1994); while irreversible sorption or deposition of the microbes on the porous medium is greatly impacted by the transport velocity through its impact on retention time (Bolster et al., 1998). This was also validated in this study. The same bacterial strain had the same sorption isotherms but different deposition coefficient at different flow rates (4.64 $hr^{-1}$, 4.39 $hr^{-1}$ and 4.17 $hr^{-1}$ for *P. fluorescens*, *P. putida* and *P.* sp. at a flow rate of 0.06 ml/sec respectively and 7.74 $hr^{-1}$, 7.33 $hr^{-1}$ and 6.96 $hr^{-1}$ at a flow rate of 0.1 ml/sec). To investigate the reason that the BTCs of the same microbes at different flow rates nearly superimposed, equation (20) is rearranged that incorporated equation (16) and the concentration dependent retention time

is expressed in term of microbial sorption isotherms and fraction recovery (obtained by integration of the BTCs):

$$\frac{t(c')}{t_0} = \frac{\frac{\rho_b(1-\theta)}{\theta}\frac{dS}{dC}+1}{1+Ln(fr)-\frac{Ln^2(fr)}{Pe}} \tag{23}$$

In equation (23), the term $\frac{Ln^2(fr)}{Pe}$ can be neglected for Pe > 100 due to the insignificant role of hydrodynamic dispersion on microbial transport under this condition (Unice and Logan, 2000; Schweich and Sardin, 1981). Microbial isotherms ($\frac{dS}{dC}$) is not impacted by the flow rate (Dohse and Lion, 1994), neither is the fraction recovery (*fr*) (Chen and Strevett, 2001). Based on equation (23), as the term $\frac{Ln^2(fr)}{Pe}$ was neglected in this research (Pe = 152.8 for the flow rate of 0.06 ml/sec and Pe = 254.6 for 0.1 ml/sec), the concentration dependent retention time was independent of transport velocity, which made the BTCs of the same microbes nearly superimposed at different flow rates. It should also be noted that for conditions where Pe < 100, or hydrodynamic dispersion cannot be ignored, the BTCs will be different for different flow rates.

**Conclusion**

The main achievement of this study is to provide a way of determination of microbial adsorption isotherms using column experiments, which cannot be achieved using the traditional batch methods due to the difficulty of distinguishing between reversible and irreversible sorption. A further advantage of the column methods is that a high solid to solution ratio close to that is encountered in the natural system of interest is used for the

determination of microbial sorption isotherms. Also, a surface thermodynamic explanation of the concave-shaped microbial sorption isotherms was also reached in this study and the impact of transport velocity on the microbial BTCs was discussed. This study will be of great importance in understanding the fate and transport of microbes in the subsurface, and in guidance of *in-situ* bioremediation.

**Acknowledgements**

The work was support in part by National Science Foundation through Grant No. BES-9733969 to the University of Oklahoma.

**References**

1. Annable, M.D., Rao P.S.C., Hatfield K., Graham W.D., Wood A.L., and Enfield C.G. (1998) Partitioning Tracers for Measuring Residual NAPL: Field-Scale Test Results. *J. Environ. Eng.*, 124: 498-503.

2. Bellin C.A. and Rao P.S.C. (1993) Impact of Bacterial Biomass on Contaminant Sorption and Transport in Subsurface Soil, *Appl. Environ. Microbiol.*, 59:1813-1820.

3. Bolster C. H., Hornberger G. M., Mills A. L. and Wilson J. L. (1998) A Method for Calculating Bacterial Deposition Coefficients Using the Fraction of Bacteria Recovered from Laboratory Columns, *Environ. Sci. Technol.*, 32:1329-1332.

4. Bürgisser C.S., Černík M., Borkovec M. and Sticher H. (1992) Determination of Nonlinear Adsorption Isotherms from Column Experiments: An Alternative to Batch Studies, *Environ. Sci. Technol.*, 27: 943-948.

5. Chen, G. and Strevett, K.A. (2002) Surface Free Energy Relationships Used to Evaluate Microbial Transport, *J. Environ. Eng.*, 128:1-8.

6. Dohse D.M. and Lion L.W. (1994) Effect of Microbial Polymers on the Sorption and Transport of Phenanthrene in a Low-Carbon Sand, *Environ. Sci. Technol.*, 4:541-548.

7. Elimelech M. and O'Melia C.R. (1990) Kinetic of Deposition of Colloidal Particles in Porous Media, *Environ. Sci. Technol.*, 24:1528-1536.

8. Fontes D.E., Mills A.L., Hornberger G.M. and Herman J.S. (1991) Physical and Chemical Factors Influencing Transport of Microorganisms through Porous Media, *Appl. Environ. Microbiol.*, 57:2473-2481.

9. Gamerdinger A.P., van Rees K.C.J., Rao P.S.C. and Jessup R.E. (1994) Evaluation of *in situ* Columns for Characterizing Organic Contaminant Sorption during Transport, *Environ. Sci. Technol.*, 28:376-382.

10. Gannon J.T., Mingelgrin U., Alexander M. and Wagenet R.J. (1991) Bacterial Transport through Homogeneous, *Soil Biol. Biochem.* 23:1155-1160.

11. Grasso D., Smets B.F., Strevett K.A. and Machinist B.D., van Oss C. J., Giese R. F. and Wu W. (1996) Impact of Physiological State on Surface Thermodynamics and Adhesion of Pseudomonas aeruginosa, *Environ. Sci. Technol.*, 30:3604-3608.

12. Hancock I. And Poxton I. (1988) *Bacterial Cell Surface Techniques*, John Wiley & Sons, New York.

13. Harvey R.W. and Garabedian S.P. (1991) Use of Colloid Filtration Theory in Modeling Movement of Bacteria through a Contaminated Sandy Aquifer, *Environ. Sci. Technol.*, 25:178-185.

14. Hornberger G.M., Mills A.L. and Herman J.S. (1992) Bacterial Transport in Porous Media: Evaluation of a Model Using Laboratory Observations, *Water Resources Research*, 28:915-938.

15. Jenkins M.B. and Lion L.W. (1993) Mobile Bacteria and Transport of Polynuclear Aromatic Hydrocarbons in Porous Media, *Appl. Environ. Microbiol.*, 59:3306-3313.

16. Jin M., Delshad M., Dwarakanath V., McKinney D.C., Pope G.A., Sepehrnoori K., Tiburg C., and Jackson R.E. (1995) Partitioning Tracer Test for Detection, Estimation, and Remediation Performance Assessment of Subsurface Phase Liquid, *Water Resour. Res.*, 31(5), 1201-1211.

17. Karapanagioti H.K., Kleineidam S., Ligouis B., Sabatini D. A. and Grathwohl P. (1999) Phenanthrene Sorption with Heterogeneous Organic Matter in a Landfill Aquifer Material, *Physics and Chemistry of the Earth*. 24:535-541.

18. Knox R.C., Sabatini D.A. and Canter L.W. (1993) *Subsurface Transport and Fate Processes*, Lewis Publishers, New York.

19. Ku C., Joseph D., Henry Jr., Ranjani S. and Lloyd R. (1985) Particle Transfer from a Continuous Oil to a Dispersed Water Phase: Model Particle Study, *J. Colloid Interface Sci.*, 106:377-387.

20. Magee B.R., Lion L.W. and Lemley A.T. (1991) Transport of Dissolved Organic Macromolecules and Their Effect on the Transport of Phenanthrene in Porous Media, *Environ. Sci. Technol.*, 25:323-331.

21. Marshall K. C., Breznak J. A., Calleja G. B., Mcfeters G. A. and Rutter P. R. (1984) *Microbial Adhesion and Aggregation*, Springer-Verlag, New York.

22. Meinders J.M., van der Mei H.C. and Bussher H.J. (1995) Deposition Efficiency and Reversibility of Bacterial Adhesion under Flow, *Journal of Colloid and Interface Science*, 176:329-341.

23. Nkedi-Kizza P., Rao P.S.C. and Hornsby A.G. (1987) Influence of Organic Cosolvents on Leaching of Hydrophobic Organic Chemicals through Soils, *Environ. Sci. Technol.*, 21:1107-1111.

24. Powelson D.K. and Mills A.L. (1998) Water Saturation and Surfactant Effects on Bacterial Transport in Sand Columns, *Soil Science*, 163:694-704.

25. Schweich D. and Sardin, M. (1981) Adsorption, Partition, Ion Exchange and Chemical Reaction in Batch Reactors or in Columns – a Review, J. Hydrol., 50 : 1 – 33.

26. van oss, C.J. (1994) *Interfacial Forces in Aqueous Media*, Marcel Dekker, New York.

27. Unice K.M. and Logan B.E. (2000) Insignificant Role of Hydrodynamic Dispersion of Bacterial Transport, *J. Environ. Eng.*, 126: 491- 500.

28. van Loosdrecht, M.C.M., Lyklema, J., Norde, W. and Zehnder, A.J.B. (1989) Bacterial Adhesion: A Physicochemical Approach, Microb. Ecol., 17: 1-15.

29. Wålinder M.E. and Gardner D.J. (1999) Factors Influencing Contact Angle Measurements on Wood Particles by Column Wicking, *J. Adhesion Sci. Technol*, 13:1363-1374.

# CHAPTER 7

# EFFECT OF FLOW RATE ON MICROBIAL TRANSPORT


## Abstract

Effect of flow rate on microbial transport in the subsurface was investigated by a column transport study of *Escherichia coli*, *Pseudomonas fluorescens*, and *Pseudomonas aeruginosa* through a model medium of silica gel and an alluvial loam from Central Oklahoma Aquifer (COA). Retardation factor was independent of flow rate (16.19 and 61.27 for *E. coli*, 8.17 and 15.97 for *P. fluorescens*, and 10.13 and 18.15 for *P. aeruginosa* in silica gel and COA, respectively) while deposition coefficient increased with the increase of flow rate by a factor of 1. Microbial fraction recovery was not a function of flow rate (24.4% and 1.96% for *E. coli*, 30.8% and 3.64% for *P. fluorescens*, and 27.5% and 2.72% for *P. aeruginosa* in silica gel and COA, respectively regardless of flow rates).



Key words: Microbial transport, flow rate, *Escherichia coli*, *Pseudomonas fluorescens*, and *Pseudomonas aeruginosa*.


## Introduction

The movement and spreading of microbes in the subsurface is impacted by the flow rate and can be described by a combined model that incorporates the Deep-Bed Filtration Model into a simple Convection-Dispersion Model (ignoring biodegradation) (Chen and Strevett, 2001; Harvey and Garabedian, 1991):

$$\theta\frac{\partial C}{\partial t}+(1-\theta)\rho_b\frac{dS}{dt}=D\theta\frac{\partial^2 C}{\partial x^2}-v\theta\frac{\partial C}{\partial x}-\theta k_c C \quad (1)$$

where $\theta$ is the porosity ($m^3/m^3$); C microbial concentration in solution (number of cells/$m^3$); t elapsed time from the initial microbial injection (sec); $\rho_b$ sediment bulk density ($g/m^3$); S concentration of reversibly adsorbed microbes on the porous medium (cells/g); D hydrodynamic dispersion coefficient ($m^2$/sec); v interstitial pore water velocity (m/sec); x longitudinal coordinate (m); and $k_c$ deposition coefficient that indicates the rate of irreversible sorption of microbes in the porous medium ($sec^{-1}$).

The reversible sorption of microbes in porous media can be expressed in term of solution concentration (Knox *et al.*,1993):

$$\frac{dS}{dt}=\frac{dS}{dC}\frac{\partial C}{\partial t} \quad (2)$$

By substituting equation (2) into equation (1) and rearranging, a one-dimension transport can be expressed as:

$$(1+\frac{1-\theta}{\theta}\rho_p\frac{dS}{dC})\frac{\partial C}{\partial t}=D\frac{\partial^2 C}{\partial x^2}-v\frac{\partial C}{\partial x}-k_c C \quad (3)$$

where $1+\frac{1-\theta}{\theta}\rho_b\frac{dS}{dC}$ is defined as retardation factor, R, and is the average transport velocity of bacteria ($v_{av}$) relative to that of water ($v_w$), such that $R = v_{av}/ v_w$. Thus, retardation factor is the parameter that describes reversible sorption (i.e., retardation) of microbes when passing through the porous media. The average retardation factor of microbial transport in porous media can be estimated using the first temporal moment of microbial BTCs (Dohse and Lion, 1994):

$$R = \frac{\int_0^\infty \frac{C}{C_0}\theta d\theta}{\int_0^\infty \frac{C}{C_0} d\theta} - \frac{\theta_p}{2} \qquad (4)$$

where $\theta$ is the pore volume and $\theta_p$ is the pulse width. Deposition coefficient $k_c$ that describes the irreversible sorption of microbes in porous media can be calculated as (Bolster *et al.*, 1998):

$$k_c = \frac{v}{L}\{-\mathrm{Ln}(fr) + \frac{[\mathrm{Ln}(fr)]^2}{Pe}\} \qquad (5)$$

where L is the length of the column; *fr* microbial fraction recovery from the outlet and Pe=vL/D Peclet number.

The objective of this study is to investigate the effect of flow rate on microbial transport in the subsurface, specifically, the effect of flow rate on microbial retardation and deposition during their transport in the subsurface. This was achieved by a column transport study of *E. coli*, *P. fluorescens*, and *P. aeruginosa* through a model medium of silica gel and an alluvial loam from Central Oklahoma Aquifer (COA).

**Experimental Protocol**

*E. coli* (JM109) was a generous gift from the Department of Botany and Microbiology at the University of Oklahoma. It was cultured on Nutrient Broth (Difco 0003) at 37°C until late stationary state. *P. fluorescens* (P-17) and *P. aeruginosa* were obtained from ATCC (Catalog No. 17559 and 15152) and grown on Nutrient Broth (Difco 0003) at 26°C and 30°C, respectively until late stationary state. Quantification was achieved

through a biochemical assay using Adenosine Triphosphate (ATP) analysis (Turner Design, Sunnyvale, CA) as described before (Chen and Strevett, 2001). The transport of three bacterial strains through porous media of silica gel and COA was evaluated in column experiments, which were conducted using a column from Kimble-Kontes (Vineland, NJ) with 2.5-cm ID × 15-cm length (Table 7.1). Silica gel and COA were initially saturated with 10 pore volumes of sterilized NPDI, which was introduced at the inlet of the column by a peristaltic pump (Masterflex, Cole-Parmer, Vernon Hills, IL) at a series of flow rates of 0.03, 0.06, 00.8 and 0.10 ml/sec. The median grain radius of silica gel was assumed to be 100 μm according to U.S. standard sieve sizes and their corresponding open dimension (Holtz and Kovacs, 1981). Before being packed in the column, it was sterilized at 121°C for 20 min. The median grain radius size of COA was 65 μm with 38% passing a 200 sieve. The organic fraction and hydraulic conductivity were reported to be $0.340 \pm 0.20$ and $(8.2 \pm 1.3) \times 10^{-5}$ cm/s (Karapanagioti et al., 1999). Due to concerns about structural and chemical alterations, COA was not sterilized. Instead, it was air dried and stored desiccated to minimize the presence of an active bacterial population. Hydrodynamic dispersion coefficient was determined separately using a conservative pulse tracer (chloride) before the introduction of bacteria as described before (Chen and Strevett, 2001).

For each run, 10 ml of bacterial solution whose concentration was predetermined by ATP analysis (Chen and Strevett, 2001) was injected via a syringe using an injection port. The column was continuously flushed with sterilized NPDI until a background ATP signal was detected from the elution collected by a fraction collector. The concentrations of

ATP were then used to generate breakthrough curves (BTCs) for each bacterium. Each run was performed in triplicate. After each run, mass balance was performed. Bacterial contents inside the column were measured by making the medium a suspended solution to perform an ATP measurement.

**Table 7.1 Summary of the Parameters Used in Column Experiment**

| Microorganisms | Radius |
|---|---|
| *E. coli* | 0.5 μm |
| *P. fluorescens* | 0.3 μm |
| *P. aeruginosa* | 0.3 μm |

| Porous Media | Radius | Porosity | Density |
|---|---|---|---|
| Silica gel | ~ 100 μm | 0.51 | 2.65 g/cm$^3$ |
| COA | ~ 65 μm | 0.48 | 2.62 g/cm$^3$ |

| Column Experiment | |
|---|---|
| Column | 2.5-cm ID x 15-cm Length |
| Flow Rate | 0.03, 0.06,0.08 and 0.10 ml/sec |
| *Pe* | 13.9 (silica gel) and 76.4(COA) |
| Pulse Width | 0.133 pore volumes |

**Results and Discussion**

Retardation factor was observed to be independent of flow rate, and the microbes had the same retardation factor when transporting in the same medium at different flow rates (16.19 and 61.27 for *E. coli*, 8.17 and 15.97 for *P. fluorescens*, and 10.13 and 18.15 for *P. aeruginosa* in silica gel and COA, respectively). This is understandable as based on its definition that retardation factor is a function of microbial sorption isotherms rather than flow rate. Equilibrium is usually assumed during microbial transport in porous media, which minimizes the effect of flow rate on sorption isotherms.

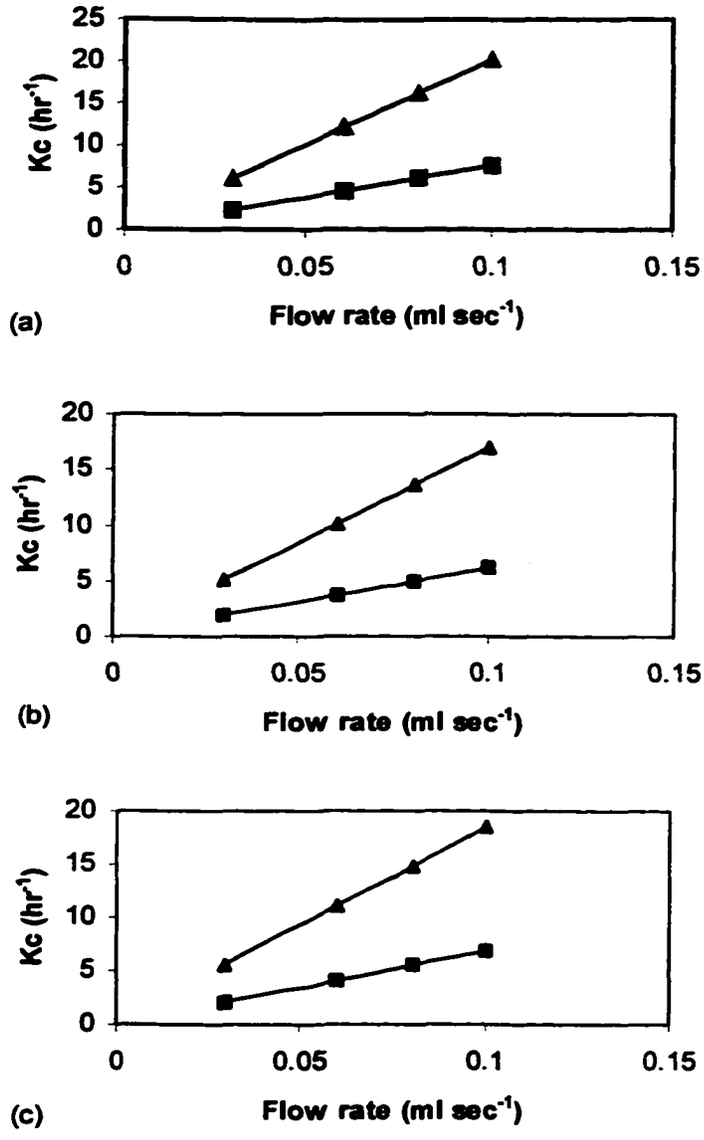


**Figure 7.1** Deposition coefficient, $k_c$ versus flow rate (a) *E. coli*, (b) *P. fluorescens*, and (c) *P. aeruginosa* in (■)silica gel and (▲) COA

Deposition coefficient, on the other hand, is effected by flow rate by a factor of 1 (Figure 7.1). According to equation (5), besides flow rate, deposition coefficient is also a function of Pe and fraction recovery. Pe is obviously a function of flow rate, which is defined as Pe = vL/D. Fraction recovery is not a function of flow rate (24.4% and 1.96% for *E. coli*, 30.8% and 3.64% for *P. fluorescens*, and 27.5% and 2.72% for *P. aeruginosa* in silica gel and COA, respectively regardless of flow rates). Unice and Logan (2000) have demonstrated that the impact of dispersion on microbial transport is insignificant. Therefore, it can be concluded from equation (5) that flow rate impacts microbial deposition by a factor of 1.

Fraction recovery is determined by interfacial interaction free energies between microbes and medium surfaces The interfacial interactions consist of DLVO forces and hydrodynamic forces (Chen and Strevett, 2002). DLVO forces between biotic microbes and abiotic surfaces that should be considered in aqueous media include: apolar, or Lifshitz-van der Waals (LW) interactions; polar, electron-donor/electron-acceptor, or Lewis acid-base (AB) interactions; and electrostatic (EL) interactions (van Oss, 1994). The drag forces due to hydrodynamics can be calculated by (Tchnobanoglous and Burton, 1991):

$$F = 0.5\rho A v^2 C_D^2 \qquad (6)$$

where ρ is the liquid density ($g/m^3$); A projected microbial surface area facing the flow; $C_d$ drag coefficient and can be calculated by (Tchnobanoglous and Burton, 1991):

$$C_D \cong \frac{24}{\mathrm{Re}} \qquad \text{for } \mathrm{Re} < 1 \qquad (7)$$

$$C_D = \frac{24}{\mathrm{Re}} + \frac{3}{\sqrt{\mathrm{Re}}} + 0.34 \qquad \text{for } 1 < \mathrm{Re} < 1000 \qquad (8)$$

$$C_D \cong 0.4 \qquad \text{for } \mathrm{Re} > 1000 \qquad (9)$$

where Re is the Reynolds number and defined as $\frac{\rho v D}{\mu}$. D is the characteristic length or pore diameter and μ Fluid viscosity (dynamic) ($1.02 \times 10^{-3}$ Nsec/$M^2$ for water at 20°C).

Deposited cells on medium surfaces were assumed at the minimum equilibrium distance of 1.57 Å (van Oss, 1994) where the flow rate was minimal, thus drag forces due to hydrodynamics on deposited cells can be neglected according to equation (6) and DLVO forces were the actual driving forces in determining microbial fraction recovery. As DLVO forces were not a function of flow rate, fraction recovery was kept constant.

**Acknowledgements**

The work was support in part by National Science Foundation through Grant No. BES-9733969 to the University of Oklahoma.

**References**

1. Bolster C. H., Hornberger G. M., Mills A. L. and Wilson J. L. (1998) A Method for Calculating Bacterial Deposition Coefficients Using the Fraction of Bacteria Recovered from Laboratory Columns, *Environ. Sci. Technol.*, 32:1329-1332.

2. Chen, G. and Strevett, K.A. (2002) Surface Free Energy Relationships Used to Evaluate Microbial Transport, *J. Environ. Eng.*, 128:1-8.

3. Dohse D.M. and Lion L.W. (1994) Effect of Microbial Polymers on the Sorption and Transport of Phenanthrene in a Low-Carbon Sand, *Environ. Sci. Technol.*, 4:541-548.

4. Harvey R.W. and Garabedian S.P. (1991) Use of Colloid Filtration Theory in Modeling Movement of Bacteria through a Contaminated Sandy Aquifer, *Environ. Sci. Technol.*, 25:178-185.

5. Holtz, R. D. and Kovacs, W. D. (1981) *An Introduction to Geotechnical Engineering*, Prentice-Hall, Inc., Englewood Cliffs, NJ.

6. Karapanagioti, H. K., Kleineidam, S., Ligouis, B., Sabatini, D. A. and Grathwohl, P. (1999) Phenanthrene Sorption with Heterogeneous Organic Matter in a Landfill Aquifer Material, *Physics and Chemistry of the Earth.* 24:535-541.

7. Knox R.C., Sabatini D.A. and Canter L.W. (1993) *Subsurface Transport and Fate Processes*, Lewis Publishers, New York.

7. Tchobanoglous, G. and Burton, F. (1991) *Wastewater Engineering, Treatment, Disposal and Reuse*, MaGraw-Hill, Inc., New York.

8. Unice, K. M. and Logan, B. E. (2000) Insignificant Role of Hydrodynamic Dispersion of Bacterial Transport, *J. Environ. Eng.*, 126: 491- 500.

9. van oss, C.J. (1994) *Interfacial Forces in Aqueous Media*, Marcel Dekker, New York.

# CHAPTER 8

# IMPACT OF BACTERIAL EXTRACELLULAR POLYMERS ON LINDANE TRANSPORT


## Abstract

The extracellular polymers (ECPs) extracted from *Pseudomonas aeruginosa*, *Escherichia coli* JM109, and *Bacillus subtilis* cultures in their stationary phase at a concentration of 30 mg/l enhanced the transport of a model pesticide (lindane) in a sand column by 46.1%, 31.8% and 19.3% (decrease in retardation factor), respectively. This was because lindane had a larger partition coefficient value between the aqueous phase and the extracellular polymers (ECPs) ($K_d^{om}$) than between the aqueous phase and the medium matrix ($K_d^{s}$), and the ECPs had a smaller partition coefficient value between the aqueous phase and the medium matrix ($K_{dom}^{s}$) than lindane ($K_d^{s}$). Among the ECPs examined, the ECPs extracted from *P. aeruginosa* had the greatest efficiency in facilitating lindane transport, followed by *E. coli* JM109 and *B. subtilis*. It was concluded that when $K_d^{om}$ reached a certain value (greater than 10 ml/g), $K_{dom}^{s}$ would be the determining factor in facilitating lindane transport. Increase of the ECP concentration increased the efficiency in facilitating lindane transport until the ECP concentration reached 35 ± 5 mg/l. Above 35 ± 5 mg/l, the increase of the efficiency with the increase of the ECP concentration became moderate.



Key words: extracellular polymers (ECPs), lindane, transport, retardation factor, *Escherichia coli*, *Bacillus subtilis*, and *Pseudomonas aeruginosa*.

## Introduction

The movement of organic contaminants such as pesticides through the subsurface is of great importance when attempting to predict the spread of the contaminants and their potential impact on human health. The transport of most hydrophobic organic contaminants is usually retarded because of their sorption onto the porous matrix (Knox et al., 1993). However, these contaminants can migrate farther than predicted in the presence of some macromolecules or colloids, which is referred to as facilitated transport (Magee *et al.*, 1991; Enfield and Bengtsson 1988; Enfield *et al.*, 1982; Jury *et al.*, 1986 and Vinten *et al.*, 1983). Current research has focused on the use of biotic colloids such as dissolved organic macromolecules (Magee *et al.*, 1991) to facilitate the transport of the contaminants because the biotic colloids are potentially biodegradable (Jenkins and Lion, 1993). Extracellular polymers (ECPs) have been demonstrated to be an ideal biotic colloid that can facilitate the transport of some contaminants because the main components of the ECPs are polysaccharides, proteins, and nucleic acids, which are biodegradable (McCarthy and Zachara, 1989). For example, Falatko and Novak (1992) observed that a mixed bacterial polymer solution increased the solubility of gasoline in batch experiments and reduced the retardation in a sand-filled column, and Dohse and Lion (1994) found that the ECPs extracted from a Gram-negative ($G^-$) motile rod can act as agents that enhanced phenanthrene transport in natural system.

For ECPs to act as an effective carrier, two important criteria must be met: (1) The ECPs should be more mobile than the contaminants; (2) The ECPs should be able to bind the contaminants (Dohse and Lion, 1994). Based on above criteria, the ECPs must have a

smaller partition coefficient value between the aqueous phase and the medium matrix than the contaminants. Secondly, the contaminants must have a larger partition coefficient between the aqueous phase and the ECPs than that between the aqueous phase and the medium matrix.

The enhancement of lindane transport by the ECPs was described by a simple transport model to explain the movement, losses and retardation due to sorption, and spreading of lindane in the porous media. Since the examination of longitudinal lindane transport was the primary objective, the situation can be simplified by a one-dimensional equation (Freeze and Cherry, 1979):

$$\eta\frac{\partial C}{\partial t}+\rho_b\frac{\partial S}{\partial t}=D\eta\frac{\partial^2 C}{\partial x^2}-v\eta\frac{\partial C}{\partial x}-\eta R_d \qquad (1)$$

where $\eta$ is the porosity ($m^3/m^3$); C lindane concentration ($g/m^3$); t time elapsed from the initial injection of lindane (sec); $\rho_b$ the medium bulk density ($g/m^3$); S the concentration of reversibly sorbed lindane on the porous media (g/g); D the coefficient of hydrodynamic dispersion ($m^2$/sec); v the interstitial pore water velocity (m/sec); x the longitudinal coordinate (m); and $R_d$ the rate of loss due to degradation or other reasons such as slow desorption kinetics ($g/m^3$·sec).

If the reversible sorption of lindane onto the porous medium matrix is assumed to be linear and the sorption is rapid with respect to advection, and $R_d$ is ignored, the time variation of lindane on the solid and in solution can be related as (Knox *et al.*,1993):

$$\frac{\partial S}{\partial t}=\frac{\partial S}{\partial C}\frac{\partial C}{\partial t}=K_p\frac{\partial C}{\partial t} \qquad (2)$$

where $K_p$ is the partition coefficient of lindane between the aqueous phase and the porous medium matrix ($m^3/g$).

By substituting equation (2) into equation (1) and rearranging, one-dimensional transport can be expressed as:

$$(1+\frac{\rho_b}{\eta}K_p)\frac{\partial C}{\partial t} = D\frac{\partial^2 C}{\partial x^2} - v\frac{\partial C}{\partial x} - R_d \qquad (3)$$

where $(1+ \rho_d \cdot K_p/\eta)$ is defined as retardation factor, R, and is the ratio of average transport velocity of lindane ($v_{av}$) relative to that of water ($v_w$), or $R = v_w/ v_{av}$. By dividing equation (3) by R,

$$\frac{\partial C}{\partial t} = D^* \frac{\partial^2 C}{\partial x^2} - v^* \frac{\partial C}{\partial x} - R_d^* \qquad (4)$$

where $D^* = D/R$ is referred to as the effective coefficient of hydrodynamic dispersion; $v^* = v/R$ the effective interstitial pore water velocity; and $R_d^* = R_d/R$ the effective loss rate. Therefore, the retardation factor is an indicator of the "lag" of lindane transport due to reversible sorption.

The objectives of this study were to characterize the effects of the ECPs extracted from three commonly found bacteria on lindane (a model pesticide) transport in porous matrices. The results of the proposed research will provide an important guideline for ECP field applications.

## Materials

Lindane, the *gamma* isomer of 1,2,3,4,5,6-hexachlorocyclohexane (aqueous solubility 7.3 mg/l at 20°C, 1 atm) (Worthing, 1983) is a halogenated organic insecticide that has been used worldwide in agricultural applications. Due to its high toxicity and persistence in soil, the use of lindane has been prohibited in many countries. However, lindane residuals in the soil are still a critical problem, which attracts more and more attention. Lindane used in this research was obtained from Sigma (catalog No. H4625, approximately 99%). Similar to other chlorocarbon pesticides, it degrades slowly in the environment (half-life > 100 days) (Waldron, 1992).

Porous media used for this research included alluvial sand from the Canadian River Alluvium (CRA) (Norman, OK) and alluvial loam from the Central Oklahoma Aquifer (COA) (Norman, Oklahoma). The median grain size of CRA (collected at 0 – 0.16 m depth) was 89 μm with 7.0% passing a 200 sieve. The organic fraction and hydraulic conductivity were reported to be $0.0480 \pm 0.0056$ and $(1.6 \pm 0.3) \times 10^{-3}$ cm/s. The median grain size of COA was 65 μm with 38% passing a 200 sieve. The organic fraction and hydraulic conductivity were reported to be $0.340 \pm 0.200$ and $(8.2 \pm 1.3) \times 10^{-5}$ cm/s (Karapanagioti et al., 1999). Due to concerns of the structural and chemical alterations, neither CRA nor COA was sterilized. Instead, both were air dried and stored desiccated until use to minimize the bacterial activity. Lindane biodegradability screening was performed in microcosms with CRA and COA matrix as inocula in mineral based salts media. No significant (95% CI) loss (data not shown) was observed for a period of 14 days.

The ECPs used herein were extracted from *Escherichia coli* JM109, *Bacillus subtilis*, and *Pseudomonas aeruginosa*. *E. coli* JM109 was supplied by Department of Botany and Microbiology at the University of Oklahoma. *B. subtilis* and *P. aeruginosa* were obtained from ATCC (American Type Culture Collection) (Catalog No. 6051a, and 9027). *Escherichia coli* JM109 was cultured on Luria Broth media (Sigma L-3522) at 37°C; *B. subtilis* and *P. aeruginosa* were cultured on Nutrient Broth (Difco 0003) at 26°C and 30°C, respectively. The activity of *E. coli* JM109, *P. aeruginosa*, and *B. subtilis* against lindane was not performed since these bacteria were not directly applied to the column.

**Experimental Protocols**

*Physiological state determinations* Bacteria were harvested at stationary phase to obtain the maximum ECP productions. Stationary state was quantified using Adenosine Triphosphate (ATP) analysis based on the fact that the ATP content per cell is constant (Karl, 1980). 50 μl of the culture broth was sampled every 30 minutes for 60 hrs to determine the growth curves for each microbial species. The light emission produced by the reaction of ATP extracted from cells with luciferase as measured by a luminometer (Turner Design, TD-20/20) was compared to an ATP standard ($2.5 \times 10^{-8}$ g/ml ATP which is equivalent to $5 \times 10^{7}$ bacteria per ml) (Turner Design, 10 μg/ml ATP in HEPES buffer) to determine the number of viable bacterial cells. Thus, growth curves of the number of viable bacterial cells versus time were obtained, which were used as the references for the determination of the stationary phase for different species. *Escherichia coli* JM109, *P. aeruginosa* and *B. subtilis* were then cultured until they reached their

stationary phase by measuring their viable bacterial cells and then harvested for the extraction of the ECPs.

*Extraction of ECPs* The procedure for the extraction of ECPs was modified from techniques used by Dohse and Lion (1994) and Brown and Lester (1980). The bacterial strains collected at stationary phase (100 ml subsamples) were centrifuged at 4000 *g* (at 25°C) (IEC, International Centrifuge, Cat. No.783) for 15 min to separate the strains from the media. After washing twice with Nano-pure deionized water (NPDI), the strains were resuspended in NPDI by agitating on a Wrist Action Shaker (Burrell Scientific, Model 75) for 30 min and then centrifuged again at 8000 *g* (at 25°C) for 20 min followed by separate treatments of the supernatant and the pellet fractions. To extract soluble ECPs, the supernatant was filtered through a well-rinsed 0.22 μm cellulose acetate filter to remove any remaining cells and then the ECPs were precipitated by mixing with an equal volume of acetone. The precipitant was collected and transferred to a round bottom flask connected to a rotoevaporator. The evaporation process was allowed to proceed until the precipitation turned to a honey-color, viscous consistency and then freeze dried. The membrane-bound ECPs were extracted from the pellet of the second centrifugative. After the addition of EDTA (tetrasodium salt, 2% by weight, 100 ml), the pellets were agitated by vortex and then refrigerated for 30 min to solublize membrane-bound ECPs, then the suspension was centrifuged at 12000 *g* for 50 min at 5°C. The resulting supernatants obtained upon centrifugation were subsequently filtered through a well-rinsed 0.22 μm cellulose acetate filter, then freeze dried. The ECPs collected from

different procedures were combined and prior to use, ECPs were redissolved to make different concentration solutions.

*Isotherm Experiments* Batch isotherms were used to determine the sorption of lindane and the ECPs on the porous medium matrix as well as lindane on the ECPs. Linear isotherms were assumed and the partition coefficient, $K_p$, was determined as described by Knox *et al.* (1993). To determine the sorption of lindane on the medium matrix and the ECPs, a series of 25 ml vials containing lindane solutions (10 ml) at the concentration of 0.01, 0.05, 0.1, 0.5, 1, and 5 mg/l and 4 g media or 4 g ECPs each (sealed with Teflon-lined screw caps) (including blank controls) were agitated on a Wrist Action Shaker (Burrel Scientic, Model 75) for 24 hrs (pre-determined to be sufficient) to reach equilibrium. To determine the sorption of the ECPs on the medium matrix, similar series of vials containing the ECP solutions (10 ml) at the concentration of 1, 5, 10, 20, 30, and 50 mg/l and 4 g media each (including blank controls) were agitated for 24 hrs (pre-determined to be sufficient) to reach equilibrium.

For the determination of the partition coefficient of lindane between the aqueous phase and the medium matrix, the solutions were centrifuged at 5000 *g* for 15 min, after which lindane concentration in the supernatant was analyzed using a Gas Chromatograph (HP5880) with an Electron Capture Detector (Nickel 63 ECD). Helium was the carrier gas and the operation conditions were as following: injector temperature: 300°C; detector temperature: 225°C; oven temperature: initial 100°C for 1 min, then increased by

10°C/min for 12.5 min and kept at 225°C for 9 min. The measured lindane concentration was then fit into equation (5) to estimate the partition coefficient of lindane.

$$q = \frac{(C_o - C_{eq})V}{M} = K_p C_{eq} \quad (5)$$

where q is the mass of lindane sorbed normalized by the mass of the media (g/g); $C_o$ the initial concentration of lindane ($g/m^3$); $C_{eq}$ lindane equilibrium concentration ($g/m^3$); V the volume of lindane solution ($m^3$); M the mass of the media (g).

For the determination of the partition coefficient of lindane between the aqueous phase and the ECPs, the solutions were centrifuged at 12000 *g* for 20 min. The supernatants were then put in an electric field (FisherBiotech Horizontal Electrophoresis System, Fisher Scientific) to remove the soluble ECPs before the concentration of lindane was measured, which was based on the assumption that the ECPs were charged (Wolfaardt *et al.*, 1998). It was confirmed in this research that the ECPs were negatively charged by their negative ζ-potential values in the range of –10 mV to –20 mV (data not shown).

For the determination of the partition coefficient of the ECPs between the aqueous phase and the medium matrix, the solutions were vacuum-filtered (0.22 μm nylon supported plain filter, Osmonic., Inc.). The concentration of the ECPs was evaluated in filtrate in term of Chemical Oxygen Demand (COD). The relationship between the ECP concentration and COD was predetermined using known mass concentrations of the ECPs. The ECP concentration values were fit into equations (5) to estimate the partition coefficient of the ECPs.

*Measurement of surface thermodynamics* The ECP surface thermodynamics was estimated by contact angle measurement (Contact Angle Meter, Tantec) following the method described by Grasso *et al.* (1996) and Smets *et al.* (1999). The ECPs extracted from different species were redissolved by acetone and deposited on a glass surface. After evaporation of the solvent, three liquids with known surface thermodynamic parameters, diiodomethane, glycerol and water, were used for the contact angle measurement (replicated 15-20 times). The average values of the results were fit into Young-Dupré's equation (6) for the estimation of the ECP surface thermodynamic parameters (van Oss, 1994).

$$(1+\cos\theta)\gamma_L = 2(\sqrt{\gamma_S^{LW}\gamma_L^{LW}} + \sqrt{\gamma_S^+\gamma_L^-} + \sqrt{\gamma_S^-\gamma_L^+}) \quad (6)$$

where $\gamma^{LW}$ is the Liftshitz-van der Waals component of surface tension of the ECPs (with the subscript of s) or the liquids (subscript of L) ($mJ/m^2$); $\gamma^+$ and $\gamma^-$ the electron-acceptor and electron-donor parameter of Lewis acid/base component of the surface tension of the ECPs (subscript of s) or the liquids (subscript of L) ($mJ/m^2$).

Surface thermodynamic characteristics of the ECPs were evaluated using the total free energies of the interactions between the ECPs,1, immersed in water, 3, $\Delta G_{131}^{TOT}$, based on equations (7) – (9) (van Oss, 1994):

$$\Delta G_{131}^{TOT} = \Delta G_{131}^{LW} + \Delta G_{131}^{AB} \quad (7)$$

$$\Delta G_{131}^{LW} = -2(\sqrt{\gamma_3^{LW}} - \sqrt{\gamma_1^{LW}})^2 \quad (8)$$

$$\Delta G_{131}^{AB} = -4(\sqrt{\gamma_1^+} - \sqrt{\gamma_3^+})(\sqrt{\gamma_1^-} - \sqrt{\gamma_3^-}) \quad (9)$$

where $\Delta G_{131}^{LW}$ is the free energy of the van der Waals interaction between the ECPs ($mJ/m^2$) and $\Delta G_{131}^{AB}$ the free energy of the Lewis acid/base interaction between the ECPs ($mJ/m^2$). In general, the Lewis acid/base interaction dominated the surface thermodynamics with the free energy at least one order greater in magnitude than van der Waals interaction (Smets *et al.*, 1999 and Grasso and Smets, 1998).

The interactions between the ECPs were assumed as a semi-infinite flat parallel slabs configuration and were evaluated at the distance of closest approach where physical "contact" can occur. At this distance, the electrostatic interaction can be neglected compared with Lifshitz-van deer Waals and Lewis acid/base interactions (Loosdrecht *et al.*, 1989).

*Column Experiments* Column experiments for lindane transport in the absence and presence of ECPs were conducted using a 2.5-cm ID × 15-cm length column (Kimble Konte). The 2.5-cm ID × 15-cm length column was chosen to avoid side-wall effects and short-circuiting (Knox *et al.*, 1993). The media used for the column experiments, CRA and COA, were initially saturated with 10 pore volumes of NPDI (prefiltered by a 0.22 μm cellulose acetate filter), which was introduced at the inlet of the column by a peristaltic pump (Masterflex, Cole-Parmer) at a flow rate of 0.03 ml/sec. For each run, lindane alone in solution (10 ml, 7.3 mg/l) or lindane (10 ml, 7.3 mg/l) in the presence of different ECPs at different concentrations was injected by a syringe-pump to the column inlet. The column was then flushed with 250 pore-volumes of NPDI to reduce the

lindane concentration to below detection limit (BDL) and the elution was collected by a fraction collector.

Eluted samples were analyzed, from which the break through curves (BTCs) were obtained. For pulse input of a column experiment, the retardation factor, R, can be estimated using the data by the first temporal moment of the ECP BTCs, i.e.(Dohse and Lion, 1994):

$$R = \frac{\int_0^\infty \frac{C}{C_0}\theta d\theta}{\int_0^\infty \frac{C}{C_0} d\theta} - \frac{\theta_p}{2} \qquad (10)$$

where $\theta$ is the pore volume; and $\theta_p$ the pulse width as defined by Dohse and Lion (1994) which is equal to 0.13 in this study. Each run was done in triplicate.

*Infrared Spectroscopy Study* ECP components were analyzed using Infrared Spectroscopy (IR) (Perkin-Elmer, 283B). ECPs extracted from different microorganisms were mixed with potassium bromide to make a crystal medium. Each ECP sample was evaluated in triplicates and the inconsistency of the peaks of relative transmission was within 5% (95% CI). The frequencies of the peaks were referred to the library of reference curves (Barnes, 1944).

**Results and Discussions**

*Lindane transport in the absence of the ECPs* From integrating the BTCs (Figure 8.1), 85.1 ± 0.5 % and 80.3 ± 0.2 % of lindane were recovered from CRA and COA columns

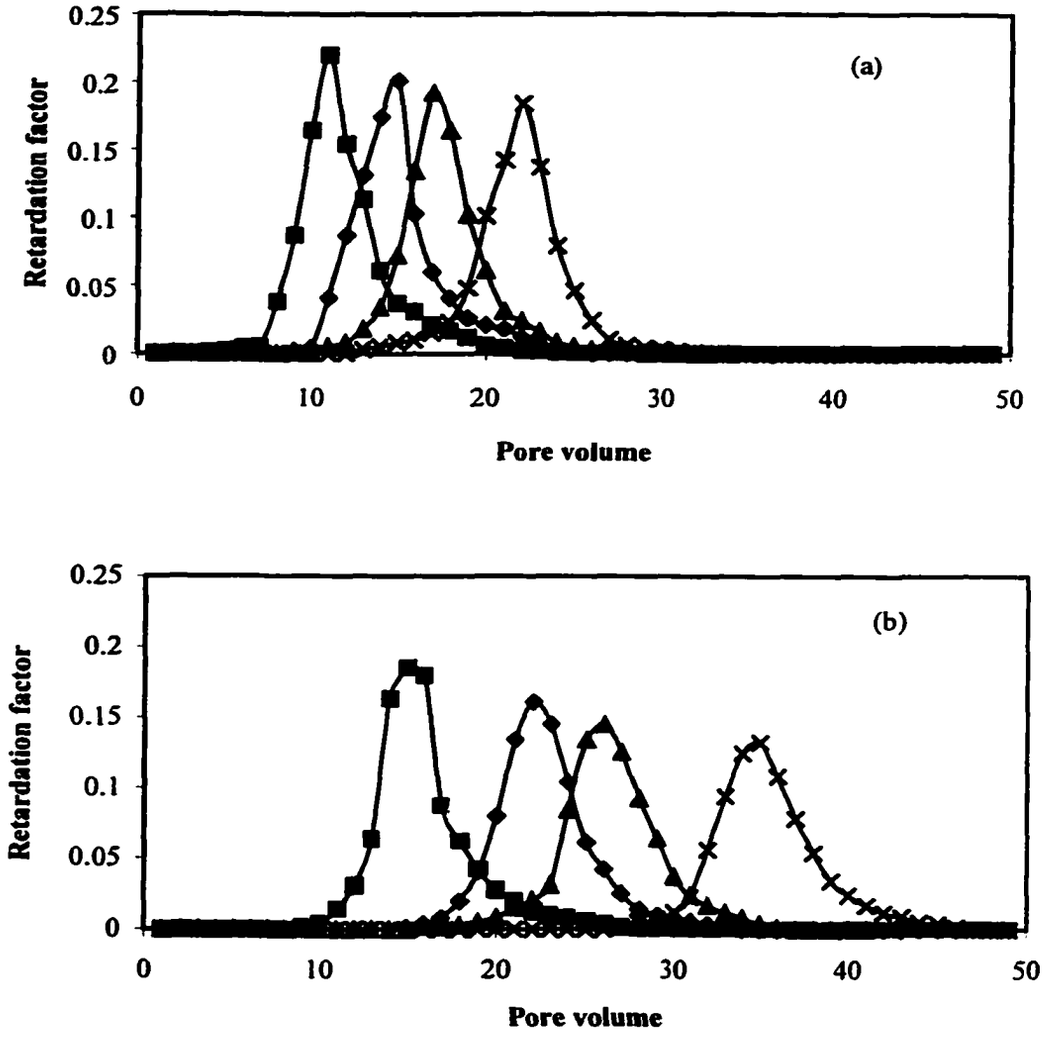


**Figure 8.1** Break through curves of lindane in the absence and presence of extracellular polymers (30 mg/l) extracted from different microorganisms in a (a) CRA and (b) COA column × Lindane in the absence of the ECPs, ■ Lindane in the presence of the ECPs extracted from *P. aeruginosa*, ◆ Lindane in the presence of the ECPs extracted from *E. coli* JM109, ▲ Lindane in the presence of the ECPs extracted from *B. subtilis*.

respectively (Table 8.1). Because no significant lindane biodegradation was observed in the preliminary experiment with the matrix, the loss of lindane due to biodegradation was assumed minimal (validated by mass balance). Therefore, the remaining 15% to 20% of the input that was not recovered was assumed to be sorbed to sites or regions of the porous matrix that displayed slow desorption kinetics. In the presence 30 mg/l ECPs extracted from *P.aeruginosa*, *E. coli* JM109, and *B. subtilis*, the percentage of lindane recovered from CRA and COA columns increased by 15.3% and 15.3%, 9.6% and 4.3%, and 3.5% and 4.0%, respectively. This suggested that most of the lindane that could not be recovered in the absence of the ECPs was due to the slow desorption kinetics.

From isotherm experiments, the average partition coefficient values of lindane, $K_p$, between the aqueous phase and CRA, COA were calculated at 6.47 ± 0.67 ml/g, 11.50 ± 1.14 ml/g, respectively based on 5 replicate isotherm experiments (Figure 8.2). Hence, the predicted retardation factor values from the batch isotherm experiments by its definition, $R = 1 + \rho_d \cdot K_p/\eta$, were 28 and 56 for CRA and COA respectively ($\rho_d/\eta$ values for CRA and COA: 4.22 g/l and 4.80 g/l). The experimental results obtained were 21.7 ± 1.8 (based on 85.1% lindane recovery in CRA) and 35.3 ± 1.9 (80.3% lindane recovery in COA) (Table 8.1). Because only 85.1% and 80.3% of lindane were recovered, the R values determined from equation (10) were underestimated.

**Table 8.1 Retardation factor and fraction recovery of lindane in the absence and presence of the ECPs at a concentration of 30 mg/l**

CRA

| | Retardation factor | Recovery (%) |
|---|---|---|
| In the absence of ECPs | 21.7 ± 1.8 | 85.1 ± 0.5 |
| ECPs extracted from P. aeruginosa | 11.7 ± 1.6 | 98.1 ± 0.4 |
| ECPs extracted from *E. coli* JM109 | 14.8 ± 1.9 | 93.3 ± 0.6 |
| ECPs extracted from B. subtilis | 17.5 ± 1.2 | 88.1 ± 0.7 |

COA

| | Retardation factor | Recovery (%) |
|---|---|---|
| In the absence of ECPs | 35.3 ± 1.9 | 80.3 ± 0.2 |
| ECPs extracted from P. aeruginosa | 15.8 ± 1.4 | 92.6 ± 0.8 |
| ECPs extracted from *E. coli* JM109 | 22.5 ± 2.4 | 87.0 ± 1.1 |
| ECPs extracted from B. subtilis | 26.3 ± 0.8 | 83.5 ± 0.9 |

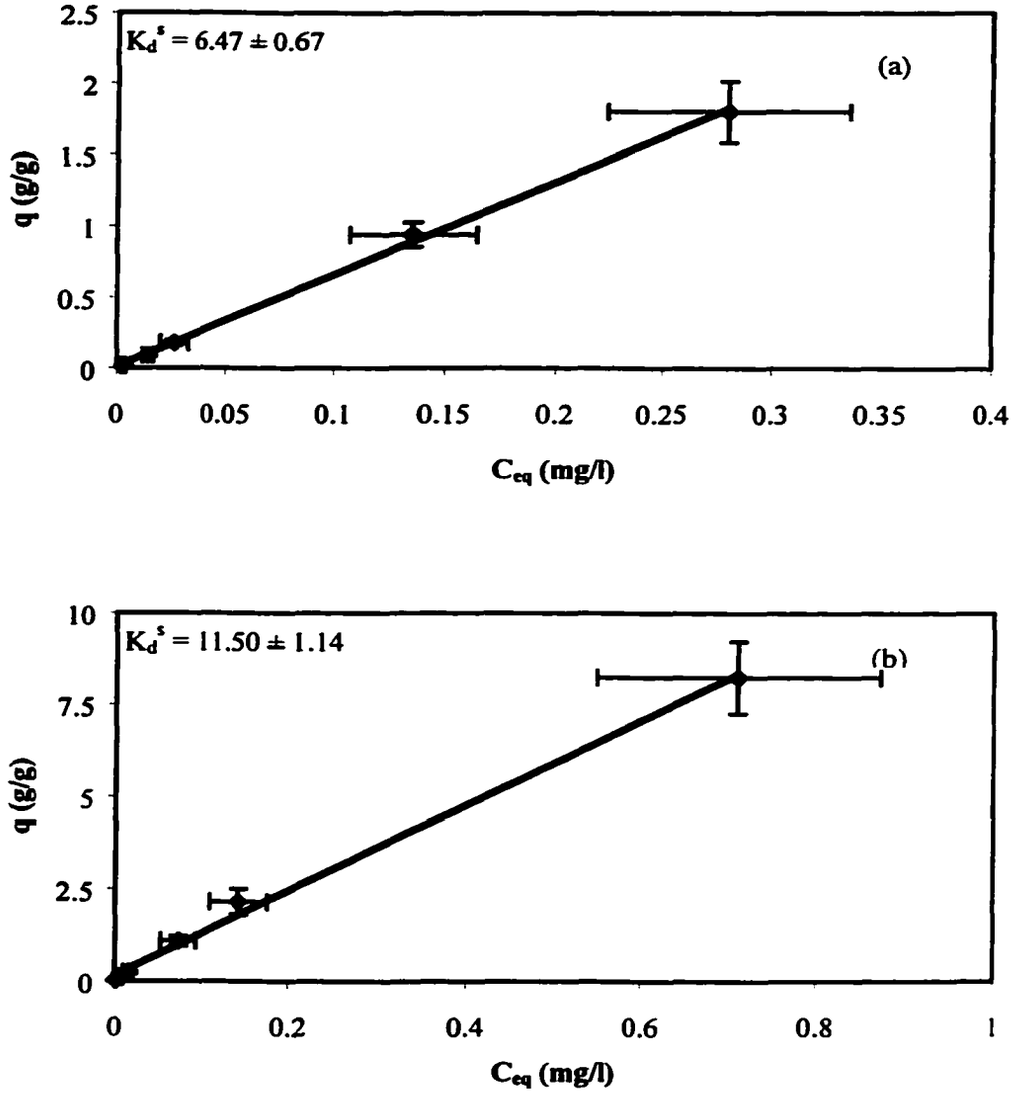


**Figure 8.2** Linear sorption isotherm of lindane in (a) CRA and (b) COA

*Lindane transport in the presence of the ECPs* The partition coefficient values of lindane between the aqueous phase and the ECPs extracted from *P. aeruginosa*, *E. coli* JM109, and *B. subtilis* were 49.28 ± 6.72 ml/g, 38.83 ± 4.92 ml/g, and 41.46 ± 4.57 ml/g, respectively (Figure 8.3). Therefore, Lindane would bind to the ECPs instead of the medium matrix because lindane had a larger partition coefficient value between the aqueous phase and the ECPs than between the aqueous phase and the medium matrix. In addition, the ECPs would be more mobile than lindane due to the smaller partition coefficient for the ECPs between the aqueous phase and the medium matrix than lindane (Figure 8.2 and 8.4). Hence, the two criteria of an effective carrier for facilitating lindane transport were observed, therefore, the ECPs should enhance lindane transport.

*Impact of lindane transport by the ECPs extracted from different microorganisms in the same porous medium matrix* Assume that the ECPs in the aqueous phase moved with a velocity equal to that of the aqueous phase, a modified expression for the retardation factor in the presence of a carrier that is also subject to retardation was derived by Magee *et al.* (1991) as following:

$$R^* = \frac{(1 + k_d^{om}DOM + k_d^s \rho_b / \eta)}{1 + \dfrac{k_d^{om}DOM}{1 + k_{dom}^s \rho_b / \eta}} \qquad (11)$$

where DOM is the carrier concentration; $K_d^{om}$ the partition coefficient of the contaminant between aqueous phase and the carrier; $K_d^s$ the partition coefficient of the contaminant between the aqueous phase and the sorbent; and $K_{dom}^s$ the partition coefficient of the carrier between the aqueous phase and the sorbent. As shown in equation (11), in the presence of different ECPs, the retardation of lindane in the same medium matrix will

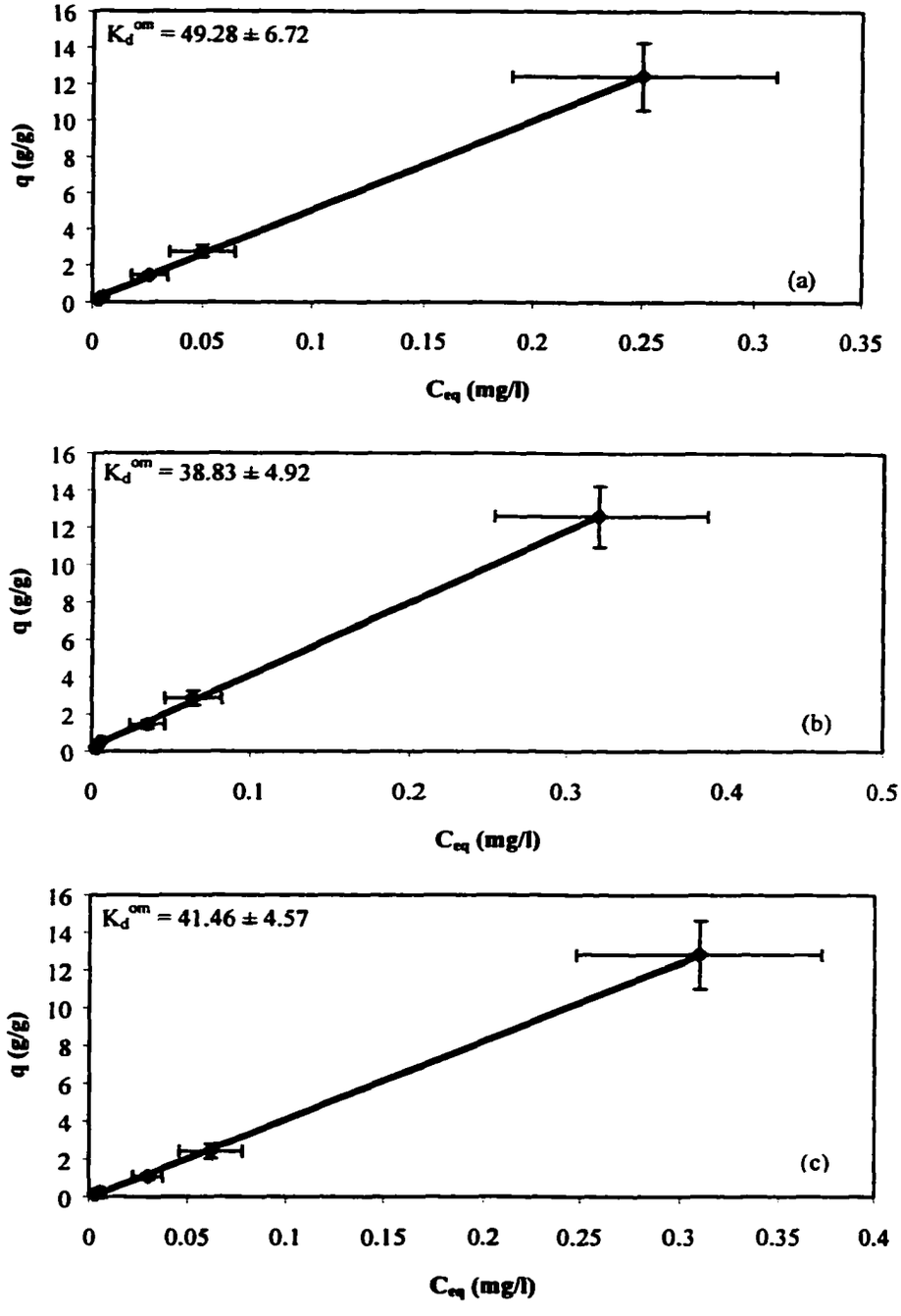


**Figure 8.3** Linear sorption isotherm of lindane in the ECPs extracted from (a) *P. aeruginosa*, (b) *E. coli*JM109, and (c) *B. subtilis*

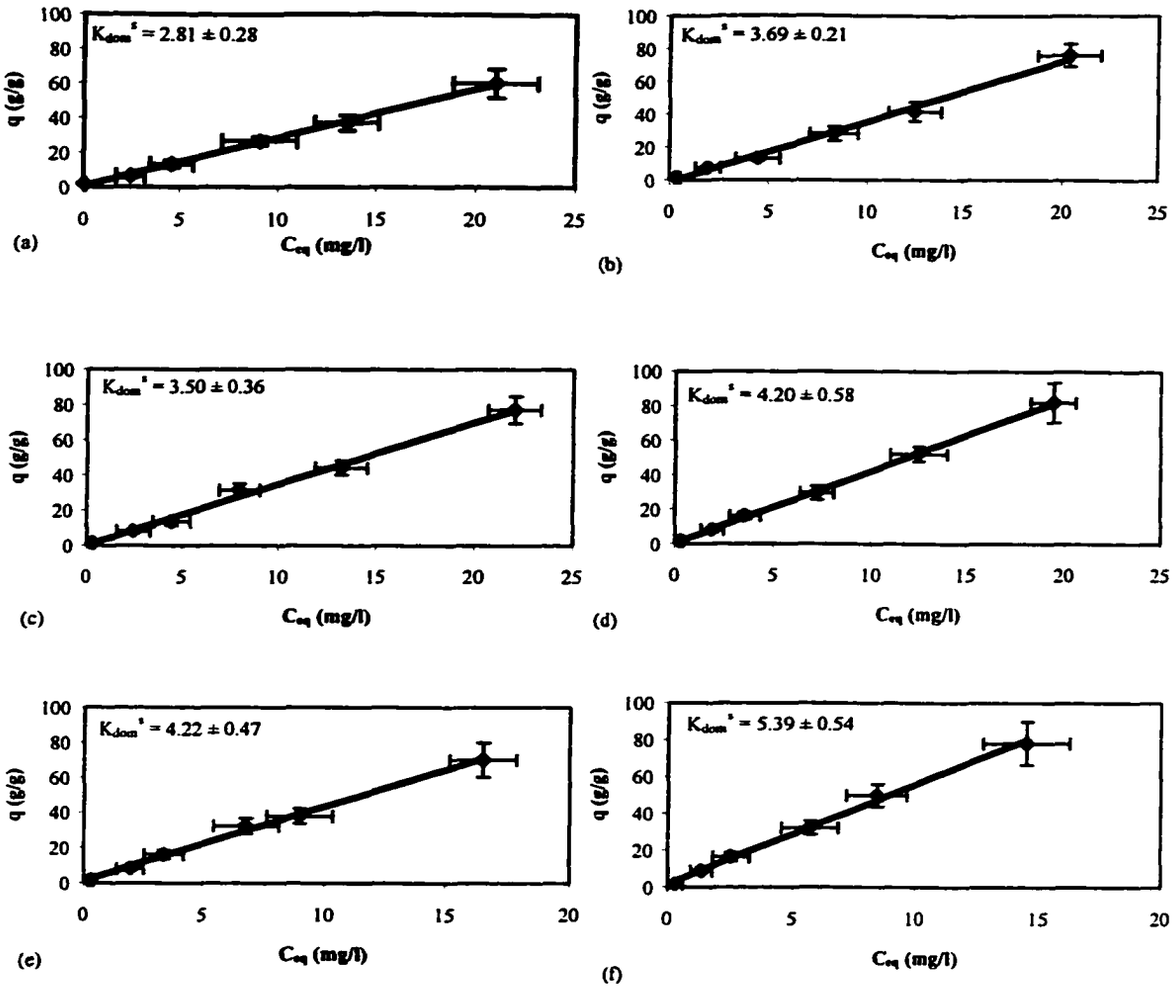


**Figure 8.4** Linear sorption isotherm of the ECPs in the media matrix (a) the ECPs extracted from *P. aeruginosa* in CRA, (b) the ECPs extracted from *P. aeruginosa* in COA, (c) the ECPs extracted from *E. coli*JM109 in CRA, (d) the ECPs extracted from *E. coli*JM109 in COA, (e) the ECPs extracted from *B. subtilis* in CRA, (f) the ECPs extracted from *B. subtilis* in COA

depend on the two partition coefficients involving the carrier, $K_d^{om}$ and $K_{dom}^{s}$. A smaller $K_{dom}^{s}$ value will result in a greater retardation reduction. However, the impact of $K_d^{om}$ on the enhancement efficiency is not clear just from equation (11). To predict the impact of $K_d^{om}$ on lindane transport, theoretically calculated $R^*$ values versus $K_d^{om}$ for different $K_{dom}^{s}$ of the transport of lindane in CRA and COA columns are plotted in Figure 8.5 (a) and (b) respectively (DOM = 30 mg/l). As shown in Figure 8.5, when $K_d^{om}$ values are small (less than 5 ml/g), $K_d^{om}$ plays an important role in determining the retardation factor; while when $K_d^{om}$ are greater than 10 ml/g, $K_{dom}^{s}$ is the determining factor in facilitating lindane transport. As all the ECP $K_d^{om}$ values were greater than 10 ml/g (Figure 8.3), $K_{dom}^{s}$ was the determining factor in facilitating lindane transport. The ECPs extracted from *P. aeruginosa* had the smallest $K_{dom}^{s}$ value followed *E. coli* JM109 and *B. subtilis* (Figure 8.4), thus the ECPs extracted from *P. aeruginosa* should be the most efficient in facilitating lindane transport, *B. subtilis* the least, and *E. coli* JM109 in between. The column experimental observations supported this conclusion. As shown in Table 8.1, the retardation factor values of lindane in COA were decreased by 55.2%, 36.4%, and 25.5% by the ECPs extracted from *P. aeruginosa*, *E. coli* JM109, and B. subtilis, respectively (at the concentration of 30 mg/l). Similar observations were made for CRA (46.1%, 31.8%, and 19.3%).

*Impact of lindane transport by the same ECPs in different medium matrices* For the constant $K_d^{om}$, $R^*$ will depend on the two distribution coefficients involving the medium matrix, $K_d^{s}$ and $K_{dom}^{s}$. Based on the isotherm experimental data and equation (11), the predicted retardation factor values of lindane in the presence of the ECPs extracted from

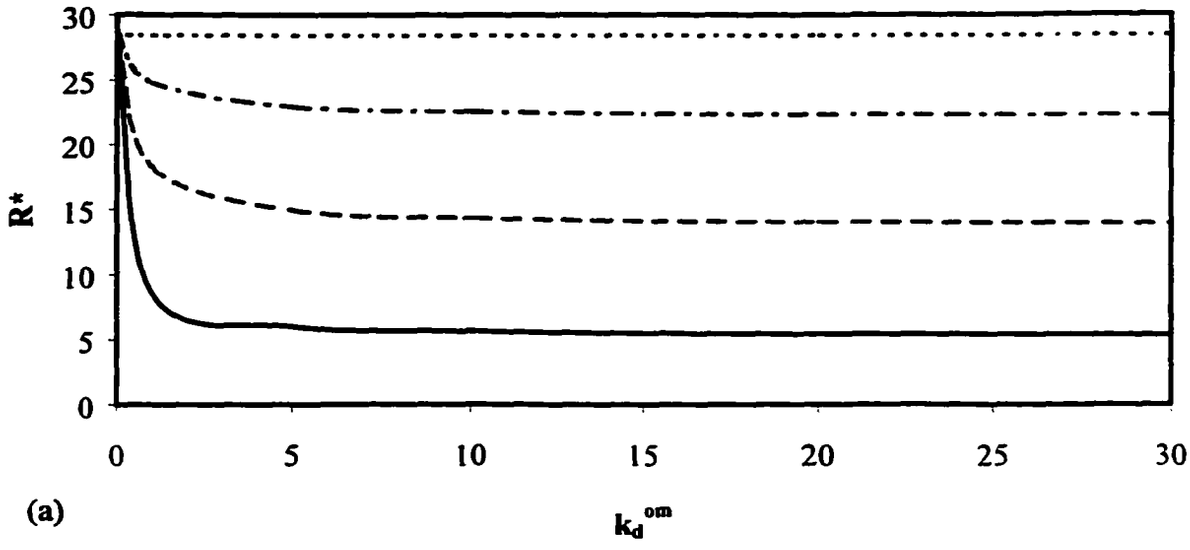


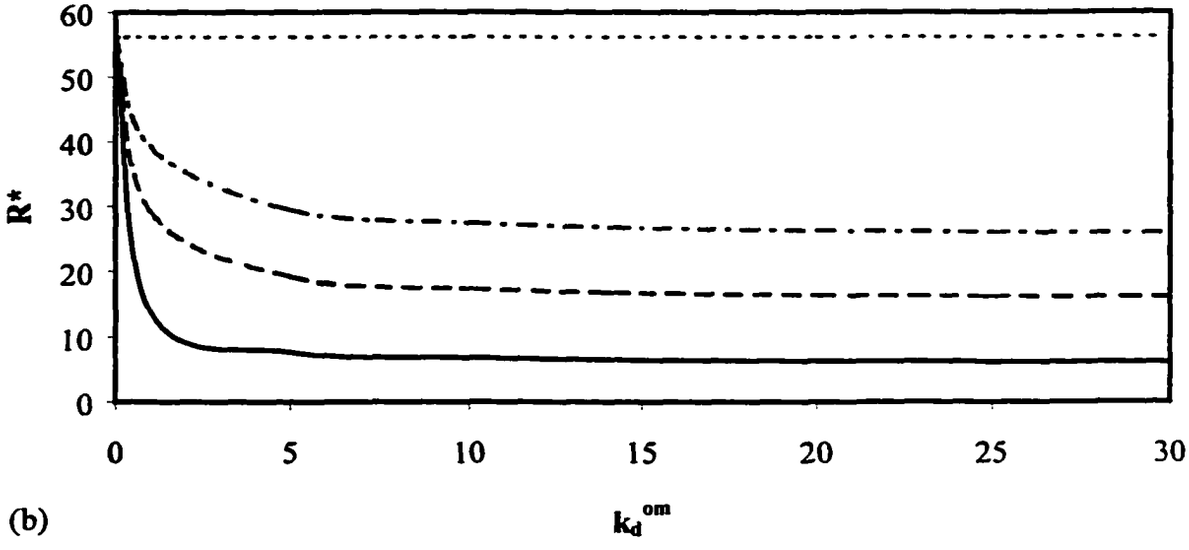


**Figure 8.5** Effect of $K_{om}^{d}$ on the retardation factor of lindane at different $K_{dom}^{s}$ values for (a) CRA and (b) COA —- $K_{dom}^{s} = 1$, – – – $K_{dom}^{s} = 3$, – · – $K_{dom}^{s} = 5$, ..... $K_{dom}^{s} = K_d^{s}$.

*P. aeruginosa* at the concentration of 30 mg/l for CRA and COA were 13 and 18, respectively. Thus, the facilitating efficiency of lindane transport [$(R-R^*)/R \times 100\%$] in CRA and COA due to the presence of the ECPs should be 40% and 49%. According to this prediction, COA should have a greater efficiency in the ECP facilitated transport of lindane than CRA. This prediction was consistent with the column experiments. As shown in Table 8.1, the retardation factor of lindane in CRA and COA was reduced by 50.2% and 55.2% respectively in the presence of the ECPs extracted from *P. aeruginosa* (at the concentration of 30 mg/l). The higher values from column experiments were because higher fraction recoveries were obtained in the presence of the ECPs than in the absence, which resulted in less underestimated R values. Similar observations were made for the ECPs extracted from *E. coli* JM109 (23% and 36% as calculated versus 31.8% and 36.4% from column experiments) and *B. subtilis* (13% and 22% versus 19.3% and 25.5%).

*Surface thermodynamic and infrared spectroscopy (IR) study of the ECPs* To further understand the behavior of the ECPs in facilitating lindane transport, surface thermodynamic and infrared spectroscopy (IR) study of the ECPs were performed to investigate the chemical structures of the ECPs. As shown in Table 8.2, the total surface free energy ($\Delta G_{131}^{TOT}$) of the ECPs extracted from *B. subtilis*, *E. coli* JM109, and *P. aeruginosa* was 30.4 mJ/m$^2$, 46.9 mJ/m$^2$, and 58.9 mJ/m$^2$, respectively, which was listed in order of increasing hydrophilicity ($\Delta G_{131}^{TOT} > 0$, van Oss, 1994).

**Table 8.2 Surface Thermodynamic Properties of the ECPs**

| ECPs | *P. aeruginosa* | *E. coli* JM109 | B. subtilis |
|---|---|---|---|
| θ (°) (Diiodomethane) | 49 ± 2 | 46 ± 4 | 42 ± 4 |
| θ (°) (Glycerol) | 56 ± 3 | 58 ± 4 | 62 ± 3 |
| θ (°) (Water) | 20 ± 3 | 22 ± 5 | 22 ± 2 |
| $\gamma^+$ (mJ/m2) | 0.062 | 0.23 | 0.90 |
| $\gamma^-$ (mJ/m2) | 68.5 | 61.2 | 51.8 |
| $\gamma^{LW}$ (mJ/m2) | 34.8 | 36.5 | 38.6 |
| $\Delta G_{131}^{LW}$ (mJ/m2) | -3.0 | -3.8 | -4.8 |
| $\Delta G_{131}^{AB}$ (mJ/m2) | 62.0 | 50.7 | 35.2 |
| $\Delta G_{131}^{TOT}$ (mJ/m2) | 58.9 | 46.9 | 30.4 |

Figure 8.6 indicated the ECPs were composed of a variety of different functional groups of aldehydes (RCOH) (peaks shown at the frequency of 1700 $cm^{-1}$), ketones (RCOR) (1680 $cm^{-1}$), carboxylic acids (RCOOH, $RCOO^-$) (1690 $cm^{-1}$, 1600 $cm^{-1}$), carbonyl groups ($CH_3CO$-) (1320 $cm^{-1}$), peptide bond (-CO-NH-) (1500 $cm^{-1}$), ethers (-$CH_2$-O-, $CH_3$-O-, -C-O-C-) (1000 $cm^{-1}$, 980 $cm^{-1}$, 1060 $cm^{-1}$), ethenyl groups (-CH=CH-, >C=$CH_2$, -CH=$CH_2$) (700 $cm^{-1}$, 830 $cm^{-1}$, 860 $cm^{-1}$), etc., as well as hydrogen (H-) (2900 $cm^{-1}$) and (hydroxyl) (OH-) (3600 $cm^{-1}$), which were contributed by the water (Barnes *et al.*,1944). Functional groups of aldehydes, ketones, carboxylic acids contribute to the ECP hydrophilicity; while ethenyl groups contribute to the ECP hydrophobicity (Myers, 1988). Therefore, the ECPs had a dual moiety. As shown in Figure 8.6, the peak intensity at frequencies between 1800 $cm^{-1}$ and 1600 $cm^{-1}$ are much stronger than that of between 1000 $cm^{-1}$ and 700 $cm^{-1}$, so the hydrophilicity was prominent, which was consistent with the results from the surface thermodynamic study.

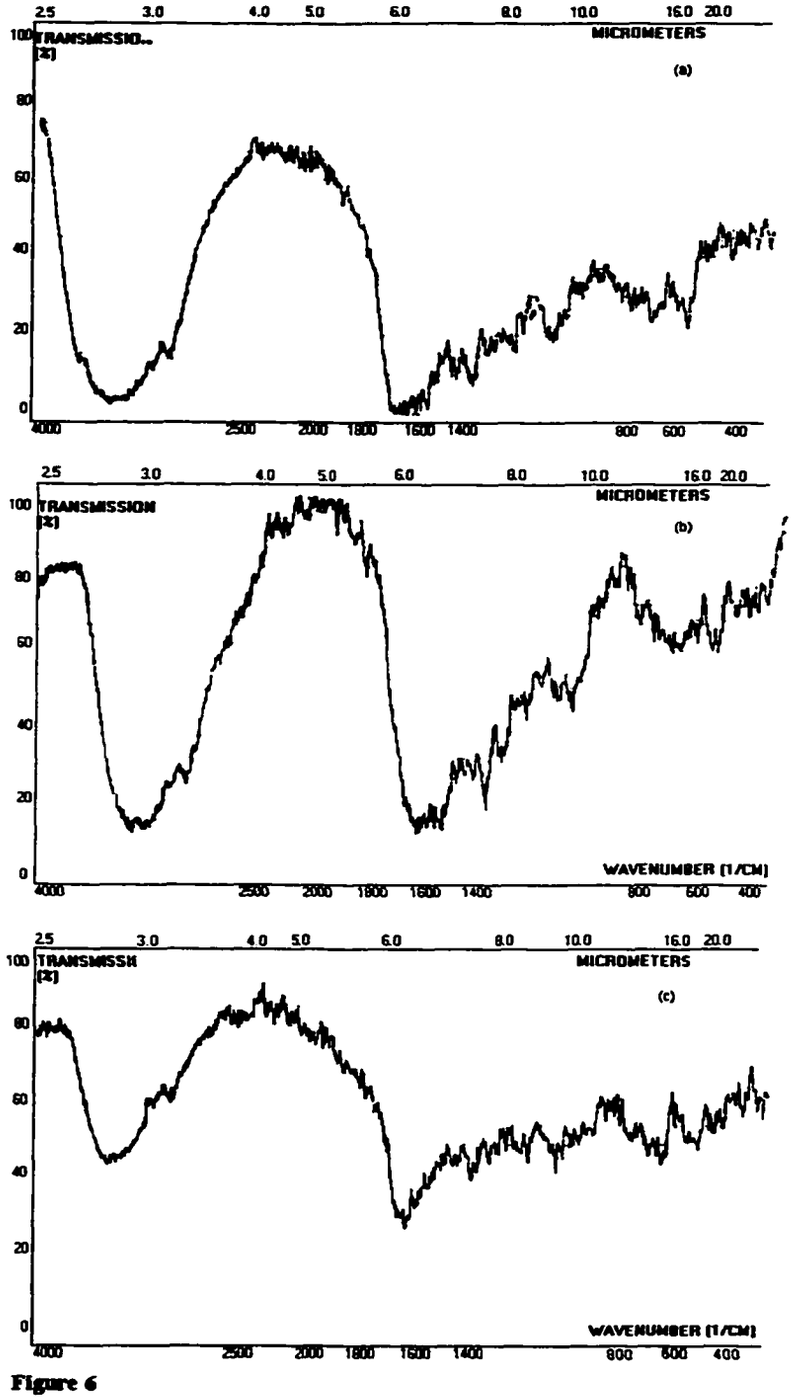


**Figure 6**

**Figure 8.6** Infrared spectroscopy of the ECPs extracted from (a) *P. aeruginosa*, (b) *E. coli*JM109, and (c) *B. subtilis*

*Impact of ECP concentrations on lindane transport* The impact of ECP concentration on lindane transport was quantified by the study of lindane transport in the presence of the ECPs at different concentrations. As shown in Figure 8.7, the lindane retardation factor values decreased greatly with the increase of ECP concentration until the ECP concentration reached 35 ± 5 mg/l. Above 35 ± 5 mg/l, decrease of the retardation factor became moderate. This behavior was similar to the observation made with a synthetic surfactant when reaching the critical micelle concentration (CMC) (Rosen, 1989). As the increase of the ECP concentration increases the binding capacity, hence, when the ECPs are present at a low concentration (less than 20 mg/l), the facilitated lindane transport is limited by the binding capacity. Conversely, when the ECPs are present at a high concentration (greater than 35 ± 5 mg/l), the facilitated lindane transport is limited by the ECP mobility (reflected by $K_{dom}^{5}$). From Figure 8.7, it can be seen that 30 mg/l is the most effective and cost-efficient ECP concentration that can be used in field applications. Below 30 mg/l, the ECPs worked less efficiently as compared with 30 mg/l. Beyond 30 mg/l, the facilitating efficiency did not increase significantly (95% CI) with the increase of the ECP concentration.

**Summary**

This research investigated the enhancement of the ECPs extracted from commonly found bacteria on the transport of lindane through porous medium matrix. The dual moiety properties of the ECPs: (1) more mobile than lindane and (2) the ability to bind lindane, allowed the ECPs to be an effective carrier for facilitating lindane transport. This study concluded that when the partition coefficient of lindane between the aqueous phase and

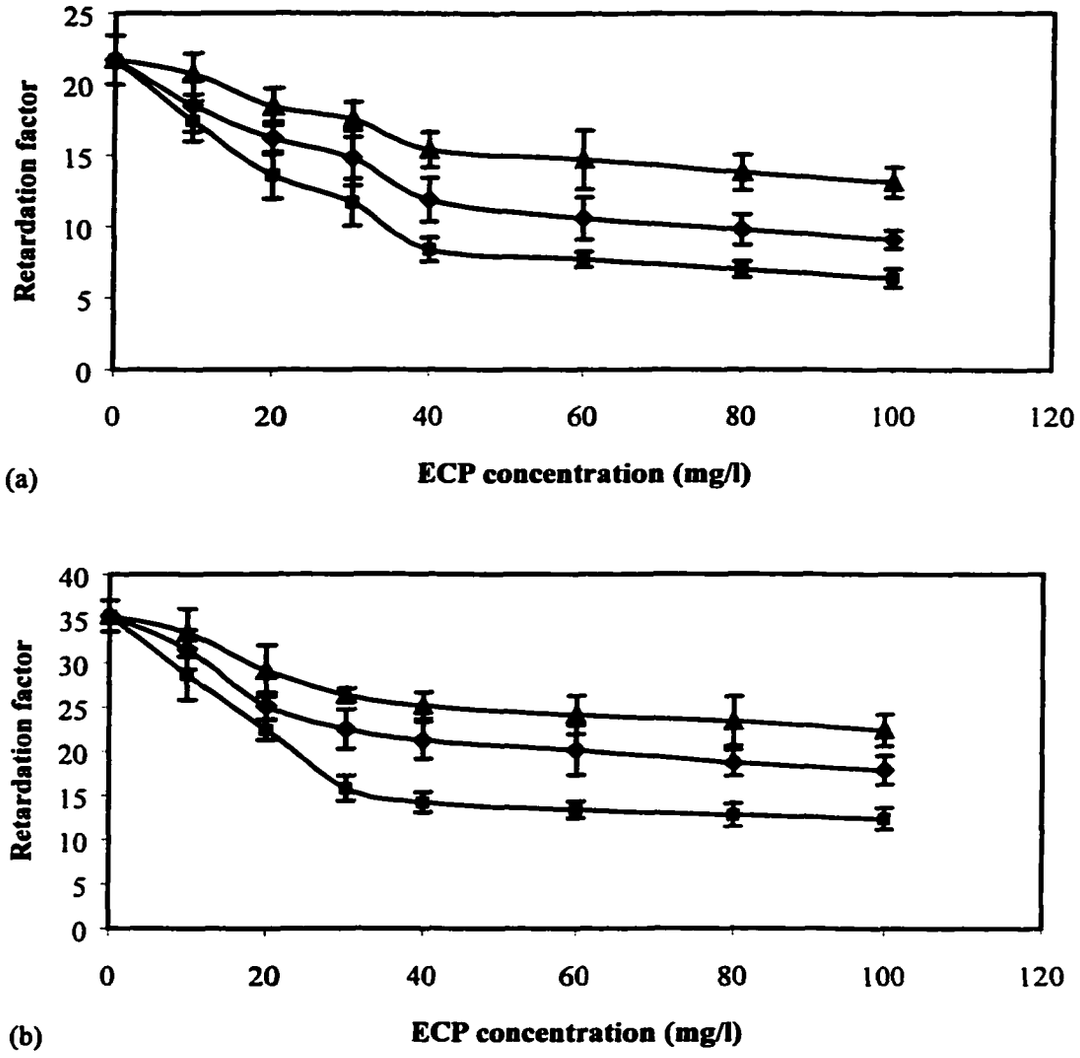


**Figure 8.7** Effect of ECP concentration on the facilitated lindane transport in (a) CRA and (b) COA ■ ECPs extracted from *P. aeruginosa*, ◆ ECPs extracted from *E. coli* JM109, ▲ ECPs extracted from *B. subtilis*.

the ECPs, $K_d^{om}$, was greater than 10 ml/g, the efficiency of the facilitated lindane transport by the ECPs was determined by the ECP mobility which was reflected by the partition coefficient of the ECPs between the aqueous phase and the medium matrix, $K_{dom}^{s}$. The quantification of the ECP concentration on the facilitating efficiency provides the guideline for the optimization of an effective ECP application when the ECPs are utilized for *in-situ* biodegradation.

**Acknowledgements**

The work was support in part by National Science Foundation through Grant No. BES-9733969 to the University of Oklahoma.

**References:**

1. Barnes R.B., Gore R.C., Liddel U. and Williams V.Z. (1944) *Infrared Spectroscopy, Industrial Applications and Bibliography*, Reinhold Publishing Corporation, New York.

2. Brown M. J. and Lester J. N.(1980) Comparison of Bacterial Extracellular Polymer Extraction Methods, *Appl. Environ. Microbiol.*, 40:179-185.

3. Dohse D. M. and Lion L. W.(1994) Effect of microbial polymers on the sorption and transport of phenanthrene in a low-carbon sand, *Environ. Sci. Technol.*, 28:541-548.

4. Enfield C.G. and Bengtsson G. (1988) Macromolecular Transport of Hydrophobic Contaminants in Aqueous Environment, *Ground Water*, 26: 64-70.

5. Enfield C.G., Walter D.W., Carsell R.F. and Cohen S.Z. (1982) Approximating Transport of Organic Pollutants to Groundwater, *Ground Water*, 20:711-722.

6. Falatko D.M. and Novak J.T. (1992) Effect of Biological Produced Surfactants on the Mobility and Biodegradation of Petroleum Hydrocarbons, *Water Environ. Res.*, 64:163-169.

7. Freeze R.A. and Cherry J.A. (1979) *Groundwater*, John Wiley & Sons, Inc., New York.

8. Grasso D. and Smets B.F. (1998) Equilibrium Modeling of Pseudomonad Aggregation and Partitioning To Dolomite, *J. Dispersion Science and Technology*, 19: 1081-1106.

9. Grasso D., Smets B.F., Strevett K.A. and Machinist B.D. (1996) Impact of Physiological State on Surface Thermodynamics and Adhesion of Pseudomonas aeruginosa, *Environ. Sci. Technol*, 30:3604-3608.

10. Jenkins M. B. and Lion L. W. (1993) Mobile Bacteria and Transport of Polynuclear Aromatic Hydrocarbons in Porous Media, *Appl. Environ. Microbiol.*, 59:3306-3313.

11. Jury W.A., Elabd H. and Resketo M. (1986) Field Study of Napropamide Movement through Unsaturated Soil, *Water Resource*, 22:749-755.

12. Karl D.M. (1980) Cellular Nucleotide Measurement, *Microbiol. Review* 44: 740-796.

13. Karapanagioti, Kleineidam S., Ligouis B., Sabatini D. A. and Grathwohl P. (1999) Phenanthrene Sorption with Heterogeneous Organic Matter in a Landfill Aquifer Material, *Physics and Chemistry of the Earth*. 24:535-541.

14. Knox R.C., Sabatini D.A. and Canter L.W. (1993) *Subsurface Transport and Fate Processes*, Lewis Publishers, New York.

15. Loosdrecht M.C.M., Lyklema J., Norde W. and Zehnder A.J.B. (1989) Bacterial Adhesion: A Physicochemical Approach, *Microbial Ecology*, 17:1-15.

16. Magee B.R., Lion L.W. and Lemley A.T. (1991) Transport of Dissolved Organic Macromolecules and Their Effect on the Transport of Phenanthrene in Porous Media, *Environ. Sci. Technol*, 25:323331.

17. McCarthy J.F.and Zachara J.M. (1989) Subsurface Transport of Contaminants, *Environ. Sci. Technol.*, 23:496-502.

18. Myers D.(1988) *Surfactant Science and Technology*, VCH.

19. Rosen M.J. (1989*) Surfactants & Interfacial Phenomena*, 2nd ed., Wiley, New York.

20. Smets B.F., Grasso D., Engwall M.A. and Machinist B.J. (1999) Surface Physicochemical properties of *Pseudomonas fluorescens* and Impact on Adhesion and Transport through Porous Media, *Colloids and Surfaces B: Biointerfaces* 14: 121-139.

21. van Oss C.J. (1994) *Interfacial Forces in Aqueous Media*, Marcel Dekker, Inc. New York.

22. Vinten A., Yaron J.A.B. and Ney P.H. (1983) Vertical Transport of Pesticides into Soil when Adsorbed on Suspended particles, *J. Agric. Food Chem.*,31:662-666.

23. Waldron A.C. (1992) *Pesticides and Groundwater Contamination*, The Ohio State University Bulletin 820.

24. Worthing C.R. (1983) *The Pesticide Manual: A World Compendium*, 7th ed., The British Crop Protection Council, Croydon, England.

25. Wolfaardt G.M., Lawrence J.R., Robarts R.D. and Caldwell D.E. (1998) In situ Characterization of Biofilm Exopolymers Involved in the Accumulation of Chlorinated Organics, *Microb. Ecol.*, 35:213-223.

# CHAPTER 9

# CONCLUSIONS

The application of natural attenuation of organic contaminants or in *in-situ* bioremediation is severely limited by the understanding of microbial migration in the subsurface. Though discovery of viable populations of microorganisms in the subsurface at unexpected locations has been one of the major findings at the end of this century, microbial migration is still not clearly understood (Bekins, 2000). Biological, chemical, and hydrologic factors all impact microbial transport in the subsurface. So far much work has been done in describing how physical and chemical variations in the subsurface result in changes in microbial migration, and yet, further insights into the subsurface as a habitat for microorganisms requires the understanding of microbial and medium subsurface properties. This research investigated the surface thermodynamics of the typical rod-shaped bacterial strains of *Enterobacteriaceae*, *Pseudomonadaceas*, *Bacillaceae* and their interactions among themselves as well as with the medium matrix. Traditional and extended DLVO forces, including van der waals, Lewis acid/base and electrostatic forces were used in quantifying microbe-microbe and microbe-surface interactions and models that can be used for the calculation of these interactions based on independently determined microbial and medium surface thermodynamics were developed. The impact of physiological states and carbon and nitrogen conditions on surface thermodynamics was also examined and relationships of physiological states and carbon and nitrogen conditions with microbial thermodynamic properties were derived.

Hydrogeological and microbiological expertise is needed to review methods that can be used for subsurface microbial transport studies. Various mathematical expressions used to model microbial processes in porous media have been established with limitations and capabilities. However, the mechanisms by which microorganisms attach and detach from porous media and are transported by groundwater is essential for understanding and developing strategies to distribute microorganisms in contaminated subsurface systems. A microbial transport model that described both reversible and irreversible microbial sorption in porous media was established and was linked to microbial and medium surface thermodynamics. The dependence of the microbial transport on their surface thermodynamics, or microbial physiological states and carbon and nitrogen conditions was investigated and quantified through lab-scale column experiments in different media. In addition, mechanisms that accounted for reversible and irreversible microbial sorption were reached and a novel method was developed that can be used for the determination of microbial sorption isotherm from column experiments. The efficacy of the extended DLVO theory for quantifying microbial-surface interactions was confirmed in column experiments.

The influence of subsurface microorganisms is now recognized to range from subsurface physicochemical properties to global chemical mass balances (Bekins, 2000). The locations and activities of these organisms are controlled by subsurface chemical and physical properties that have traditionally been studied by hydrogeologists. Thus microbial transport in the subsurface will be a combined discipline of vadose zone hydrology, soil physics, interface geochemistry, and microbiology. This research has

developed a rational forecasting framework for describing microbial transport processes in saturated medium systems. The next step following this research is to apply the fundamental principles of microbial transport in the subsurface and to develop engineering strategies to design and operate practical groundwater technologies such as active bioremediation system where fundamental subsurface transport principles can be used. It should be noted that modeling of microbial subsurface transport processes is a difficult process due to the complexities associated with various underlying processes. With the expansion of interest in this field, new techniques and strategies have been formulated to facilitate studies of subsurface microbial processes.

**References:**

1. Bekins, B.A. (2000) Groundwater and Microbial Processes Theme Issue - Guest Editor's Preface, *Hydrogeology Journal*, 8: 2-3.

## APPENDIX I

## REFERENCES


1. Absolom, D. R., Lamberti, F. V., Policova, Z., Zingg, W., van Oss, C. J. and Neumann, A. W. (1983) Surface Thermodynamics of Bacterial Adhesion, *Appl. Environ. Microbiol.* 46:90-97.

2. Annable, M. D., Rao, P. S. C., Hatfield, K., Graham, W. D., Wood, A. L., and Enfield, C. G. (1998) Partitioning Tracers for Measuring Residual NAPL: Field-Scale Test Results. *J. Environ. Eng.*, 124: 498-503.

3. Barnes, R.B., Gore, R.C., Liddel, U. and Williams, V.Z. (1944) *Infrared Spectroscopy, Industrial Applications and Bibliography*, Reinhold Publishing Corporation, New York.

4. Bekins, B.A. (2000) Groundwater and Microbial Processes Theme Issue - Guest Editor's Preface, *Hydrogeology Journal*, 8: 2-3.

5. Bellin, C.A. and Rao, P.S.C. (1993) Impact of Bacterial Biomass on Contaminant Sorption and Transport in Subsurface Soil, *Appl. Environ. Microbiol.*, 59:1813-1820.

6. Bolster, C. H., Hornberger, G. M., Mills, A. L. and Wilson, J. L. (1998) A Method for Calculating Bacterial Deposition Coefficients Using the Fraction of Bacteria Recovered from Laboratory Columns, *Environ. Sci. Technol.*, 32:1329-1332.

7. Brown, M. J. and Lester, J. N.(1980) Comparison of Bacterial Extracellular Polymer Extraction Methods, *Appl. Environ. Microbiol.*, 40:179-185.

8. Bürgisser, C.S., erník, M., Borkovec, M. and Sticher, H. (1992) Determination of Nonlinear Adsorption Isotherms from Column Experiments: An Alternative to Batch Studies, *Environ. Sci. Technol.*, 27: 943-948.

9. Chattopadhyay, S. and Puls, R. W. *Environ. Sci. Technol.* 1999, 33: 3609 – 3614.

10. Chen, G. and Strevett, K. A. (2001) Impact of Surface Thermodynamics on Bacterial Transport, *Environ. Microbiol.*, 3: 237-245.

11. Chen, G. and Strevett, K.A. (2002) Surface Free Energy Relationships Used to Evaluate Microbial Transport, *J. Environ. Eng.*, 128:408-415.

12. Dabros, T and van de Ven, T.G.M. *Colloids Polym. Sci.* 1983, 261: 694-707.

13. Dohse, D. M. and Lion, L. W. (1994) Effect of Microbial Polymers on the Sorption and Transport of Phenanthrene in a Low-Carbon Sand, *Environ. Sci. Technol.*, 4:541-548.

14. Elimelech, M. and O'Melia, C. R. (1990) Kinetic of Deposition of Colloidal Particles in Porous Media, *Environ. Sci. Technol.*, 24:1528-1536.

15. Elimelech, M. and O'Melia, C.R. (1990) Effect of Particle Size on Collision Efficiency in the Deposition of Brownian Particles with Electrostatic Energy Barriers, *Langmuir*, 6: 1153-1163.

16. Ellwood, D.C. and Tempest, D.W. (1972) Effects of Environment on Bacterial Wall Content and Composition. *Adv. Microb. Physiol.*, 7:43-47.

17. Enfield, C.G. and Bengtsson, G. (1988) Macromolecular Transport of Hydrophobic Contaminants in Aqueous Environment, *Ground Water*, 26: 64-70.

18. Enfield, C.G., Walter, D.W., Carsell, R.F. and Cohen, S.Z. (1982) Approximating Transport of Organic Pollutants to Groundwater, *Ground Water*, 20:711-722.

19. Falatko, D.M. and Novak, J.T. (1992) Effect of Biological Produced Surfactants on the Mobility and Biodegradation of Petroleum Hydrocarbons, *Water Environ. Res.*, 64:163-169.

20. Faust, S.D. and Hunter, J.V. (1971) *Organic Compounds in Aquetic Environment*, Marcel Dekker, Inc., New York.

21. Fontes, D.E., Mills, A.L., Hornberger, G.M. and Herman, J.S. (1991) Physical and Chemical Factors Influencing Transport of Microorganisms through Porous Media, *Appl. Environ. Microbiol.*, 57:2473-2481.

22. Freeze, R.A. and Cherry, J.A. (1979) *Groundwater*, John Wiley & Sons, Inc., New York.

23. Gamerdinger, A. P., van Rees, K. C. J., Rao, P. S. C. and Jessup, R. E. (1994) Evaluation of *in situ* Columns for Characterizing Organic Contaminant Sorption during Transport, *Environ. Sci. Technol.*, 28:376-382.

24. Gannon, J. T., Mingelgrin, U., Alexander, M. and Wagenet, R. J. (1991) Bacterial Transport through Homogeneous, *Soil Biol. Biochem.* 23:1155-1160.

25. Goldman, J.C. and Mark, R.D. (2000) Growth of Marine Bacteria in Batch and Continuous Culture under Carbon and Nitrogen Limitation, *Limn. Ocean.*, 45: 789-801.

26. Gooses, K. and Schwarzenbach, R. P. (2001) Linear Free Energy Relationship Used to Evaluate Equilibrium Partitioning of Organic Compounds, *Environ. Sci. Technol.* 35: 1-9.

27. Grasso, D. and Smets, B.F. (1998) Equilibrium Modeling of Pseudomonad Aggregation and Partitioning To Dolomite, *J. Dispersion Science and Technology*, 19: 1081-1106.

28. Grasso D., Smets B. F., Strevett K. A., Machinist B. D., van Oss C. J., Giese R. F. and Wu W. (1996) Impact of Physiological State on Surface Thermodynamics and Adhesion of Pseudomonas aeruginosa, *Environ. Sci. Technol.*, 30:3604-3608.

29. Hancock, I. and Poxton, I. (1988) *Bacterial Cell Surface Techniques*, John Wiley & Sons, New York.

30. Harvey, R. W. and Garabedian, S. P. (1991) Use of Colloid Filtration Theory in Modeling Movement of Bacteria through a Contaminated Sandy Aquifer, *Environ. Sci. Technol.*, 25:178-185.

31. Holtz, R. D. and Kovacs, W. D. (1981) *An Introduction to Geotechnical Engineering*, Prentice-Hall, Inc., Englewood Cliffs, NJ.

32. Hornberger, G. M., Mills, A. L. and Herman, J. S. (1992) Bacterial Transport in Porous Media: Evaluation of a Model Using Laboratory Observations, *Water Resources Research*, 28:915-938.

33. Jenkins, M. B. and Lion, L. W. (1993) Mobile Bacteria and Transport of Polynuclear Aromatic Hydrocarbons in Porous Media, *Appl. Environ. Microbiol.*, 59:3306-3313.

34. Jin, M., Delshad, M., Dwarakanath, V., McKinney, D. C., Pope, G. A., Sepehrnoori, K., Tiburg, C., and Jackson, R. E. (1995) Partitioning Tracer Test for Detection, Estimation, and Remediation Performance Assessment of Subsurface Phase Liquid, *Water Resour. Res.*, 31(5), 1201-1211.

35. Johnson, P. R. and Elimelech, M. (1995) Dynamics of Colloid Deposition in Porous Media: Blocking Based on Random Sequential Adsorption, Langmuir, 11: 801-812.

36. Jury, W.A., Elabd, H. and Resketo, M. (1986) Field Study of Napropamide Movement through Unsaturated Soil, *Water Resource*, 22:749-755.

37. Karapanagioti, Kleineidam, S., Ligouis, B., Sabatini, D. A. and Grathwohl, P. (1999) Phenanthrene Sorption with Heterogeneous Organic Matter in a Landfill Aquifer Material, *Physics and Chemistry of the Earth.* 24:535-541.

38. Karickhoff, S. W., Brown, D. S. and Scott, T. A. (1979) Sorption of Hydrophobic Pollutants on Natural Sediments, *Water Res.* 13:241-248.

39. Karl, D.M. (1980) Cellular Nucleotide Measurement, *Microbiol. Review* 44: 740-796.

40. Knox, R.C., Sabatini, D.A. and Canter, L.W. (1993) *Subsurface Transport and Fate Processes*, Lewis Publishers, New York.

41. Ku C., Joseph D., Henry Jr., Ranjani S. and Lloyd R. (1985) Particle Transfer from a Continuous Oil to a Dispersed Water Phase: Model Particle Study, *J. Colloid Interface Sci.*, 106:377-387.

42. Liu, D., Johnson, P.R. and Elimelech, M. (1995) Colloid Deposition Dynamics in Flow through Porous Media: Role of Electrolyte Concentartion, *Environ. Sci. Technol.*, 29: 2963-2973.

43. Loosdrecht, M.C.M., Lyklema, J., Norde, W. and Zehnder, A.J.B. (1989) Bacterial Adhesion: a Physicochemical Approach, *Microb. Ecol.*, 17:1-15.

44. Magee, B. R., Lion, L. W. and Lemley, A. T. (1991) Transport of Dissolved Organic Macromolecules and Their Effect on the Transport of Phenanthrene in Porous Media, *Environ. Sci. Technol.*, 25:323-331.

45. Mahanty, J. and Ninham, B. W. (1976) *Dispersion Forces*, Academic Press, New York.

46. Marmur, A. (1979) A Kinetic Approach to Primary and Secondary Minimum Coagulations and Their Combination, *J Colloid Interface Sci.*, 72: 41-48.

47. Marshall, K. C., Breznak, J. A., Calleja, G. B., Mcfeters, G. A. and Rutter, P. R. (1984) *Microbial Adhesion and Aggregation*, Springer-Verlag, New York.

48. McCarthy, J.F.and Zachara, J.M. (1989) Subsurface Transport of Contaminants, *Environ. Sci. Technol.*, 23:496-502.

49. McCarty, P.L. (1975) Stoichiometry of Biological Reactions, *Progr. Water Technol.*, 7: 157-172.

50. McEldowney, S. and Fletcher, M. (1986) Effect of Growth Conditions and Surface Characteristics of Aquatic Bacteria on Their Attachment to Solid Surfaces, *J. Gen. Microbiol.* , 132:513-523.

51. Meinders, J. M., van der Mei, H. C. and Bussher, H. J. (1995) Deposition Efficiency and Reversibility of Bacterial Adhesion under Flow, *Journal of Colloid and Interface Science*, 176:329-341.

52. Meinders, J. M., Noordmans, J., Busscher, H. J. (1992) Simultaneous Monitoring of the Adsorption and Desorption of Colloidal Particles during Deposition in a Parallel Plate Flow Chamber, *J. Colloid Interface Sci.* 152: 265 –280.

53. Mercer, R. J., Ford, M. R., Stitz, L. J. and Bradbeer, C. (1993) Growth Rate Effect on Fundamental Transport Properties of Bacterial Populations, *Biotech. Bioeng.*, 42:1277-1286.

54. Monod, J. (1949) The Growth of Bacterial Cultures, *Ann. Rev. Microbiol.*, 3: 371-394.

55. Myers, D.(1988) *Surfactant Science and Technology*, VCH.

56. Nikaido, H. and Yaara, M. (1985) The Molecular Basis of Bacterial Outer Membraane Permeability, *Microbiol. Rev.* 49:1-32.

57. Nkedi-Kizza, P., Rao, P.S.C. and Hornsby, A.G. (1987) Influence of Organic Cosolvents on Leaching of Hydrophobic Organic Chemicals through Soils, *Environ. Sci. Technol.*, 21:1107-1111.

58. Ouyang, Y., Shinde, D., Mansell, R. S. and Harris, W. (1996) Colloid-Enhanced Transport of Chemicals in Subsurface Environments: A Review, *Critical Reviews in Environmental Science and Technology*, 26(2):189-204.

59. Pooley, H.M. (1976) Turnover and Spreading of Old Wall during Surface Growth of Bacillus subtilis, *J. Bacteriol.* 125:1127-1138.

60. Powelson, D. K. and Mills, A. L. (1998) Water Saturation and Surfactant Effects on Bacterial Transport in Sand Columns, *Soil Science*, 163:694-704.

61. Quagliano, J.C. and Miyazaki, S.S. (1997) Effect of Aeration and Carbon/Nitrogen Ratio on the Molecular Mass of the Biodegradation Polymer Poly-β-Hydroxybutyrate Obtained from *Azotobacter chroococcum* 6B, *Appl. Microbiol. Biotechnol.* 48:662-664.

62. Rajagopalan, R. and Tien, C. (1976) Trajectory Analysis of Deep Bed Filtration Using the Sphere in Cell Porous Media Model, *AIChE J.* 22: 523-533.

63. Rijnaarts, H. H. M., Norde, W., Bouwer, E. J., Lyklema, J. and Zehnder, A. J. B. (1995) Reversibility and Mechanism of Bacterial Adhesion, *Colloids Surf. B: Biointerfaces*, 4: 5 – 22.

64. Rijnaarts, H. H. M., Norde, W., Bouwer, E. J., Lyklema, J. and Zehnder, A.J.B. (1996) Bacterial Deposition in Porous Media Related to the Clean-Bed Collision Efficiency and Substratum-Blocking by Attached Cells. *Envion. Sci. Technol.* 30:2869-2876.

65. Rijnaarts, H. H. M., Norde, W., Bouwer, E. J., Lyklema, J. and Zehnder, A.J.B. (1996) Bacterial Deposition in Porous Media: Effects of Cell-Coating, Substratum Hydrophobicity, and Electrolyte Concentration, *Environ. Sci. Technol.* 30: 2877 – 2883.

66. Rosen, M.J. (1989*) Surfactants & Interfacial Phenomena*, 2nd ed., Wiley, New York.

67. Schaaf, P. and Talbot, J. J. Chem. Phys. 1989, 91: 4401- 4409.

68. Schweich, D. and Sardin, M. (1981) Adsorption, Partition, Ion Exchange and Chemical Reaction in Batch Reactors or in Columns – a Review, J. Hydrol., 50 : 1 – 33.

69. Singleton, P. (1997) *Bacteria in Biology, Biotechnology and Medicine*, John Wiley & Sons, New York.

70. Smets, B.F., Grasso, D., Engwall, M.A. and Machinist, B.J. (1999) Surface Physicochemical properties of *Pseudomonas fluorescens* and Impact on Adhesion and Transport through Porous Media, *Colloids and Surfaces B: Biointerfaces* 14: 121-139.

71. Stenstrom, A. T. (1989) Bacterial Hydrophobicity, an Overall Parameter for the Measurement of Adhesion Potential to Soil Particles, *Appl. Environ. Micobiol.*, 55:142-147.

72. Sutherland, I.W. and Wilkinson, J.F. (1965) Depolymerase for Bacterial Expolysaccharides Obtained from Phage-Infected bacteria, *J. Gen. Microbiol.*, 39:373-383.

73. Tchobanoglous, G. and Burton, F.L. (1991*) Wastewater Engineering, Treatment, Dispsal, and Reuse*, Third Eddition, Metcalf & Eddy, Inc., New York.

74. Tien, C., Turian, R. M. and Pandse, H. (1979) Simulation of the Dynamics of Deep Bed Filters, *AIChE J.*, 25: 385-395.

75. Unice, K. M. and Logan, B. E. (2000) Insignificant Role of Hydrodynamic Dispersion of Bacterial Transport, *J. Environ. Eng.*, 126: 491- 500.

76. van der Mei, H. C., Cowan, M. M. and Busscher, H. J. (1991) Physicochemical and Structural Studies on Acinetobacter calcoaceticus RAG-1 and MR-481--Two Standard Strains in Hydrophobicity Tests, *Curr. Microbiol.*, 23:337-341.

77. van Loosdrecht M. C. M., Lyklema J., Norde W., Schraa, G. and Zhender A. J. B. (1987) The Role of Bacterial Cell Wall Hydrophobicity in Adhesion, *Appl. Environ. Micobiol.*, 53:1893-1897.

78. van Loosdrecht, M.C.M., Lyklema, J., Norde, W. and Zehnder, A.J.B. (1989) Bacterial Adhesion: A Physicochemical Approach, *Microb. Ecol.*, 17: 1-15.

79. van oss, C.J. (1994) *Interfacial Forces in Aqueous Media*, Marcel Dekker, New York.

80. Vinten, A., Yaron, J.A.B. and Ney, P.H. (1983) Vertical Transport of Pesticides into Soil when Adsorbed on Suspended particles, *J. Agric. Food Chem.*,31:662-666.

81. Waldron, A.C. (1992) *Pesticides and Groundwater Contamination*, The Ohio State University Bulletin 820.

82. Wålinder, M. E. and Gardner, D. J. (1999) Factors Influencing Contact-angle Measurements on Wood particles by Column Wicking, *J. Adhesion Sci. Technol.*, 13:1363-1374.

83. Winget, P., Cramer, C. J. and Truhlar, D. G. (2000) Prediction of Soil Sorption Coefficients Using a Universal Solvation Model, *Environ. Sci Technol.* 34:4733 – 4740.

84. Wolfaardt, G.M., Lawrence, J.R., Robarts, R.D. and Caldwell, D.E. (1998) In situ Characterization of Biofilm Exopolymers Involved in the Accumulation of Chlorinated Organics, *Microb. Ecol.*, 35:213-223.

85. Worthing, C.R. (1983) *The Pesticide Manual: A World Compendium*, 7th ed., The British Crop Protection Council, Croydon, England.

## APPENDIX II

### *E. coli* HB101 Growth Curve

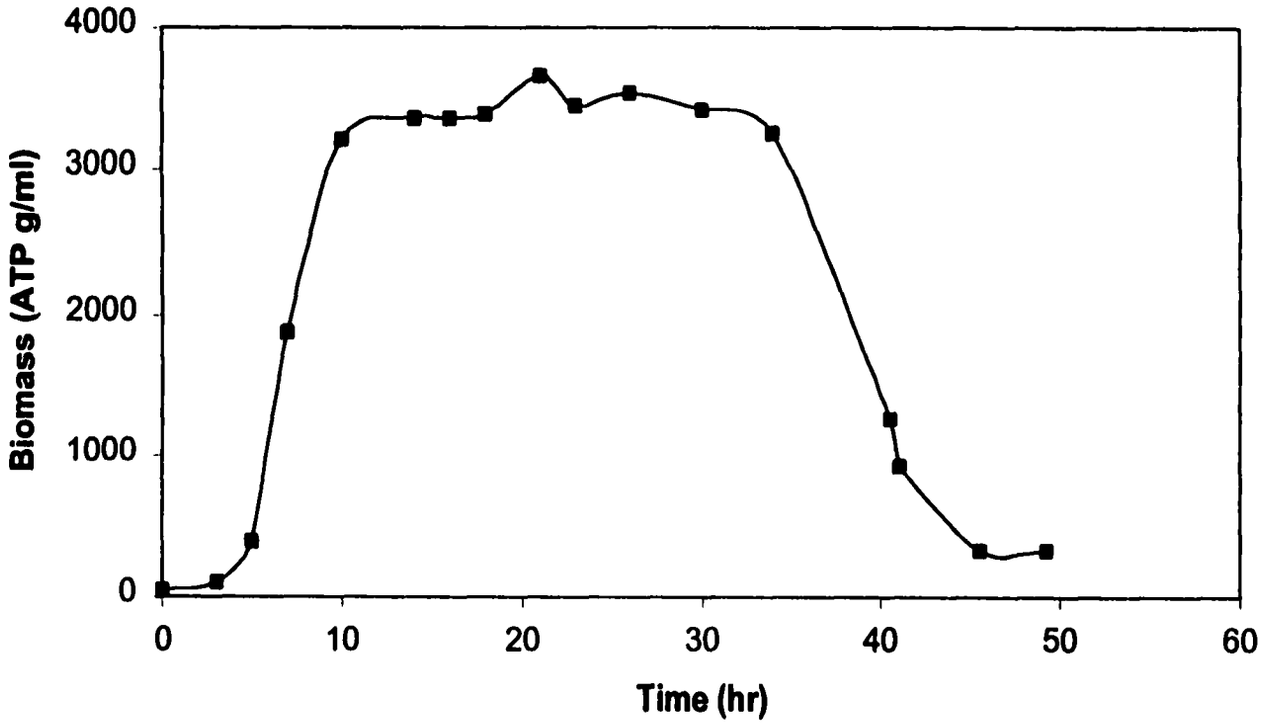

## APPENDIX III

### *E. coli* JM109 Growth Curve

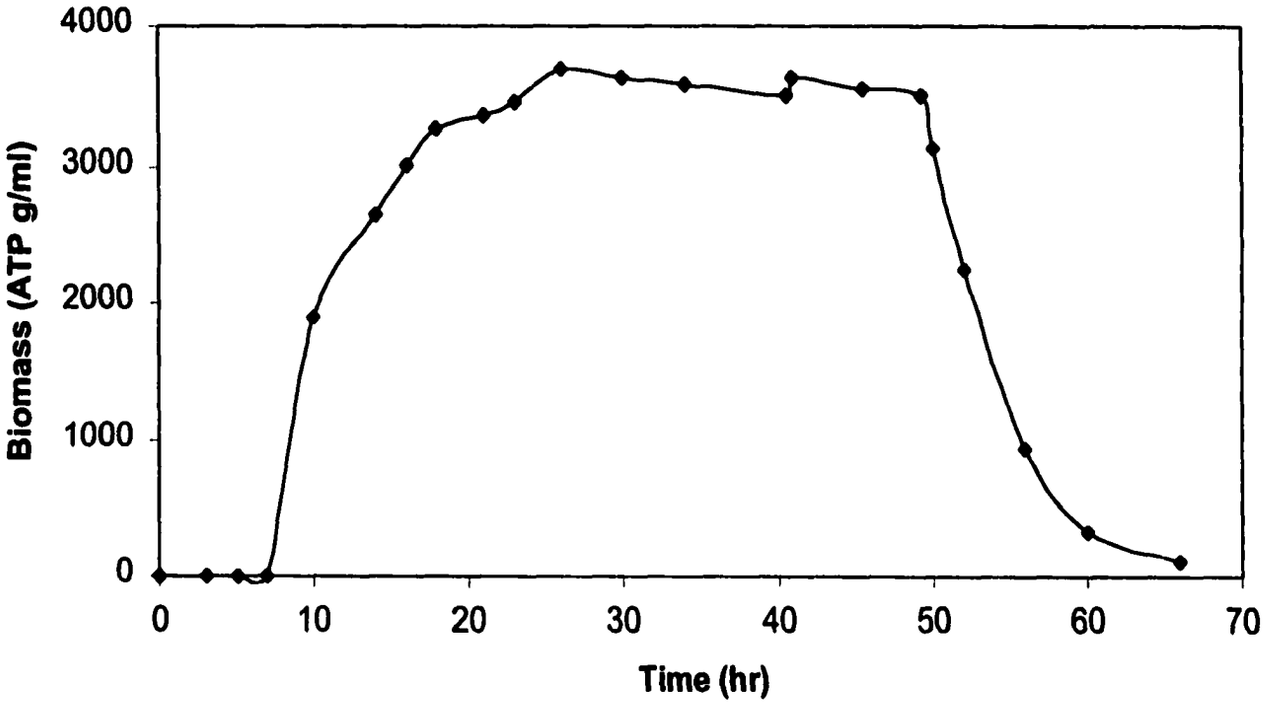

## APPENDIX IV

### *E. coli* k12 Growth Curve

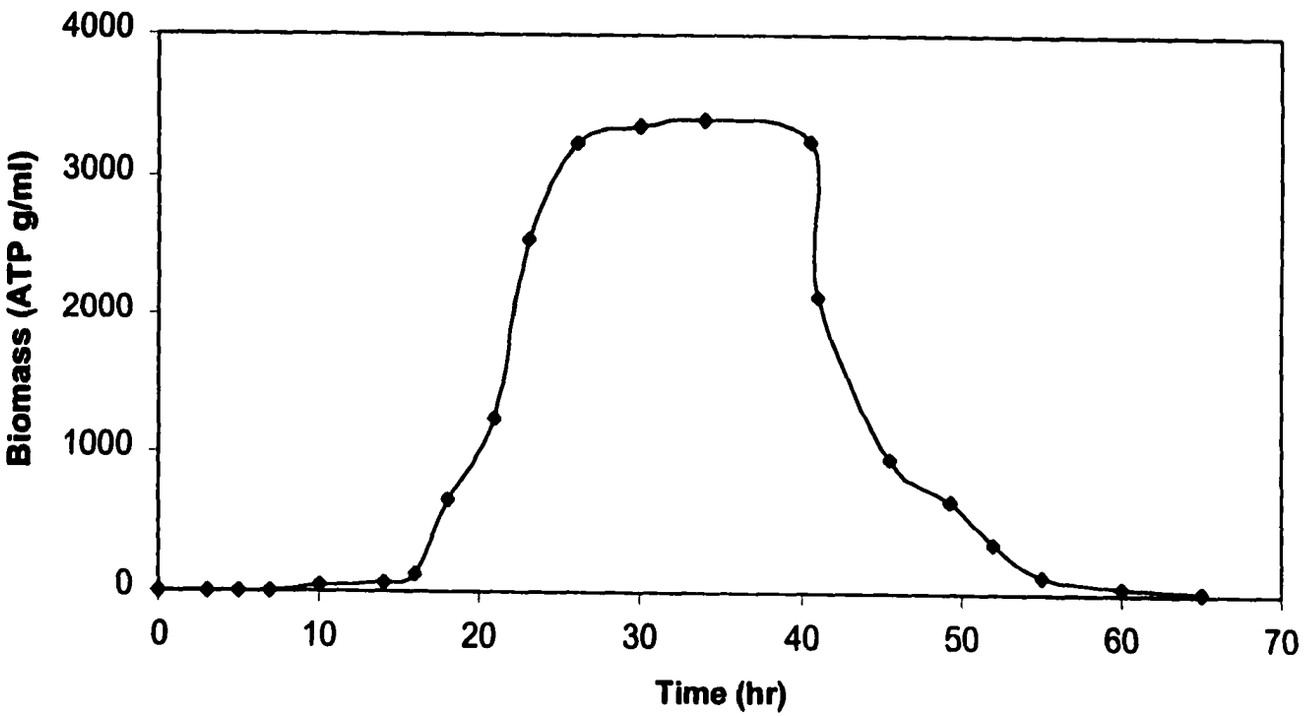

## APPENDIX V

### *P. fluorescens* Growth Curve

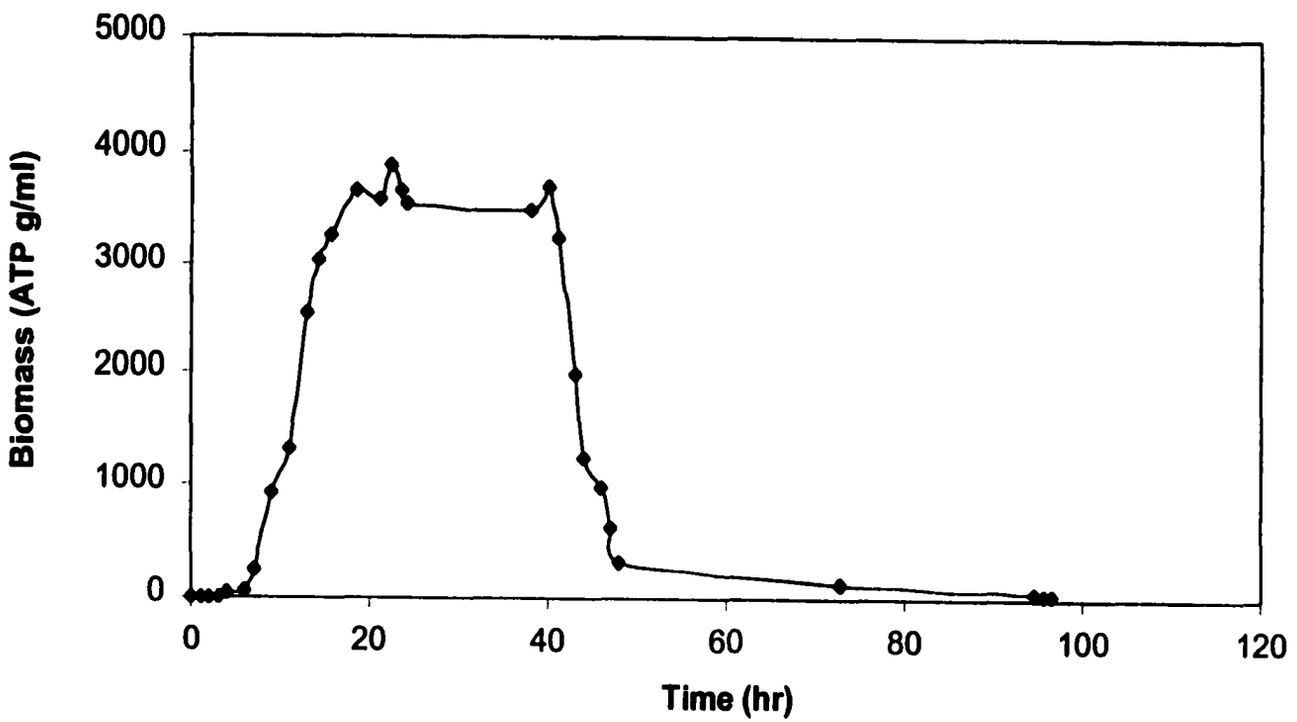

## APPENDIX VI

### *P. aeruginosa* Growth Curve

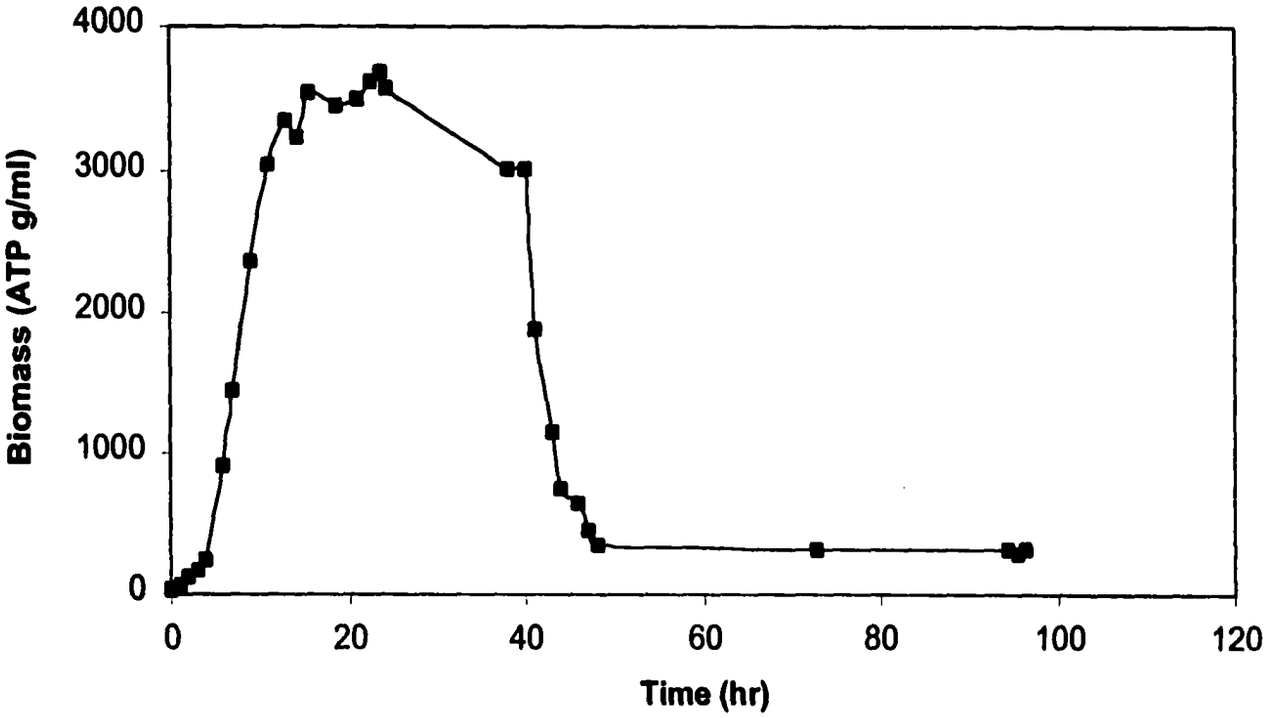

## APPENDIX VII

### *P. putida* Growth Curve

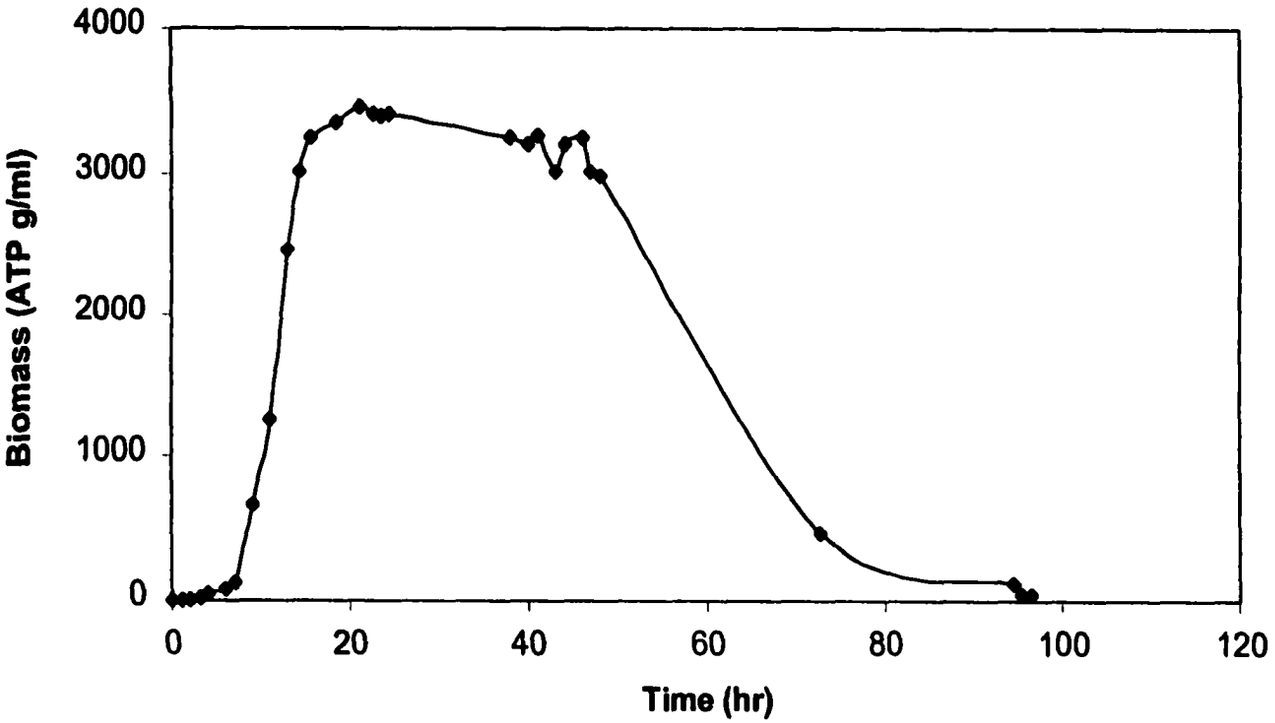

## APPENDIX VIII

### *P.* sp Growth Curve

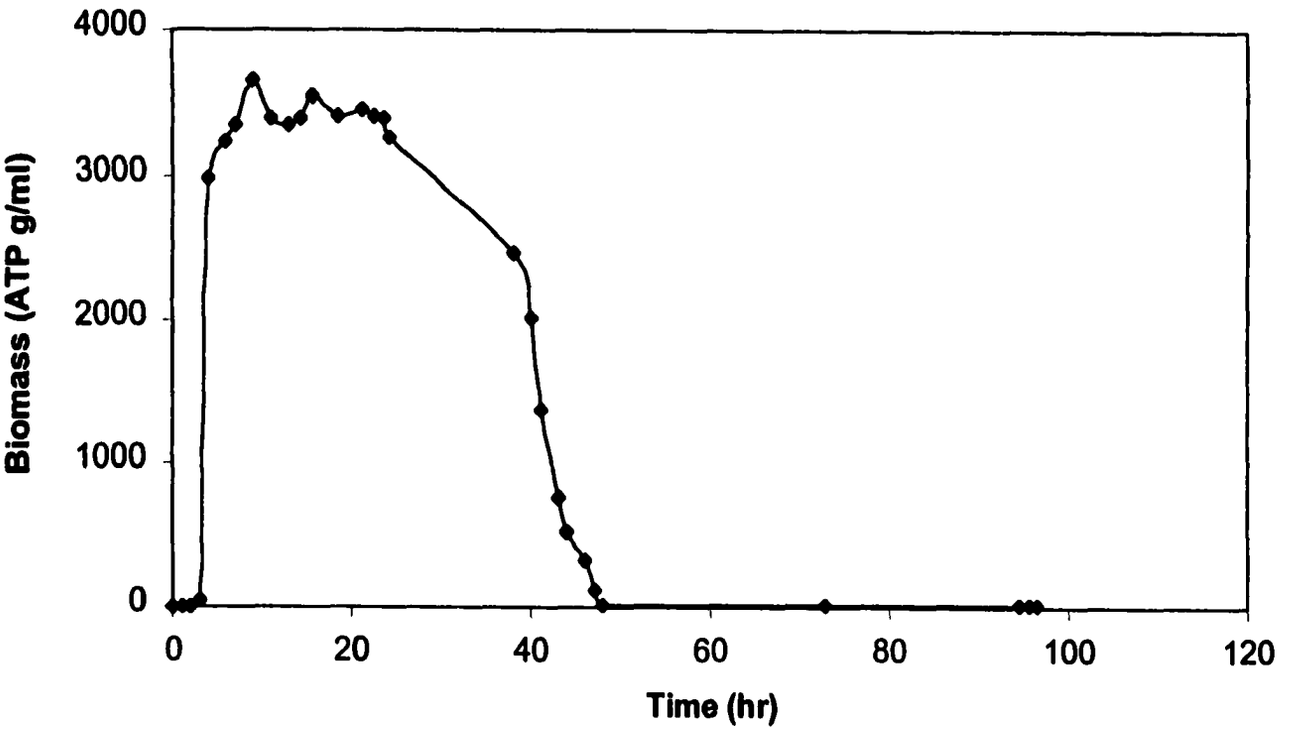

## APPENDIX IX

### *B. subtilis* Growth Curve

